PURIFICATION AND KINETIC CHARACTERISATION OF CLASS 3 BOVINE CORNEAL ALDEHYDE DEHYDROGENASE

A Thesis presented in partial
fulfilment of the requirements
for the degree of

Master of Science
in Chemistry

at

Massey University

Brendon John Woodhead
1999

Acknowledgements.

I would like to thank my family and fiancee Nicola for their emotional and financial support as well as my supervisors, Dr. Michael J. Hardman and Dr. Paul. Buckley for their support, patience and encouragement over the last few years.

Contents.

List of Figures

List of Tables

Section 1. Introduction

1.1 Aldehydes.

Aldehydes can be found in a wide variety of places. For example, formaldehyde, acetaldehyde and acrolein are products of combustion and are present in smog and cigarette smoke (Schauenstein *et al.*, 1977). In addition, many foods, such as fruits and vegetables, are sources of aldehydes (Schauenstein *et al.*, 1977). Aldehydes can also function as communication molecules, either between species or within a species, but the majority of aldehydes which are encountered are physiologically derived intermediates in the metabolism of other compounds (Schauenstein *et al.*, 1977).

Aldehydes can be generated from numerous endogenous and exogenous sources. Endogenous aldehydes include aldehydes arising from the metabolism of amino acids, biogenic amines, carbohydrates, vitamins, steroids (Schauenstein *et al.*, 1977) and as a result of membrane lipid peroxidation (Esterbauer *et al.*, 1990). Examples of some exogenous derived aldehydes include aldehydes resulting from the oxidation of primary alcohols (Williams, 1959) and from combustion (Schauenstein *et al.*, 1977).

In general aldehydes are biologically toxic due to the highly reactive nature of their electrophilic carbonyl group which can react with cellular nucleophiles, including proteins and nucleic acids. But not all aldehydes are biologically detrimental; for example, retinoic acid, the oxidation product of retinal, is involved in embryonic differentiation, and retinal itself is required for vision (Siegenthaler, *et al.*, 1990). Some aldehydes may be chemotactic, that is they can recruit cells to sites of injury or inflammation (Dianzani, 1989).

1.2 Aldehyde-Metabolising Enzymes.

In mammals aldehydes can be metabolised by three different enzymes; aldehyde dehydrogenase (ALDH), aldehyde oxidase (ALOX), and aldo-keto reductase (ALRD) (Fig. 1). All three enzymes have widespread tissue distributions with

broad, and sometimes overlapping, substrate preferences but differing physiological functions. Only ALDH will be discussed in this thesis.

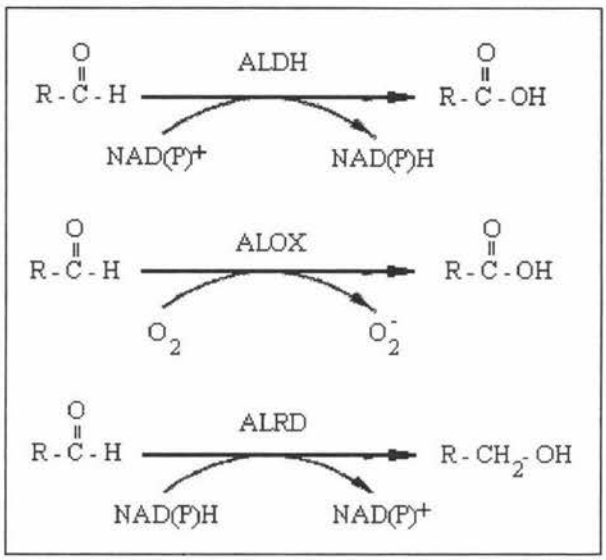

Figure 1. Reactions catalysed by aldehyde-oxidising enzyme systems.

ALDH; aldehyde dehydrogenase catalyses the oxidation of an aldehyde to its corresponding acid, using $NAD(P)^+$ as a coenzyme. *ALOX*; aldehyde oxidase catalyses the oxidation of an aldehyde to its corresponding acid using oxygen as a cofactor. *ALRD*; aldo-keto reductase catalyses the oxidation of an aldehyde to an alcohol, using NAD(P)H as a coenzyme.

1.3 Tissue and Subcellular Distribution of Aldehyde Dehydrogenase.

The ALDH family is a group of $NAD(P)^+$-dependent enzymes with common structural and functional features that catalyze the irreversible oxidation of a wide variety of aliphatic and aromatic aldehydes to their corresponding acids. Different forms of ALDH have been found in practically every cellular and subcellular compartment of the tissues examined. In humans, horses, sheep and cattle, ALDH is mainly found in the mitochondria and cytosol (Kraemer & Deitrich, 1968; Blair & Bodley, 1969; Feldman & Weiner, 1972; Crow *et al.*, 1974; Eckfeldt & Yonetani, 1976; Eckfeldt *et al.*, 1976; Sugimoto *et al.*, 1976; Greenfield & Pietruszko, 1977; Leicht *et al.*, 1978).

Within a tissue or cell, there appears to be a set of constitutively expressed ALDHs. Although there are exceptions, at least one mitochondrial and one cytosolic ALDHs is constitutive in a particular cell or tissue. In addition to the constitutive ALDHs, cytosolic inducible forms of ALDH have been identified following exposure to certain

xenobiotics, including drugs and carcinogens (Deitrich, 1971; Deitrich *et al.*, 1977; Marselos *et al.*, 1979; Torronen *et al.*, 1981; Feinstein & Cameron, 1972; Lindahl & Feinstein, 1976).

Of the tissues examined, the liver is considered to possess the highest ALDH activity. Multiple forms of ALDH have been identified for rat liver (Deitrich, 1966; Marjanen, 1972; Shum & Blair, 1972; Tottmar *et al.*, 1973; Horton & Barrett, 1975; Koivula & Koivusalo, 1975; Nakayasu *et al.* 1978; Mahoney *et al.*, 1981; Lindahl & Evces, 1984a). These forms have been differentiated largely on the basis of their kinetic properties. For the rat, mitochondrial ALDH accounts for more than 50 % of the total ALDH activity in the liver. Microsomal ALDH can account for another 35 %, while the cytosolic form makes up less than 10 % of the total rat liver ALDH activity (Marjanen, 1972; Shum & Blair, 1972; Tottmar *et al.*, 1973; Horton & Barrett, 1975; Koivula & Koivusalo, 1975; Nakayasu *et al.*, 1978; Lindahl & Evces, 1984a; Smith & Packer, 1972; Grunnet, 1973; Siew *et al.*, 1976; Nakanishi *et al.*, 1978).

The human liver also possesses multiple ALDH forms with approximately equal distribution between the mitochondria and cytosol (Duley *et al.*, 1985; Yoshida, 1990). A microsomal form has also been identified (Crow *et al.*, 1974). As with the rodent forms, both high- and low-substrate K_m forms have been identified for the human liver, with the low-K_m mitochondrial and high-K_m cytosolic forms accounting for the majority of the acetaldehyde-oxidising capacity of human liver (Kraemer & Deitrich, 1968; Greenfield & Pietruszko, 1977).

In all the species examined, brain and kidney tissues have a similar ALDH subcellular distribution to liver (Holmes, 1978; Rout & Holmes, 1985; Harada *et al.*, 1978; Holmes & VandeBerg, 1986a; Cox *et al.*, 1975; Cederbaum & Rubin, 1977; Hjelle *et al.*, 1983). However, other tissues, most notably the cornea, lung, stomach and urinary bladder, have a different subcellular distribution and activity profile from liver (Holmes & VandeBerg, 1986b; Dunn *et al.*, 1988; Evces & Lindahl, 1989; Manthey *et al.*, 1990). In these tissues the cytosolic form possesses the greatest ALDH activity, 90 % for the cornea (Holmes & VandeBerg, 1986b; Evces & Lindahl, 1989; Messiha, 1982) and 50 % in the stomach and urinary bladder (Lindahl, 1986; Rout & Holmes, 1985).

The distribution of ALDH among mammalian tissues is complex, but all tissues seem to possess a mitochondrial ALDH, and depending on the tissue and species, they may also possess a constitutive cytosolic ALDH, which may be induced under ideal conditions.

1.4 Nomenclature and Classification of ALDH.

In the past, naming of mammalian ALDHs has been based on physical or functional properties of the particular enzyme under investigation, for example "high-K_m" and "low-K_m", "mitochondrial", "cytosolic", "stomach" and "corneal" aldehyde dehydrogenases, but now ALDHs can be classified into three different classes based on their primary amino acid sequences:

- Class 1 ALDH, cytosolic constitutive and inducible ALDH forms exist
- Class 2 ALDH, only constitutive mitochondrial ALDH forms exist
- Class 3 ALDH, constitutive and tumor inducible ALDH forms exist

In general, class 1 and class 2 ALDHs function as tetramers with molecular weights of approximately 220 to 250 kDa. The tetramers are composed of four identical subunits each consisting of approximately 500 amino acids, with a molecular weight of approximately 55 kDa. The Phenobarbital (PB)-inducible ALDH (class 3 ALDH) is a dimer of identical 55 kDa subunits, each containing 501 amino acids, as is the tumor/dioxin-inducible ALDH with identical monomers of 50 kDa and 453 amino acids. Based on overall alignments and positional identities a newly deduced mammalian ALDH protein sequence can now be assigned into one of the three existing classes (Table 1).

The human and horse cytosolic ALDH, the 56-kDa androgen-binding protein, the rat phenobarbital (PB)-inducible ALDH, and the mouse retinal ALDH all share greater than 85 % positional identity and can be classified as class 1 ALDHs. All the mitochondrial ALDHs share greater than 95 % identity and can be classified as class 2 ALDHs. The tumor/dioxin-inducible ALDH, the rat constitutive microsomal ALDH and the bovine corneal protein (BCP 54) are at least 77 % identical and are considered to be class 3 ALDHs (Cooper *et al.*, 1990; 1991; Konishi & Mimura, 1992).

Table 1. Classification of mammalian ALDH.

Class 1 *(ALDH1)*	Constitutive	***Cytosolic Human Liver***
		Cytosolic Horse Liver
		Cytosolic Mouse Liver
		Cytosolic Bovine Liver
		Cytosolic Sheep Liver
		Cytosolic Dog Liver
	Inducible	***Rat PB Inducible***
		Mouse Retina
		Cytosolic Rat Liver
Class 2 *(ALDH2)*	Constitutive	***Mitochondrial Human Liver***
		Mitochondrial Horse Liver
		Mitochondrial Bovine Liver
		Mitochondrial Rat Liver
		Mitochondrial Sheep Liver
Class 3 *(ALDH3)*	Constitutive	Microsomial Rat Liver
		Bovine Corneal
	Inducible	***Tumor-specific Rat Liver***

Note: Sources identified in italics are considered the prototype ALDH enzyme for the class, based on primary structure determination. Other representatives are based on kinetic, physical and immunological properties or subcellular distribution.

1.5 Substrate Specificities.

Not only do the ALDH classes differ in tissue and subcellular distribution, so do they in substrate specificities. Some ALDHs have broad substrate specificities while others have more narrow substrate preferences. Physiological substrates have been identified for only a few ALDH isozymes in a small number of tissues. As for most enzymes, identification of potential physiological substrates has relied primarily on determination of K_m values but this is really only adequate when the subcellular concentrations of enzyme and putative substrate are known. When little is known about the concentrations, V_{max} / K_m values give a more precise measure of catalytic efficiency, as they allow for local differences in enzyme concentration and/or activity.

Small aliphatic aldehydes (e.g. acetaldehyde, propionaldehyde, malondialdehyde), biogenic aldehydes derived from neurotransmitter metabolism (Tank *et al.*, 1981; Ambroziak & Pietruszko, 1987) and 4-hydroxyalkenals from lipid peroxidation (Mitchell &

Petersen, 1987) are excellent substrates for classes 1 and 2 ALDH (Crow *et al.*, 1974; Greenfield & Pietruszko, 1977; Deitrich, 1966; Tottmar *et al.*, 1973).

Class 3 ALDH also seems to have a broad range of substrate specificities. For the liver-inducible, cornea and urinary bladder constitutive forms, experimental evidence suggests that a physiological role of ALDH is to catalyse the oxidation of medium chain (C6 to C9) aliphatic aldehydes derived from lipid peroxidation (Holmes & VandeBerg, 1986b; Evces & Lindahl, 1989) but 4-hydroxyalkenals and malondialdehyde, which are also generated by lipid peroxidation, are not substrates for class 3 ALDHs (Lindahl & Petersen, 1991).

With respect to coenzyme specificity, all ALDHs have K_m values for NAD^+ in the micromolar range (Feldman & Weiner, 1972; Crow *et al.*, 1974; Greenfield & Pietruszko, 1977; Nakayasu *et al.*, 1978; Mahoney *et al.*, 1981; Lindahl & Evces, 1984b; Ryzlak & Pietruszko, 1987; Algar & Holmes, 1989). In general, class 1 ALDHs have K_m values of 1 to 10 μM, whereas the class 2 forms have K_m values in the 20 to 50 μM range. Class 3 ALDHs have more variability, with their K_m values for NAD^+ ranging from about 5 μM for the corneal ALDH to approximately 100 μM for the microsomal form.

Although $NADP^+$ is a relatively good coenzyme for the class 3 ALDHs (K_m 60-200 μM), the catalytic constants (V_{max} / K_m) suggest that NAD^+ is probably the preferred coenzyme *in vivo*, even for the class 3 ALDHs. Classes 1 and 2 ALDH have K_m values for $NADP^+$ which are at least 10 to 100 times higher than those for NAD^+, while the catalytic constant is lower, indicating that NAD^+ functions as the coenzyme *in vivo* for these forms.

1.6 Structural Organisation of the Cornea.

The cornea is a thin transparent piece of tissue (Fig. 2A) that forms the outermost surface of the eye, providing a protective barrier to the external environment and most of the refractive power of the eye, directing light onto the retina. The cornea is composed of five layers; an external epithelial layer, Bowman's membrane, a bulky stroma layer, Descemet's membrane and the endothelium (Fig. 2B).

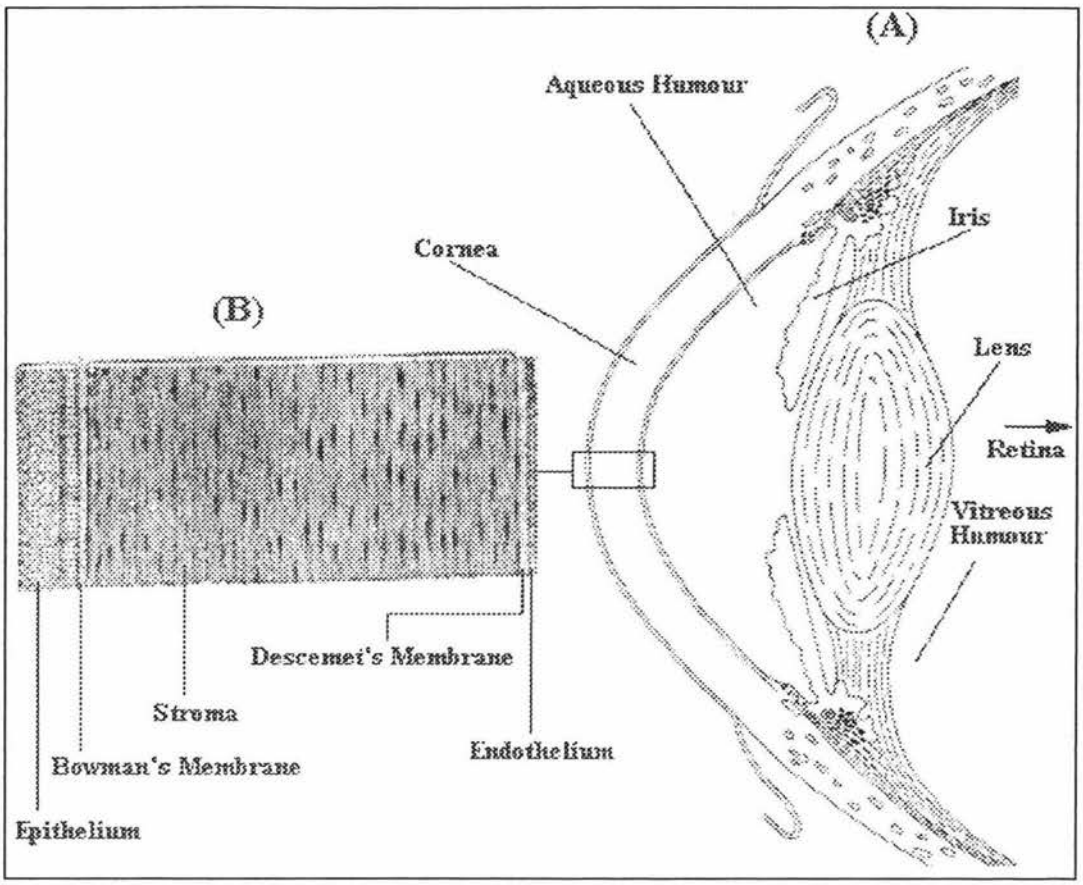

Figure 2. Structural organisation of the cornea.

(A). Lateral view of the eye showing the position of the cornea
(B). A cross-section of the cornea, showing its five different layers.

The corneal epithelium represents 10 % of the corneal thickness and functions as a major center of oxidative metabolism in the cornea. The Bowman's membrane is a randomly arrayed collagen fibril structure that merges into the stroma. The stroma constitutes approximately 90 % of the corneal thickness and is comprised of a matrix of 300-500 layers (lamellae) of collagen fibrils, surrounded by proteoglycans. Located between the stromal lamellae are keratocytes, which are flat cells that maintain the collagen fibrils and extracellular matrix. The Descemet's membrane is only 10 μm thick and separates the stroma from the endothelium. It is mainly made up of collagen, fibronectin and laminin (Millin *et al.*, 1986; Newsome *et al.*, 1981; Nakayasu *et al.*, 1986). The corneal endothelium consists of a single layer of hexagonal cells, 4-6 μm thick and 20 μm wide. The main function of the endothelial layer is to maintain a fixed stromal hydration (Klyce & Beuerman, 1988).

Both the epithelial and endothelial layers of the cornea provide a semipermeable membrane barrier to the tear film and the aqueous humor found on either side of the cornea. The proteoglycan content of the cornea attracts fluid and leads to swelling of the corneal stroma (Hedbys, 1961). This swelling pressure is relieved by the endothelial 'fluid pump' which allows fluid transfer from the swollen stroma to the aqueous humor. The epithelium also contributes to the release of intraocular pressure by moving about 15 % of the stromal fluid to the tear film by secretion of Cl^- (Beekhuis & McCarey, 1986). The intraocular pressure has a dual effect on the corneal hydration, depending on the condition of the endothelial cell layer. If the endothelium is intact the intraocular pressure decreases corneal thickness, but if the endothelium is acutely damaged as caused by glaucoma, corneal thickness increases (Olsen, 1980). Thus, regulation of stromal hydration by the endothelium and proteoglycan content can subsequently regulate the inter-fibrillar distance of the stromal collagen molecules.

1.7 Proteins of the Cornea

The normal cornea is composed of approximately 78 % water, 12-15 % collagen and 1-3 % proteoglycan (Maurice 1969). Collagen and proteoglycan are the major structural proteins of the cornea but non-collagenous structural proteins, soluble proteins, glycoproteins and lipids can also be found within the cornea and have important biological and metabolic functions.

Collagen is the major protein of the extracellular matrix, accounting for 71 % of the corneal dry weight. It forms the structural component of the corneal stroma and has a major role in providing the optical transparency of the tissue (Oxlund & Andreassen, 1980). Of the twelve known types of collagen, seven are present in the cornea.

Within the stroma, four different types of collagen can be found, Type I, III, V and VI, representing 50-55 %, less than 1 %, 8-10 % and 25-30 % of the relative dry weight of the stromal cornea respectively (Nakayasu *et al.* 1986; Zimmermann *et al.*, 1986). The other collagen types, IV, VII and VIII are components of the Bowman's layer, Descemet's membrane and can also be found in the basement membranes of the epithelium and/or endothelium (Newsome *et al.*, 1981; Zimmermann *et al.*, 1988; Kapoor *et al.*, 1986). A slow

progressive cross-linking of the corneal collagen molecules has been found to correlate with increasing age; this crosslinking results in a decrease in corneal transparency (Zimmerman *et al.*, 1988; Cannon & Foster, 1978).

Proteoglycans contain a protein core with covalently linked glycosaminoglycan chains. They act as a protein filler, interspersed between collagen fibrils and contribute to the regularity of the parallel spacing of the collagen fibres in the corneal stroma. Another function of proteoglycans, which was stated earlier, is their role in the hydration of the corneal stroma (Klyce & Beuerman, 1988). Approximately 60-70 % of the proteoglycans in the stroma consist of keratan sulphate and the rest is dermatan sulphate. Studies have shown a correlation between increasing collagen fibril diameter and decreasing concentration of keratan sulphate with age (Borcherding *et al.*, 1975; Kangas *et al.*, 1990).

Also located within the cornea are many soluble glycoproteins, peptides and enzymes, the most abundant being a 54 kDa bovine corneal protein, designated BCP54.

BCP54 was first identified by Holt and Kinoshita (1973) as a single non-serum protein, which constitutes a major fraction of the soluble proteins of the bovine cornea. In later studies it was shown that BCP54 is an intrinsic corneal protein specific for the mammalian cornea and absent from extraocular tissues (Silverman *et al.*, 1981) and is the most abundant soluble protein of the bovine cornea, constituting approximately 30 % of the total soluble corneal protein (Alexander *et al.*, 1981). Immunohistochemical studies have shown that the 54 kDa protein is present in the corneal epithelium, stromal keratocytes, endothelium and the epithelial cells of the anterior capsule of the lens (Eype *et al.*, 1987).

As BCP54 is not a structural protein like collagen or a proteoglycan, as indicated by its amino acid composition (Alexander *et al.*, 1981), BCP54 was presumed to possess some hormonal or enzymatic activity. Genetic studies of BCP54 showed that BCP54 has extensive sequence homology with the rat tumor-associated ALDH (class 3 ALDH), being 78 % identical at the nucleotide level and 82 % identical in amino acid sequence (Cooper *et al.*, 1990; 1991; Konishi & Mimura, 1992) but only 17 % identical with human class 1 and 2 ALDH (Hempel *et al.*, 1984; Hsu *et al.*, 1988). Based on this information,

BCP54 is a homologue of the tumor-associated rat ALDH, the prototype of the class 3 ALDH isozyme.

ALDH activity of BCP54 was verified by Verhagen *et al.* (1991) and by Konishi & Mimura (1992) using kinetic and immunoprecipitation assays. It was shown through these studies that BCP54 is identical to the tumor-associated ALDH, but clearly different from the normal rat liver ALDH (Lindahl and Evces, 1984b,c), and can be classified as a class 3 ALDH.

Another abundant soluble protein has recently been identified in the bovine corneal epithelium, denoted BCP11/24, due to its molecular weight of 11 kDa by SDS-PAGE and 24 kDa by gel filtration under non-denaturing conditions (Bakker *et al.*, 1992). BCP11/24 behaves identically in reduced and non-reduced SDS-PAGE and is probably not a glycoprotein. BCP11/24 has a tendency to bind non-covalently to BCP 54; this hampered its characterisation by biochemical and immunochemical techniques. Isoelectric focusing indicated microheterogeneity of BCP11/24, yielding bands with isoelectric points of 6.1, 5.9, 5.7 and 5.6. A rabbit antiserum directed against BCP11/24, that did not recognize BCP54, demonstrated that the distribution of BCP11/24 in different ocular tissues is strikingly similar to that of BCP54. It was found that, *in vitro*, BCP11/24 had a tendency to interact with BCP54, suggesting that BCP11/24 is associated with BCP54 *in vivo*, fulfilling a function which may be related to the activity of BCP54 as a corneal ALDH. In contrast to BCP54, however, BCP11/24 was not detectable in corneal endothelium. The antiserum did not detect any immunologically related molecules in corneal epithelium extracts of sheep, human or rat origin, indicating that BCP11/24 is probably not as highly conserved as BCP54 (Bakker *et al.*, 1992).

1.8 Ultraviolet Absorption by Corneal ALDH.

Approximately 80 % of the UV-B radiation in the 290-320 nm range directed towards the eye is absorbed by the cornea (Cogan & Kinsey, 1946; Bachem, 1956; Wurtman 1975; Ambach *et al.*, 1994), while less harmful visible light is allowed to be transmitted and focused onto the retina. The UV absorption properties of the cornea and the lens serves

to protect the photosensitive retinal cells against UV-induced tissue damage (Boettner & Wolters, 1962; Zigman, 1983).

Investigations (Pitts, 1987) into the effects of UV radiation on the mammalian eye have shown that at wavelengths of less than or equal to 290 nm the ocular response is restricted almost entirely to the corneal epithelium, indicating that absorption of the radiation is almost totally by this cell layer. Stromal swelling increases significantly at wavelengths greater than 290 nm and this is thought to result from endothelial damage, particularly to the endothelial pump (Cullen *et al.*, 1984; Riley *et al.*, 1987; Doughty & Cullen, 1989; Bergmanson, 1990). At threshold levels of UV radiation the cornea is subject to photokeratitis (Le Grand, 1958; Boettner & Wolters, 1962; Scholander *et al.*, 1969; Sherashov, 1970; Hemmingsen & Douglas, 1970; Pitts, 1970, 1973; Kurzel, 1978; Ringvold, 1980). Photokeratitis is an immediate effect caused by absorption of high levels of UV radiation in the epithelial cells. The cells form layers of keratin which reduces corneal transparency and 'clouding' of the cornea results. Cataract, is a late, cumulative response to UV radiation (Bachem, 1956; Zigman, 1983) which occurs in the lens rather than the cornea. However, it has been observed that UV irradiation may cause or promote corneal endothelial cell changes associated with aging (Riley *et al.*, 1987) which may contribute to such illnesses as glaucoma.

Due to the reported high abundance of corneal ALDH from a number of mammalian species, including human (Holmes, 1988), baboon (Holmes & VandeBerg, 1986), pig, sheep, cattle (Holmes *et al.*, 1989; Abedinia *et al.*, 1990), mice (Holmes *et al.*, 1988; Rout & Holmes, 1988,1991), gray short tailed opossums (Holmes *et al.*, 1990) and rat (Messiha & Price, 1983; Evces & Lindahl, 1989), it has been proposed that one of corneal ALDH's functions may be as a UV absorbing agent (Abedinia *et al.*, 1990).

Recent histochemical studies (Downes *et al.*, 1992; Gondhowiardjo *et al.*, 1991) have shown that corneal ALDH is predominantly localised in the epithelial and endothelial layers, with species-specific differences in relative and total levels of activities between these layers being observed. The epithelial layer of the human, baboon and pig cornea exhibits the highest levels of ALDH activity, whereas sheep and cattle exhibit the highest enzyme levels in the corneal endothelium. The differences in distribution of corneal ALDH between mammalian species may be related to the relative thickness of

the corneas. Sheep and cattle corneas are much thicker than those of human, baboon and pig, and as such limit UV-B penetration. The need for a UV-B absorbing protein in the corneal epithelium may not be as critical for thick corneas (i.e. sheep and cattle) as compared with thin corneas (i.e. human, pig and baboon).

The absorbance spectrum of purified bovine corneal ALDH illustrates the potential of this protein in contributing to UV-B absorbance by the cornea (Abedinia *et al.*, 1990). The enzyme absorbs maximally at 278-280 nm, which differs slightly from the absorbance maxima of 288-290 nm for the action spectrum of abiotic UV-induced keratitis in the mammalian cornea (Cogan & Kinsey, 1946). Kurzel (1978) suggested that a direct correlation between the absorbance spectrum of the photoreceptor and the action spectrum would not be expected, since filtration by other absorbers in the cornea would directly influence the result observed, as could the presence of the enzyme-coenzyme binary complex, which absorbs UV light at wavelengths of approximately 300 nm.

Recently, Mitchel *et al.* (1995) investigated the contributions of different fractions of bovine cornea to the absorption of UV light between 240 and 320 nm. The cornea was divided into four fractions, water-insoluble (largely collagen), nonprotein small water-soluble, water-soluble protein, and a lipid-soluble fraction. It was found that the insoluble fraction, which comprises approximately 75 % of the corneal dry weight, accounted for 40-50 % of UV absorbance between 240 and 280 nm. However, in the range of 290-300 nm, the water-soluble plus lipid-soluble fractions, which represent 17 % of the cornea's dry weight, accounted for 60-65 % of the total absorption, with the water-soluble proteins alone accounting for 40-45 % of the total. The absorbance contribution of the water-soluble proteins has been attributed to their relatively high tryptophan content. The major soluble protein was found to be corneal ALDH, which is a tryptophan-rich protein accounting for approximately 30 % of the total soluble protein mass. This study supports the earlier proposal by Abedinia *et al.* (1990) and others, that one of the functions of corneal ALDH is in protecting the eye against UV-B induced tissue damage. However, just because ALDH can absorb harmful UV light, this does not mean it is not affected by UV radiation. Studies into the effects of UV-B radiation on rat corneal aldehyde dehydrogenase have shown dramatic reductions in

ALDH activity (activity level only 15 % relative to control animals) along with corneal clouding 4-6 days after a 1 hour exposure of UV-B light (peak wavelength of 302 nm) (Downes *et al.*, 1993). Structural changes to corneal ALDH have also been observed, with alterations to its quaternary structure, though there was no significant change in the peptide chain conformation. Under such conditions the enzyme continues to act as a protectant by preventing aggregation of photolabile proteins such as the eye lens gamma-crystallin (Uma *et al.*, 1996).

1.9 The Enzymatic Function of Corneal ALDH.

UV light has also been implicated in the generation of free radicals and related reactive reduced oxygen species (ROS), e.g. superoxide anion (O_2^-), hydroxy radicals (OH^-), and hydrogen peroxide (H_2O_2). ROSs can be removed through the enzyme activities of superoxide dismutase, glutathione peroxidase and catalase (Sies, 1985). The free radicals can initiate membrane lipid peroxidation processes, resulting in the formation of cytotoxic peroxidic aldehydes (Esterbauer *et al.*, 1985).

Membrane lipid peroxidation is part of the continuing process of cellular membrane synthesis and degradation. Polyunsaturated fatty acids in membrane phospholipids are susceptible to attack by ROSs, which initiate a chain-like reaction. The products of lipid peroxidation include short-lived, unstable intermediates and relatively stable carbonyl-containing compounds. The short-lived intermediates contain reactive radicals that catalyse further auto-oxidations or spontaneously rearrange to form stable products. Aldehydes account for greater than 35 % of the stable products and are known to posses cytotoxic properties due to their reactivity towards thiol compounds, including sulfhydryl groups of proteins (Grafstrom, 1990). Although the quantity of the various aldehydes produced varies with the starting lipid hydroperoxide, three are generally considered to be the major products of lipid peroxidation: malondialdehyde, hexanal and 4-hydroxynonenal (Schauenstein *et al.*, 1977; Esterbauer *et al* , 1985).

A physiological role for ALDH in the cornea as a detoxifier of the cytotoxic aldehydes generated by UV-induced lipid membrane peroxidation has been proposed (Abedinia *et al.*, 1990; Holmes & VandeBerg, 1986; Evces & Lindahl, 1989; Lindahl & Petersen, 1991).

Values of k_{cat} /K_m give an indication of substrate efficiency, and have shown that the enzyme has a distinct preference for medium chain aliphatic aldehydes such as hexanal, Δ-2-hexenal and 4-hydroxynonenal and is highly active with benzaldehyde, but inactive with malondialdehyde (Abedinia *et al.*, 1990; Lindahl & Petersen, 1991; Gondhowiardjo *et al.*, 1991; Algar *et al.*, 1990; Evces & Lindahl, 1989; King & Holmes, 1993; Yin *et al.*, 1995; Downes & Holmes, 1993). Bovine corneal ALDH exhibits a very high K_m with acetaldehyde (180 mM) (Abedinia *et al.*, 1990), which is significantly higher than for other 'high-K_m' forms of ALDH in human and mouse liver (Algar & Holmes, 1985; MacKerrell *et al.*, 1986) and mammalian liver mitochondrial and cytosolic ALDH (Greenfield & Pietruszko, 1977; Algar & Holmes, 1985; 1986). NAD^+ and $NADP^+$ both serve as cofactors for bovine corneal ALDH, although k_{cat} values are greater for NAD^+ than for $NADP^+$. Rat corneal ALDH (Evces & Lindahl, 1989), however, prefers $NADP^+$ as coenzyme and preferentially oxidizes benzaldehyde-like aromatic aldehydes as well as medium chain length (4-9 carbons) aliphatic aldehydes. Table 2 illustrates some of the kinetic properties of mammalian corneal ALDH using a range of naturally occurring aldehydes.

Table 2. Kinetic properties of mammalian corneal ALDH.

	Bovine [a]			Mouse [b]			Baboon [c]			Human [d]		
Substrates	K_m	k_{cat}	k_{cat}/K_m	K_m	k_{cat}	k_{cat}/K_m	K_m	k_{cat}	k_{cat}/K_m	K_m	k_{cat}	k_{cat}/K_m
Acetaldehyde	180	33	0.18	16	2008	128	40	798	20	67	2154	32
Hexanal	0.8	112	140	0.08	2038	25475	-----	-----	-----	0.06	2058	34300
Δ-2-Hexanal	0.4	27	67.5	0.12	2107	17558	0.29	2796	9641	0.10	3180	31800
Malondialdehyde	0	0	-----	0	0	-----	0	0	-----	0	0	-----
4-Hydroxynonenal	3.0	41	13.7	0.03	1564	52133	0.22	4398	19991	0.11	2622	23836
Benzaldehyde	3.7	57	15.4	0.11	1255	11409	0.56	4698	8389	0.20	3060	15300
NAD	0.07	228	3257	0.06	1126	18767	0.02	-----	-----	0.03	2718	90600
NADP	0.09	62	689	1.40	1985	1418	0.17	-----	-----	0.49	2328	4751

K_m values are in mM, k_{cat} values are in min^{-1}, k_{cat}/K_m values are in mM^{-1} min
[a] Abedinia *et al.*, (1990); [b] Downes & Holmes, (1993); [c] Algar *et al.*, (1991); [d] King & Holmes, 1993).

Species differences concerning the inhibition of ALDH activity by disulfiram have been reported. Rat class 3 ALDH is almost completely inhibited by disulfiram (Evces & Lindahl, 1989), whereas human class 3 ALDH (lung, stomach and corneal) (Harada *et al.*,

1980; Gondhowiardjo *et al.*, 1991), bovine corneal ALDH (Gondhowiardjo *et al.*, 1991; Konishi & Mimura, 1992), and mouse corneal ALDH (Downes & Holmes, 1993) are not affected. Inhibition studies using *p*-hydroxymercuribenzoate showed that for human, mouse and bovine corneal ALDH, activity was rapidly inactivated but the rate of inactivation by *p*-hydroxymercuribenzoate was significantly reduced in the presence of benzaldehyde and NAD^+ (King & Holmes, 1993; Downes & Holmes, 1993; Konishi & Mimura, 1992). The results of the inhibition studies differ from those for the normal rat liver ALDH or the tumor-associated ALDH (Lindahl & Evces, 1984b,c) and are indicative of an essential active cysteine. This cysteine residue is strictly conserved in the ALDH family (Cys-243 in class 3, Cys-302 in classes 1 and 2) and it is generally accepted as the catalytic thiol (Hempel *et al.*, 1993; Hempel & Pietruszko, 1981; Farres *et al.*, 1995; Kitson *et al.*, 1991; Cooper *et al.*, 1991).

1.10 The Structural Role of Corneal ALDH.

A third proposed function of corneal ALDH is as a structural protein. Studies on embryonic development of bovine (Rabaey *et al.*, 1981) and mouse (Downes & Holmes, 1992) corneas showed that corneal transparency parallels the appearance of the ALDH protein. This hypothesis is based on a 'gene sharing phenomenon' which involves the use of one gene encoding a protein that has two entirely different functions at the same time.

Functional duality has been recognised in a number of identifiable crystallin proteins in vertebrate lens, such as ε-crystallin, which is a lactate dehydrogenase (Wistow *et al.*, 1989), and δ-crystallin of birds and reptiles, which exhibits argininosuccinate lyase activity (Piatigorsky *et al.*, 1988). Many of the structural proteins of ocular lenses, commonly referred to as crystallins, are identical to specific enzymes or are the result of a recent gene duplication (Piatigorsky & Wistow, 1989). Aldehyde dehydrogenase functions in both the cornea and lens as a crystallin in certain mammals (Wistow & Kim, 1991) and cephalopods (Tomarev *et al.*, 1991). The necessity to maintain optical transparency for both the lens and cornea requires a structural protein which is stable, and resistant to deleterious influences such as UV light, free radicals and heat from the environment. ALDH, which can accumulate in a high

intracellular concentration without leading to precipitation, may possibly fulfill these criteria and function both as a structural protein and as a enzymatic protein.

The structural and enzymatic differences of corneal ALDH amongst mammalian species (Abedinia *et al.*, 1990; Holmes & VandeBerg, 1986; Holmes, 1988; Evces & Lindahl, 1989; Messiha, 1981) may be explained due to differences in adaptive development among species, based on the 'gene sharing phenomenon'. This could account for their varying tolerances to abiotic UV light. As mentioned earlier, differences in the relative thickness of the corneas and the subcellular location of corneal ALDH between mammalian species occur (Downes *et al.*, 1992; Gondhowiardjo *et al.*, 1991). For thinner human, baboon and pig corneas ALDH is predominantly localised in the epithelial layer, but for thicker sheep and cattle corneas ALDH is mainly located in the corneal endothelium. For thinner corneal epithelial cells, ALDH may be recruited more for its structural role than its other functions (Cuthbertson *et al.*, 1992). This is similar to the recruitment of enzymes in the lens to act as crystallins which aid in maintaining optical transparency of that tissue. The fact that the protein also exhibits enzymatic activity is an added bonus. Endothelial ALDH may regulate collagen cross-linking, thereby contributing to the maintenance of corneal transparency through its effect on the aldehyde derivatives of two lysine residues of lysyl oxidase. These aldehyde derivatives have been shown to undergo an aldol condensation resulting in a spontaneous intramolecular collagen fibril cross-link, and therefore a decrease in corneal transparency (Hoekzema *et al.*, 1992).

1.11 Structural features of Class 3 ALDH.

The tertiary structure of the rat class 3 ALDH-NAD^+ complex was determined at a 2.6 Å resolution (Liu *et al.*, 1996; 1997). The active form of the enzyme is a homodimer (90 x 60 x 40 Å), consisting of two 452 residue subunits which are related by a pseudo two-fold symmetry. Each monomer contains three domains, an NAD-binding domain (residues 1-81, 104-212, 397-423), a catalytic domain (residues 213-396) and a bridging domain (residues 82-103, 424-452) (Fig 3). The dimer is stabilised through a total of 63 intra-molecular hydrogen bonds. The

majority (58) of these hydrogen bonds are between the bridging domain of one subunit and the catalytic domain of the other.

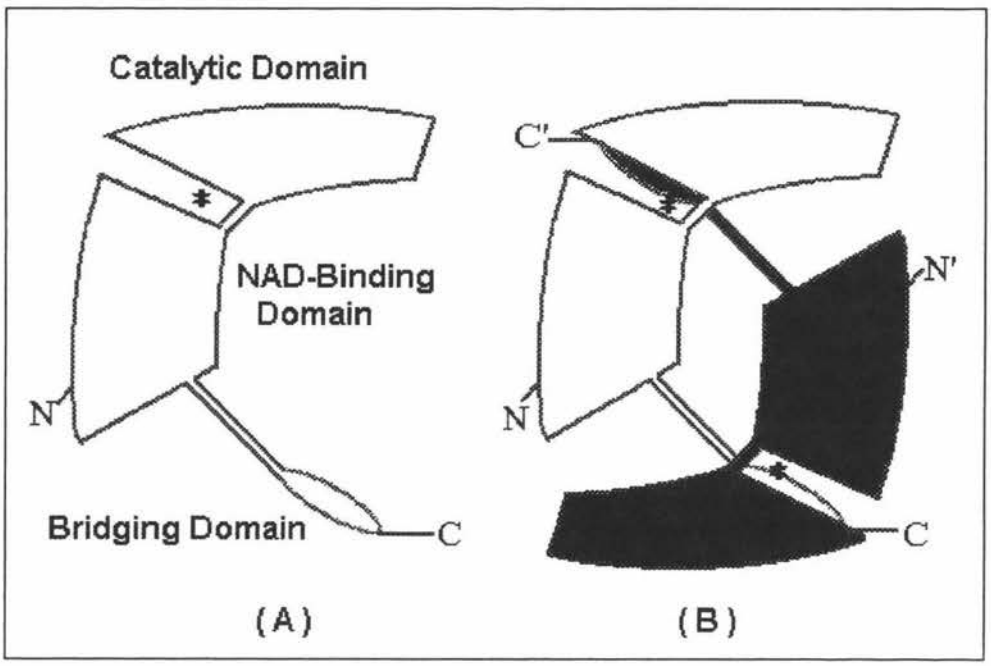

Figure 3. Schematic drawing of the ALDH monomer and dimer

(A). A simplistic drawing of the ALDH monomer, indicating the location of the three domains.

(B). A drawing showing the orientation of the two monomers within the homodimer of ALDH.

* Indicates the entrance to the funnel shaped pocket.

The domains are not drawn true to scale nor do they represent the relative 3D orientation within the ALDH structure. For a detailed view of the ALDH structure refer to Liu *et al.* (1997).

The Nucleotide-Binding Site.

Almost all known dehydrogenase structures contain a nucleotide-binding motif, the 'Rossmann fold', consisting of a core of two sets of β–α–β units, together forming six parallel β-strands flanked by α-helices (Rossmann *et al.*, 1974). In ALDH-3, however, the Rossmann fold contains only five β–strands (β1–5) connected by four α-helices (αA-αD), instead of the usual six β–strands (Lesk, 1995). Most NAD-dependent dehydrogenases have a highly conserved GXGXXG sequence motif, which identifies the dinucleotide binding site (Wierenga *et al.*, 1986). Generally, this sequence motif occurs at the N-terminus of αA, but for ALDH-3 this motif

occurs at the beginning of αD, resulting in a novel mode of NAD^+ binding. An acidic residue Glu-140 (residue 197 in classes 1 and 2) located in β2, downstream of the last Gly in the NAD-binding 'fingerprint' sequence gives rise to the specificity for NAD^+.

The Catalytic Site.

The catalytic site is located at the bottom of a deep funnel-shaped channel and is composed of residues from all three domains. The upper portion of the channel is formed by residues from the coenzyme-binding domain, whereas the nicotinamide ring of NAD^+ forms the bottom of the channel. Residues from the catalytic domain and from the bridging domain of the other subunit form part of the funnel entrance. Cys-243 is the catalytic thiol and is positioned near the bottom of the passage.

The active site structure suggests that the upper portion of the channel, formed by residues from all three domains, provides the specificity of the different forms of ALDH toward a particular aldehyde. The surface of the upper funnel is lined with a total of 35 residues of which only one (Phe-401) is highly conserved. It is therefore reasonable to assume that variation of these residues determines the aldehyde binding specificities of the different forms of ALDH. The structure of the lower portion of the funnel, formed by the highly conserved residues from both the NAD-binding and catalytic domains, as well as the presence of the catalytic thiol and nicotinamide ring, suggests that this is the catalytic site where hydride transfer from aldehyde to NAD^+ takes place (Liu *et al.*, 1996; 1997). Hydride transfer from aldehyde to NAD^+ requires the formation of a tetrahedral intermediate. A structure-based mechanism for the formation of such an intermediate complex is proposed (Liu *et al.*, 1997) (Fig. 4). For a substrate such as benzaldehyde, rotation of the Cα-Cβ single bond of Cys-243 would enable the formation of the intermediate complex where the carbonyl carbon of the aldehyde is approximately 2 Å from the catalytic thiol and about 2.5 Å from the nicotinamide NC4 atom. In this model the hydride is almost coplanar with the NAD pyridine ring, and small conformational shifts of the active site on aldehyde binding result in the pro-R specificity which has been found in all three classes of aldehyde dehydrogenases (Jones *et al.*, 1987).

Analysis of the conserved residues in the aldehyde dehydrogenase family, showed that 23 residues are strictly conserved (Hempel *et al.*, 1993); eleven glycines and three prolines are found at turns in the structure, while the remaining nine residues are found associated with the catalytic pocket (Cys-243, Glu-333 and Phe-335) or appear to stabilise adjacent secondary structural elements (Arg-25, Lys-137, Thr-318, Asn-355, Asn-388 and Ser-407). The observation that these conserved residues are found at key locations within the structure of ALDH from all classes, suggests that members of the ALDH family have similar structural folds, catalytic site structures and NAD-binding despite differences in sequence, modes of aggregation and substrate specificity (Hempel *et al.*, 1997; Liu *et al.*, 1997).

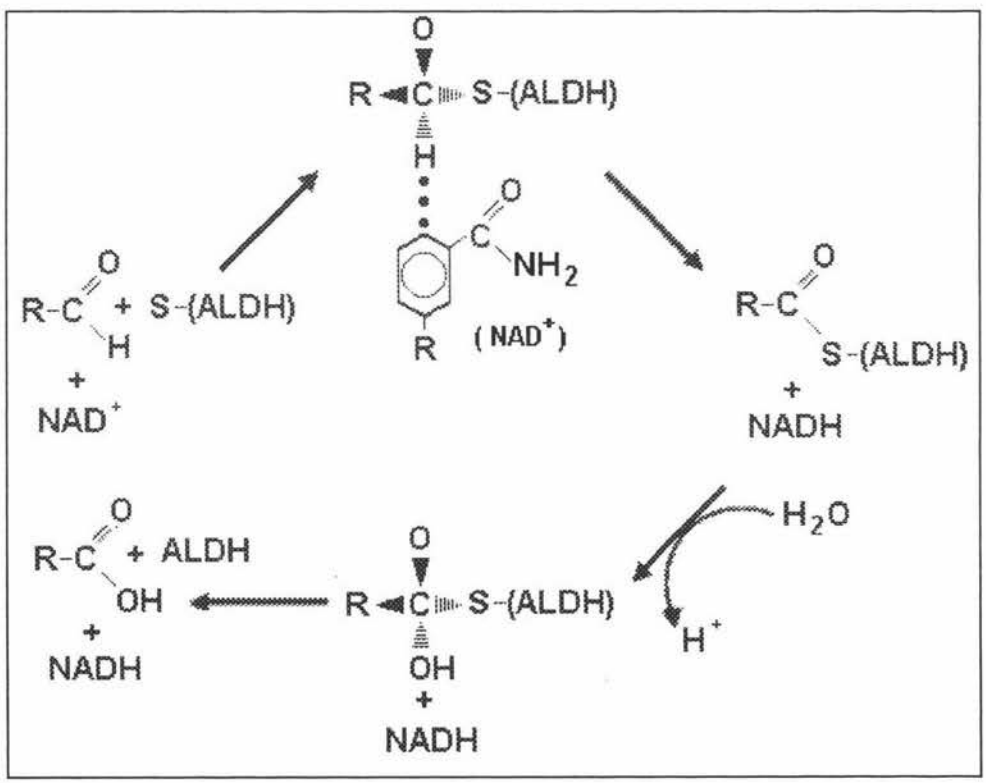

Figure 4. A schematic drawing for the structure based mechanism of aldehyde conversion to carboxylic acid.

1.12 Aims of the Study.

Bovine corneas are an easily accessible source of class 3 ALDH compared to some other mammalian species and therefore many investigations have been performed using this type of corneal ALDH. Although important biological functions of this protein have been proposed, its exact role and structure-function relationship are still not fully understood. This research is aimed at contributing to the kinetic characterisation of bovine corneal aldehyde dehydrogenase by focusing on the following:

1. Improving both protein recovery and enzyme purity.
2. Investigation of the active site by ligand binding studies using NADH.
3. Presteady-state and steady-state kinetic investigations using different aldehyde substrates and mixing conditions.

Information obtained through these investigations of bovine corneal ALDH will hopefully help in the elucidation of the structure-function relationship for all classes of mammalian ALDH, but in particular corneal ALDH.

Section 2. Purification of Class 3 Bovine Corneal Aldehyde Dehydrogenase.

2.1 Introduction.

Abedinia *et al.* (1990) reported a 48 % recovery of the bovine corneal ALDH protein following a small scale purification from 3 grams of corneal tissue. Riley (1993) carried out larger scale preparations of approximately 37 grams and obtained a 90 % protein recovery but this was probably at the expense of purity. Both investigations purified bovine corneal aldehyde dehydrogenase using a simple three step approach:

1. Extraction of soluble corneal protein.
2. Removal of protein precipitated by acid-denaturation (not ALDH)
3. Purification of ALDH using a CM-Sepharose cation-exchange column.

The purification of bovine corneal aldehyde dehydrogenase in this research is based around this basic three step approach but the procedures have been modified slightly by using different column elutions or by the inclusion extra purification steps, such as salt fractionation and dialysis.

2.2 Methods.

2.2.1 Protein Determinations.

The relative protein concentration was estimated by absorbance at 280 nm (A_{280}) and the actual protein concentration was determined by the Bradford (1976) method using bovine serum albumin (BSA) as the standard protein.

2.2.2 Sodium Dodecyl Sulphate (SDS) Gel Electrophoresis.

Polyacrylamide gels (10 % resolving and 4 % stacking) containing 1 % SDS, were prepared in a Bio-Rad mini gel slab apparatus, according to the procedure of Laemmli (1970), as modified by Ames (1974). After electrophoresis, the gels were

stained for protein with 0.25 % (w/v) Coomassie Brilliant Blue R-250 in 50 % (v/v) methanol - 10 % (v/v) acetic acid for 2 hrs and destained in a solution of 30 % (v/v) methanol - 10 % (v/v) acetic acid.

The protein molecular weight was estimated by a mobility plot using standard low molecular weight markers; phosphorylase b (94 kDa), serum albumin (67 kDa), ovalbumin (43 kDa), carbonic anhydrase (30 kDa), trypsin inhibitor (20 kDa) and α-lactalbumin (14 kDa).

2.2.3 Isoelectric Focusing and Staining.

Purified corneal ALDH preparations were subjected to isoelectric focusing according to the method of Pharmacia for precast polyacyrlamide gels over a pH range of 3-10 at 8 ^{0}C, with the voltage being increased from 0.25 kV to 1.3 kV after 1 hour and then increased to 1.6 kV after 2 hours. After isoelectric focusing, the gel was divided up into lanes and stained for either protein using Coomassie Brilliant Blue G-250, or ALDH activity using a staining mixture comprised of 50 mM phosphate buffer (pH 7.5), 0.25 mM NAD^{+}, 2.5 mM sodium pyruvate, 0.5 mM phenazine methosulfate, 3 mM methyl thiazolyl blue and one of the following aldehydes as substrate: acetaldehyde (30 mM), butylaldehyde (10 mM), hexanal (10 mM), benzaldehyde (30 mM), or propionaldehyde (10 mM).

2.2.4 Aldehyde Dehydrogenase Assay.

A quartz curvette containing 2.64 ml sodium phosphate buffer (50 mM, pH 7.5), 0.30 ml NAD^{+} (0.5 mM) and 10 µl hexanal (2 mM) was placed in a CARY UV-spectrophotometer and blanked at 340 nm. The reaction was initiated by the addition of 50 µl of experimental sample and the production of NADH was followed by the increase of absorbance at 340 nm. Control assays were also performed as outlined above, but in the absence of either coenzyme or the appropriate substrate, to ensure that ALDH activity was being measured. All enzyme assays were performed at 30°C and enzyme activity is expressed in µmol min^{-1} ml^{-1}.

2.2.5 Protein Purification 1a, Method and Results.

Bovine corneal ALDH was purified using the simple three step approach, as used by Riley (1993), this involved; extraction, acid-denaturation and a cation-exchange column. Corneas were obtained from the Feilding Freezing Works and stored at -80^{0}C until required. Corneal extracts were prepared by homogenization of the tissue using an Ultra-Turrax (Janke & Kunkel, Stausenbreisgan, Germany) homogenizer in 5 volumes of extraction buffer (50 mM triethanolamine-HCl, 0.1 mM EDTA, 0.1% (w/v) sodium deoxychlorate, and 1 mM dithiotheritol, pH 7.5). The homogenate was placed on ice for 25 minutes before being centrifuged (16000 rpm for 30 minutes at 4°C). The supernatant (sample A) was adjusted to pH 5.8 with dilute acetic acid and kept on ice for 25 minutes. The acid-denatured protein was then removed by centrifugation (16000 rpm for 15 minutes at 4°C) and the supernatant (sample B) applied to a 150 ml CM-Sepharose CL-6B chromatography column, which had been pre-equilibrated with equilibration buffer (20 mM MES, 0.1 mM EDTA, 20% glycerol, 1 mM dithiotheritol, pH 5.8). The sample was then loaded onto the column using extraction buffer (pH adjusted to pH 5.8) until the A_{280} of the eluting protein fell to the base-line. The protein was then eluted from the column by a change in pH using elution buffer 1 (100 mM MOPS, 0.1 mM EDTA, 20% glycerol, 1 mM dithiotheritol, pH 7.5) and the ALDH activity of the fractions was determined. See Figure 5 for a summary of the purification procedure.

ALDH eluted off the column as a mixture of two peaks (peaks I and II, A_{280} maxima at 96 and 112 minutes respectively) (Fig. 6). The occurrence of two peaks of ALDH activity differs from what has been reported previously (Abedinia *et al.*, 1990; Riley 1993). A possible reason for this anomaly could be that the sample was loaded onto the column using extraction instead of equilibration buffer, which could affect enzyme-column interactions and possibly lead to isozyme separation. Peak I eluted only 22 minutes after switching to elution buffer 1, indicating that the first active peak may have eluted more by a weak interaction and slow movement through the column, than by a change in pH or salt concentration. Protein in the second peak presumably has stronger column binding properties and requires a change in pH or salt concentration to disrupt the enzyme-column interactions.

Because the two peaks are overlapping, the active fractions from peaks I and II were pooled to give sample C, which gave a percentage recovery of approximately 62 % and a degree of purification of 2.4 (Table 3).

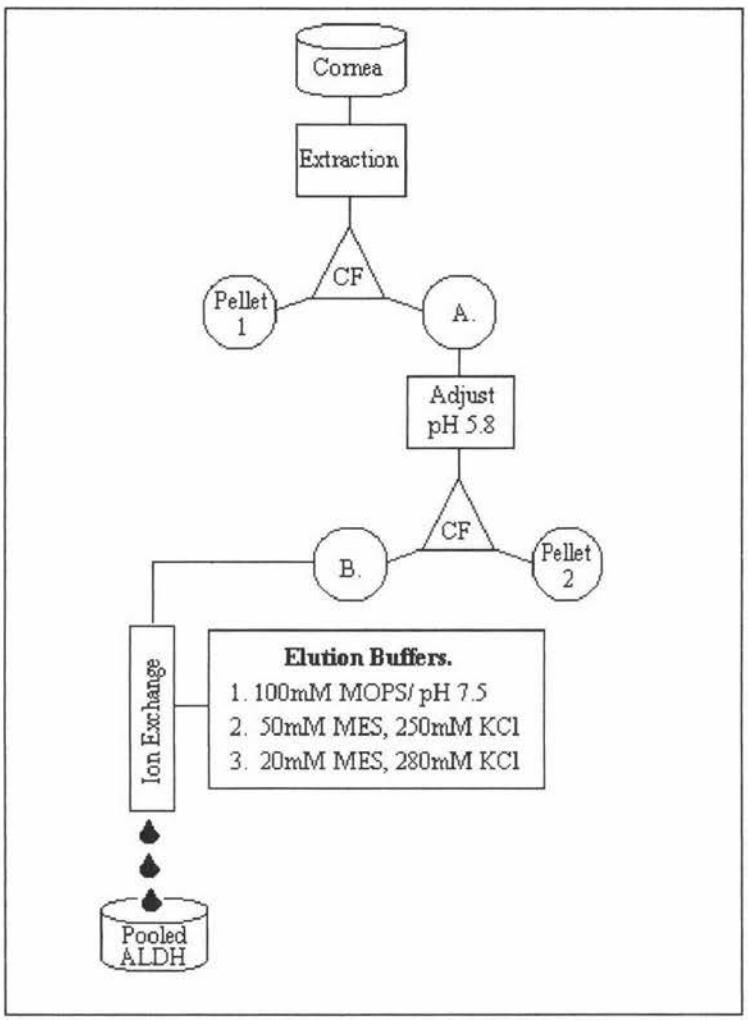

Figure 5. Procedure summary for protein purifications 1a, 1b and 1c.

All three purification procedures have the same first steps, that is extraction of soluble protein with extraction buffer, centrifugation (CF) followed by acid denaturation of the supernatant (sample A), another centrifugation to remove the acid denatured protein (pellet 2) and then application of the supernatant (sample B) to a pre-equilibrated CM-Sepharose CL-6B chromatography column. For purification 1a and 1c the column was equilibrated with equilibration buffer containing 20 mM MES, but for purification 1b the equilibration buffer contained 50 mM MES. Sample B from purification 1a was loaded onto the column with extraction buffer (pH adjusted to pH 5.8) and the ALDH eluted by a change in pH with elution buffer 1 (pH 7.5). Sample B from purification 1b was loaded onto the column with equilibration buffer (50 mM MES) and the ALDH eluted by a salt gradient generated using elution buffer 2 (50mM MES, 250 mM KCl). Sample B from purification 1c was loaded onto the column with equilibration buffer (20 mM MES) and the ALDH eluted by a salt gradient generated using elution buffer 3 (20mM MES, 280 mM KCl). The ALDH active fractions from the purifications were then pooled and frozen in small aliquots.

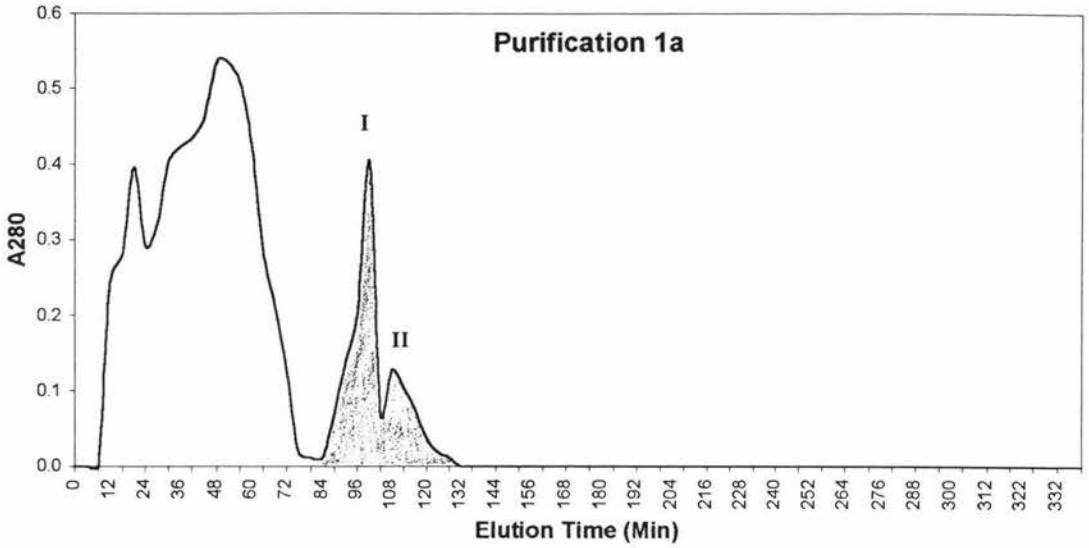

Figure 6. A_{280} versus elution time for the purification of bovine corneal ALDH using purification 1a.

Sample B was loaded onto a equilibrated CM-Sepharose CL-6B chromatography column using extraction buffer (pH adjusted to pH 5.8) at time 0 minutes. At 74 minutes protein elution was initiated by switching to elution buffer 1 (pH 7.5). Two overlapping peaks of ALDH activity were recovered (**I** and **II**, A_{280} maxima at 96 and 112 minutes respectively). Shaded area indicates ALDH activity. Flow rate: 2 ml/min

Table 3. Results of protein purification 1a.

Sample	Total Protein (mg)	Total Activity (μmol min^{-1})	Specific Activity (μmol min^{-1} mg^{-1})	% Recovery	Degree of Purification
A	658.92	27.30	0.0414	100.0	1.0
B	556.62	24.80	0.0446	90.8	1.1
C	170.62	16.88	0.0989	61.8	2.4

An indication of the purity of the enzyme is given by SDS polyacrylamide gel electrophoresis. The SDS gel for protein purification 1a (Fig. 7) showed that the pooled protein (lane 4) contained minute amounts of protein contaminant. A mobility plot gave a subunit molecular weight of approximately 54 kDa for the major band in this sample. The major protein in the crude extracts (lanes 2 and 3) corresponded in subunit molecular weight to that of the purified sample (C). This is consistent with the proposal that ALDH is the major soluble protein extracted from the cornea (Abedinia *et al.*, 1990). Moreover, the protein yield following purification indicates that bovine corneal ALDH represents 26 % of the total soluble corneal protein and approximately 1.0 % of the wet weight of bovine cornea.

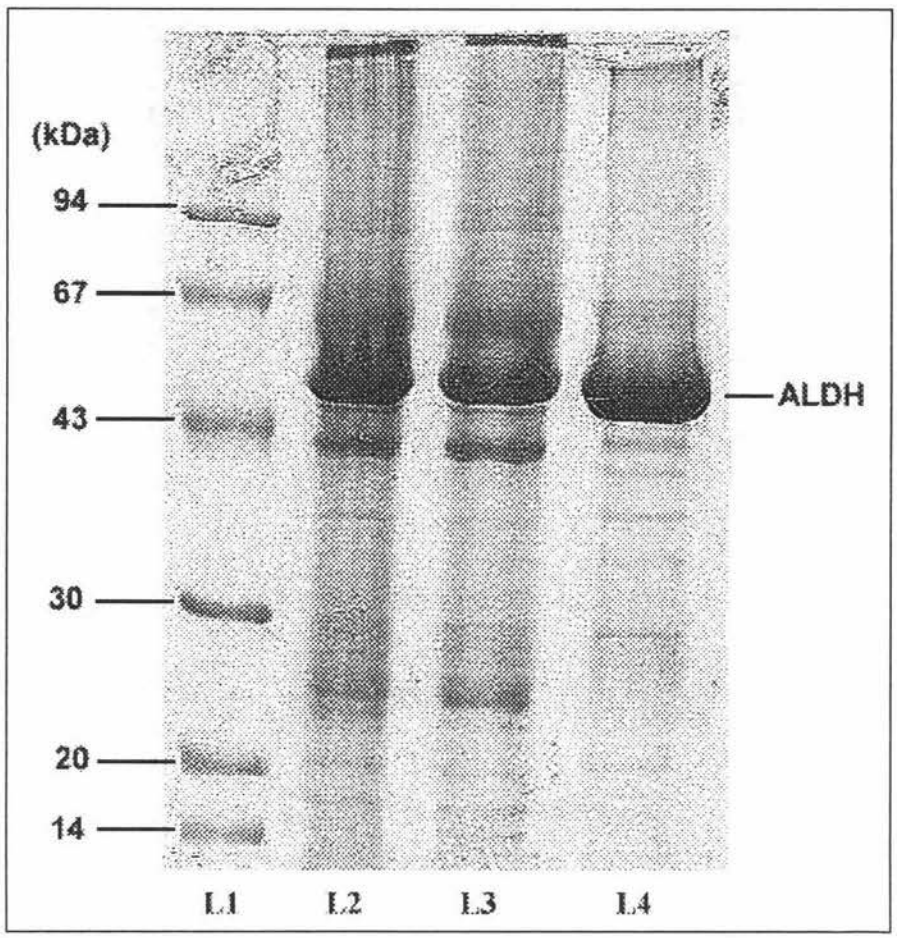

Figure 7. SDS-PAGE of purified and crude bovine corneal ALDH from purification 1a.

Lane 1, Standard low molecular weight markers. Lane 2, 10 µl crude extract of bovine cornea (sample A). Lane 3, 10 µl sample B. Lane 4, 10 µl purified bovine corneal ALDH (sample C). SDS gel electrophoresis results for the purified proteins from purification 1b and 1c were identical to that of sample C (Lane 4) of purification 1a shown above.

Isoelectric focusing (Fig. 8) of the purified protein (sample C) showed eight distinct bands (1-8) when stained with Coomassie blue. The positions of the bands corresponded to isoelectric points of 6.82, 6.69, 6.49, 6.38, 6.27, 6.10, 5.99 and 5.67 respectively. Of the eight bands only bands 2-5 exhibited ALDH activity (pI's 6.69, 6.49, 6.38 and 6.27 respectively) when stained for activity using different aldehyde substrates. The major band corresponded to band 4 (pI of 6.38) for both the protein and activity stain.

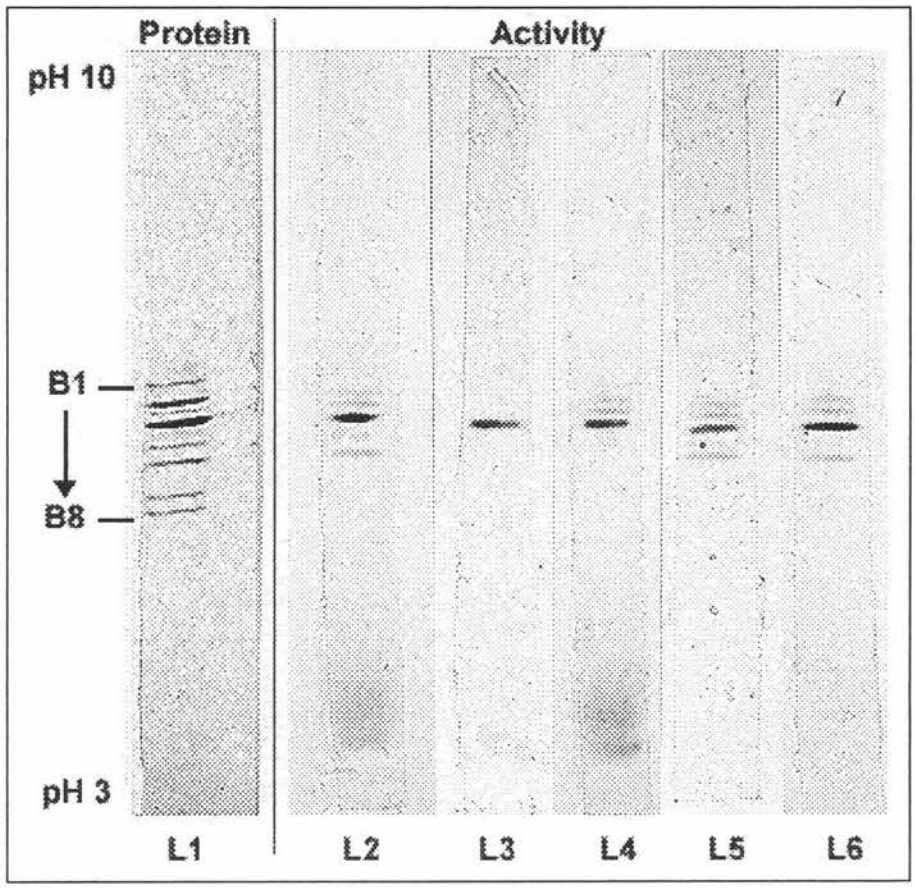

Figure 8. Isoelectric focusing and staining of purified bovine corneal ALDH.

10 µl of purified bovine corneal ALDH (sample C) was applied to lanes 1-6. After IEF the lanes were separated and stained for either protein (Lane 1) using Coomassie Blue, or ALDH activity (lanes 2-6) using; acetaldehyde (Lane 2), butylaldehyde (Lane 3), hexanal (Lane 4), benzaldehyde (Lane 5) and propionaldehyde (Lane 6).

2.2.6 Protein Purification 1b, Method and Results.

Purification of bovine corneal ALDH using Purification 1a resulted in the elution of two overlapping active ALDH peaks from a cation exchange column. Both peaks, however, gave the same subunit molecular weight of 54 kDa and contained minute amounts of protein contaminant. Protein purification 1b was designed to give greater separation of these two active peaks by eluting ALDH from the cation exchange column using a salt gradient instead of a change in pH.

The protein extraction and acid denaturation steps of protein purification 1b are the same as those of purification 1a; only the cation exchange column chromatography step is different. The MES concentration of the equilibration buffer (50 mM MES,

0.1 mM EDTA, 20 % glycerol, 1 mM dithiotheritol, pH 5.8) is increased from 20 mM to 50 mM and the supernatant after acid denaturation (sample B) is loaded onto the CM-Sepharose CL-6B chromatography column with equilibration buffer (50 mM MES) instead of the extraction buffer (pH 5.8) used in purification 1a. The protein is eluted from the column using a salt gradient generated using elution buffer 2 (50 mM MES, 250 mM KCl, 0.1 mM EDTA, 20 % glycerol, 1 mM dithiotheritol, pH 5.8). See Figure 5 for a summary of the purification procedure.

Separation of the peaks did occur, with two peaks of ALDH activity (peaks I and II) being eluted from the column (A_{280} maxima at 80 and 232 minutes respectively) (Fig. 9). A comparison of the elution times of Peak I from purification 1a and 1b (A_{280} maxima 80 and 96 minutes respectively) shows that the peak I from purification 1b elutes earlier. This may be due to the higher ionic strength of the equilibration buffer (50 mM MES). At lower ionic strengths, such as that used in purification 1a, competition for charged groups on the ion exchange column is less and substances are bound more strongly. Increasing the ionic strength increases the competition and reduces the interaction between the ALDH and the ion exchange column, resulting in its early elution. However, the ionic strength of the equilibration buffer is not sufficient to cause total ALDH elution; only after application of a salt gradient does all the enzyme elute. Peak II (A_{280} maxima at 232 minutes) is eluted off the column at an approximate ionic strength of 170 mM (Fig. 9).

Samples from both the ALDH active peaks (I and II) were analysed by SDS polyacryamide gel electrophoresis and were found to possess the same migration pattern as each other and that of purified ALDH from purification 1a, i.e. the purified protein has a subunit molecular weight of approximately 54 kDa and contains minute amounts of protein contaminant. The active fractions from peaks I and II were pooled to give sample C, with an ALDH percentage recovery of approximately 40 % and a degree of purification of 1.2 (Table 4). The percentage recovery and degree of purification were lower than expected with activity being lost either before or during the ion exchange chromatography step.

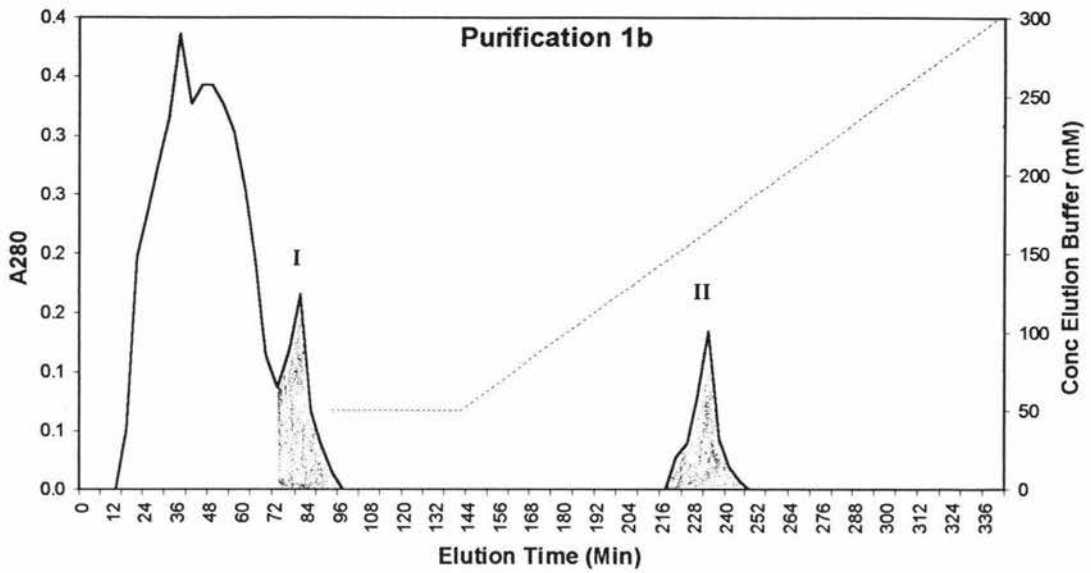

Figure 9. A_{280} versus elution time for the purification of bovine corneal ALDH using purification 1b.

Sample B was loaded onto a equilibrated CM-Sepharose CL-6B chromatography column using equilibration buffer (50 mM MES) at time 0 minutes. At 96 minutes the salt gradient (dashed line) was initiated. For 50 min, equilibration buffer (50 mM MES) was applied before the ionic strength was linearly increased from 50 mM to 300 mM over a 200 minute period using elution buffer 2 (pH 5.8). Two peaks of ALDH activity were recovered (peaks **I** and **II**, A_{280} maxima at 80 and 232 minutes respectively). Shaded area indicates ALDH activity. Flow rate: 2 ml/min

Table 4. Results of protein purification 1b.

Sample	Total Protein (mg)	Total Activity (μmol min^{-1})	Specific Activity (μmol min^{-1} mg^{-1})	% Recovery	Degree of Purification
A	293.63	6.41	0.0218	100.0	1.0
B	172.76	5.56	0.0321	86.8	1.5
C	94.71	2.54	0.0268	39.6	1.2

2.2.7 Protein Purification 1c, Method and Results.

Protein purification 1b allowed greater separation of the two overlapping peaks of ALDH activity but resulted in a low percentage recovery and degree of purification. Further modifications to the purification procedure were required to improve both enzyme recovery and purity, as well as investigating the possible causes of the observed cation-exchange elution patterns.

The protein extraction and acid denaturation steps of protein purification 1c are the same as those in purification 1a, while the cation exchange column chromatography step is similar to that of purification 1b, except the MES concentration of the equilibration and elution buffer has been changed back to 20 mM MES, as it was thought that the higher MES concentration may have led to the early elution of peak I before the application of the salt gradient. The supernatant after acid denaturation (sample B) was loaded onto the CM-Sepharose CL-6B chromatography column with equilibration buffer (20 mM MES) until the A_{280} of the eluting protein fell to the base-line. The protein was then eluted from the column using a salt gradient generated using elution buffer 3 (20 mM MES, 280 mM KCl, 0.1 mM EDTA, 20% glycerol, 1 mM dithiotheritol, pH 5.8). See Figure 5 for a summary of the purification procedure.

Two peaks of ALDH activity were eluted from the column (peaks I and II, A_{280} maxima at 104 and 320 minutes respectively) (Fig.10). Peak I eluted from the column after sample loading but before application of the salt gradient, i.e. at a ionic strength of only 20 mM, using the equilibration buffer as the loading buffer. Even though the samples for purification 1a and 1c are loaded onto the column with different buffers, peak I from both purifications, eluted at approximately the same time. However, in purification 1b, peak I eluted earlier, but this could be because of the higher MES concentration of the equilibration buffer. Elution of the first peak may be affected more by the ionic strength of the equilibration buffer than by the buffer used to load the enzyme onto the column. Peak II is eluted from the column at an approximate ionic strength of 300 mM. This is approximately twice the ionic strength used to elute peak II in purification 1b.

Table 5 shows a summary of the results of purification 1c. Peak I exhibits almost double the specific activity and degree of purification of peak II, but the total amounts of protein in the two peaks are similar. SDS-PAGE Analysis of the protein from the two peaks (I and II) demonstrated that they were identical to each other and to purified ALDH from purifications 1a and 1b (gel not shown), i.e. the purified protein has a major band with a subunit molecular weight of approximately 54 kDa and contains minute amounts of protein contaminant. The

active fractions from peaks I and II were pooled to give sample C, with an ALDH percentage recovery of approximately 45 % and a degree of purification of 2.9 (Table 5).

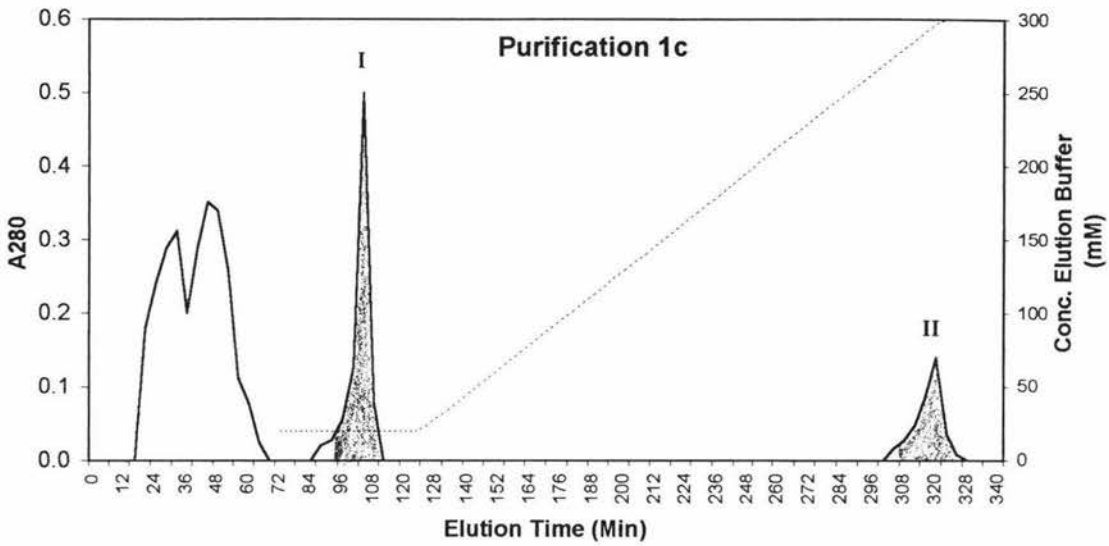

Figure 10. A_{280} versus elution time for the purification of bovine corneal ALDH using purification 1c.

Sample B was loaded onto a equilibrated CM-Sepharose CL-6B chromatography column using equilibration buffer (20 mM MES) at time 0 minutes. At 72 minutes the salt gradient (dashed line) was initiated. For 50 min, equilibration buffer was applied before the ionic strength was linearly increased from 20 mM to 300 mM over a 200 minute period using elution buffer 3 (pH 5.8). Two peaks of ALDH activity were recovered (**I** and **II**, A_{280} maxima at 104 and 320 minutes respectively). Shaded area indicates ALDH activity. Flow rate: 2 ml/min

Table 5. Results of protein purification 1c.

Sample	Total Protein (mg)	Total Activity (μmol min^{-1})	Specific Activity (μmol min^{-1} mg^{-1})	% Recovery	Degree of Purification
A	274.35	8.96	0.0327	100.0	1
B	195.03	7.67	0.0393	85.6	1.2
Peak I	19.55	2.48	0.1270	27.7	3.9
Peak II	24.3	1.46	0.0602	16.3	1.8
C	42.35	3.98	0.0940	44.5	2.9

2.2.8 Protein Purification 2, Method and Results.

Purifications 1b and 1c demonstrated that application of a salt gradient results in two separate peaks of ALDH activity from a cation exchange column, though the first active peak is eluted from the cation exchange column before the application of the salt gradient. In purification 2, a salt fractionation step was introduced before cation exchange chromatography so that most of the unwanted protein could be removed, in case column overloading may be causing the observed elution patterns.

Corneal extracts used in purification 2 were prepared in the same manner as outlined in purification 1a. After centrifugation, the protein was separated by salt fractionation using ammonium sulphate. Ammonium sulphate was added to the supernatant to give a 40 % saturation of this salt and the precipitated protein (pellet 1) removed by centrifugation (16000 rpm for 20 minutes at 4°C). A second ammonium sulphate fractionation step was performed by increasing the salt concentration to 60 % saturation and the precipitated protein (pellet 2) removed by centrifugation (16000 rpm for 20 minutes at 4°C). A third and final ammonium sulphate fractionation step was achieved by increasing the salt concentration to 80 % saturation, followed by removal of the precipitated protein (pellet 3) by centrifugation (16000 rpm for 20 minutes at 4°C). All the pellets from the centrifugations were dissolved in 5 ml of extraction buffer (pH 7.5) and, along with the supernatants, assayed for ALDH activity and analysed by SDS-PAGE (Fig. 11). Most of the ALDH protein (54 kDa) from the first salt fractionation step was located within the supernatant (lane 3) but pellet 1 contained a small amount of ALDH and other protein contaminants (lane 4). The second fractionation step resulted in a large fraction of the ALDH precipitating out in pellet 2 (lane 6) but a small amount stayed in solution (lane 5). The final salt fractionation step resulted in all the remaining protein precipitating out of solution (lane 8), as indicated by the absence of protein in the supernatant (lane 7). Pellet 2 from the second salt fractionation step exhibited the most ALDH activity and was used for further purification steps.

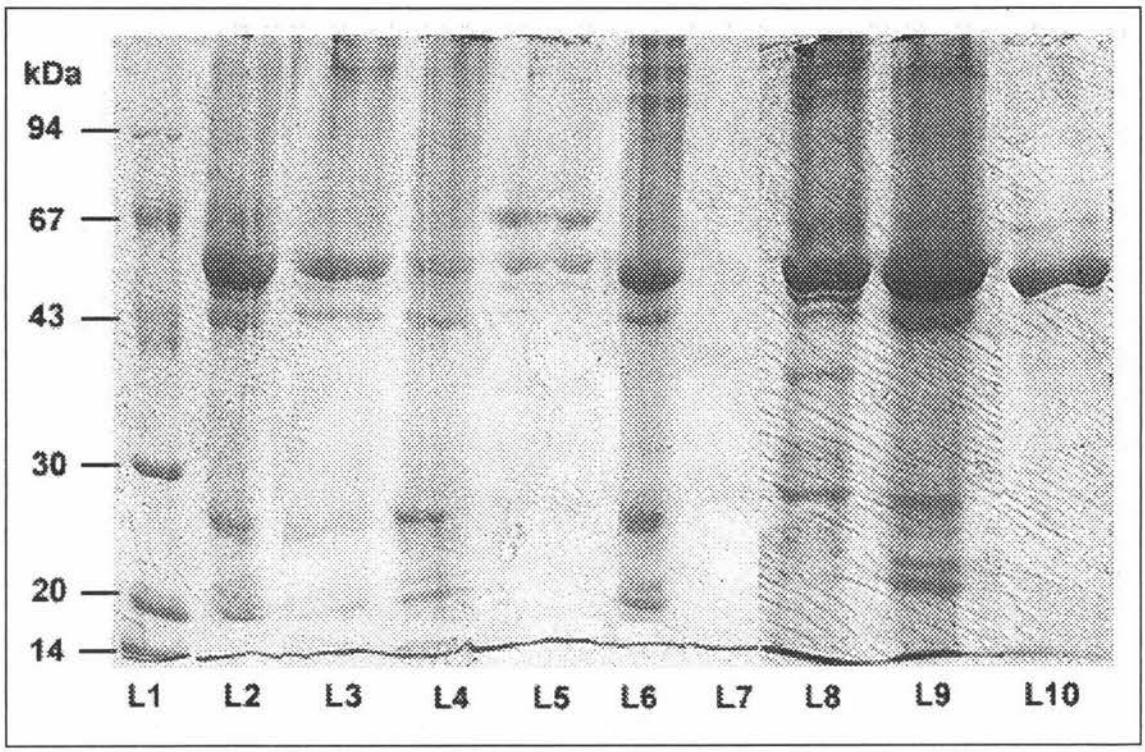

Figure 11. SDS-PAGE of purified and crude bovine corneal ALDH from purification 2.

Lane 1, Standard low molecular weight markers. Lane 2, 5 µl crude extract of bovine cornea (sample A). Lane 3, 5 µl sample super 1. Lane 4, 5 µl sample pellet 1. Lane 5, 10 µl sample super 2. Lane 6, 2 µl sample pellet 2. Lane 7, 10 µl sample super 3. Lane 8, 5 µl sample pellet 3. Lane 9, 5 µl sample B. Lane 10, 10 µl purified bovine corneal ALDH (sample C).

The dissolved pellet 2 was dialysed overnight against 1000 ml extraction buffer (pH 7.5). The sample was then adjusted to pH 5.8 and allowed to stand on ice for 25 minutes before being centrifuged (16000 rpm for 15 minutes at 4°C). The supernatant (sample B) was loaded onto a pre-equilibrated CM-Sepharose CL-6B chromatography column using extraction buffer (pH adjusted to pH 5.8) until the A_{280} of the eluting protein fell to the base-line. Initially a salt gradient generated using elution buffer 3 (20 mM MES, 280 mM KCl, 0.1 mM EDTA, 20 % glycerol, 1 mM dithiotheritol, pH 5.8) was applied to the column in the hope of eluting the enzyme but no fractions with ALDH activity were eluted. The elution buffer was then switched to elution buffer 1 (100 mM MOPS, 0.1 mM EDTA, 20 % glycerol, 1 mM dithiotheritol, pH 7.5) which resulted in one peak of ALDH activity being eluted from the column by a change in pH (A_{280} maximum at 252 minutes) (Fig. 12). See Figure 13 for a summary of the purification procedure.

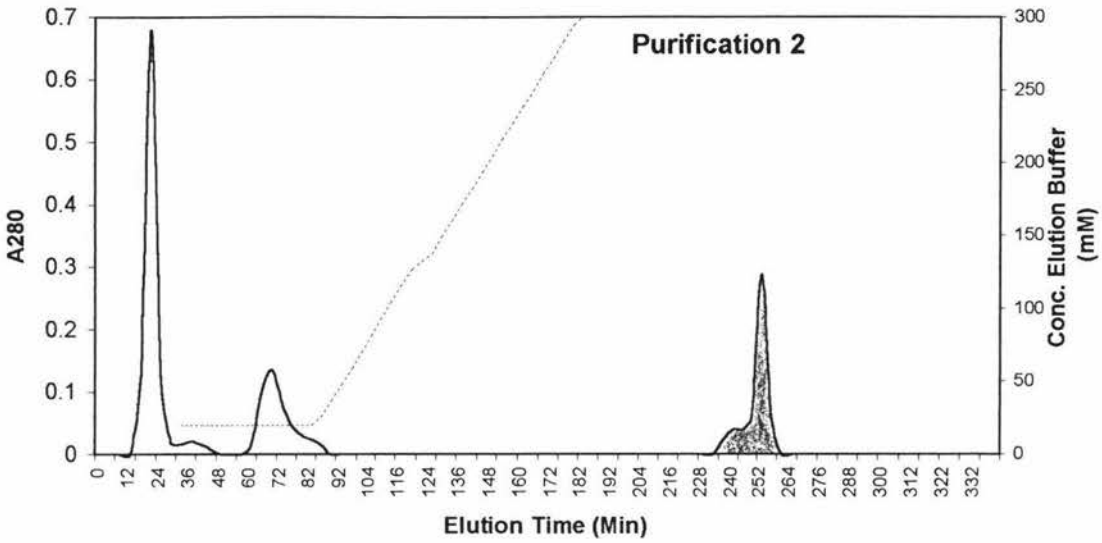

Figure 12. A_{280} versus elution time for the purification of bovine corneal ALDH using purification 2.

Sample B was loaded onto a equilibrated CM-Sepharose CL-6B chromatography column with extraction buffer (pH adjusted to pH 5.8) at time 0 minutes. At 32 minutes the salt gradient (dashed line) was initiated. For 50 min, equilibration buffer (20 mM MES) was applied before the ionic strength was linearly increased from 20 mM to 300 mM over a 100 minute period using elution buffer 3 (pH 5.8). At 204 minutes elution by salt gradient was stopped and switched to elution by a change in pH using elution buffer 1 (pH 7.5). One peak of ALDH activity was recovered (A_{280} maximum at 252 minutes). Shaded area indicates ALDH activity. Flow rate: 2 ml/min

Table 6. Results of protein purification 2.

Sample	Total Protein (mg)	Total Activity (μmol min^{-1})	Specific Activity (μmol min^{-1} mg^{-1})	% Recovery	Degree of Purification
A	350.40	15.13	0.0432	100.0	1.0
P1	12.55	0.53	0.0422	3.5	1.0
S1	187.62	11.78	0.0628	77.8	1.5
P2	78.10	4.88	0.0624	32.0	1.5
S2	104.98	2.16	0.0206	14.3	0.5
P3	35.00	1.25	0.0357	8.3	0.8
S3	31.90	0.00	0.0000	0.0	0.0
B	59.33	4.72	0.0795	31.2	1.8
C	38.40	3.85	0.1003	25.5	2.3

The ALDH active fractions were pooled to give sample C, with an ALDH percentage recovery of approximately 26% and a degree of purification of 2.3 (Table 6). When examined by SDS-PAGE, the purified pooled protein consisted of a major band with a subunit molecular weight of approximately 54 kDa but contained minute amounts of protein contaminant (Fig.11, Lane 10).

The introduction of a salt fractionation before the cation exchange column resulted in the successful removal of some of the protein contaminants, thereby reducing the amount of protein applied to the column. However, modifications to the percent salt saturation would be required if the ALDH protein was to be obtained within one step.

After cation exchange only one peak of ALDH activity was eluted, but this elution occurred due to a change in pH rather than by application of a salt gradient. A possible explanation for this observation could be in the choice of dialysis buffer and/or the ionic strength of the sample, since both can effect the net charge of the protein and hence its column binding properties. Extraction buffer (pH 7.5) was used as the dialysis buffer, but the buffer reservoir was not changed over the 12 hour period. This may have increased the column binding properties of the protein so that the application of the salt gradient had little effect; only when the pH was changed did the enzyme elute from the column. In future the dissolved pellet should be dialysed against equilibration buffer (pH 5.8) and with frequent buffer changes.

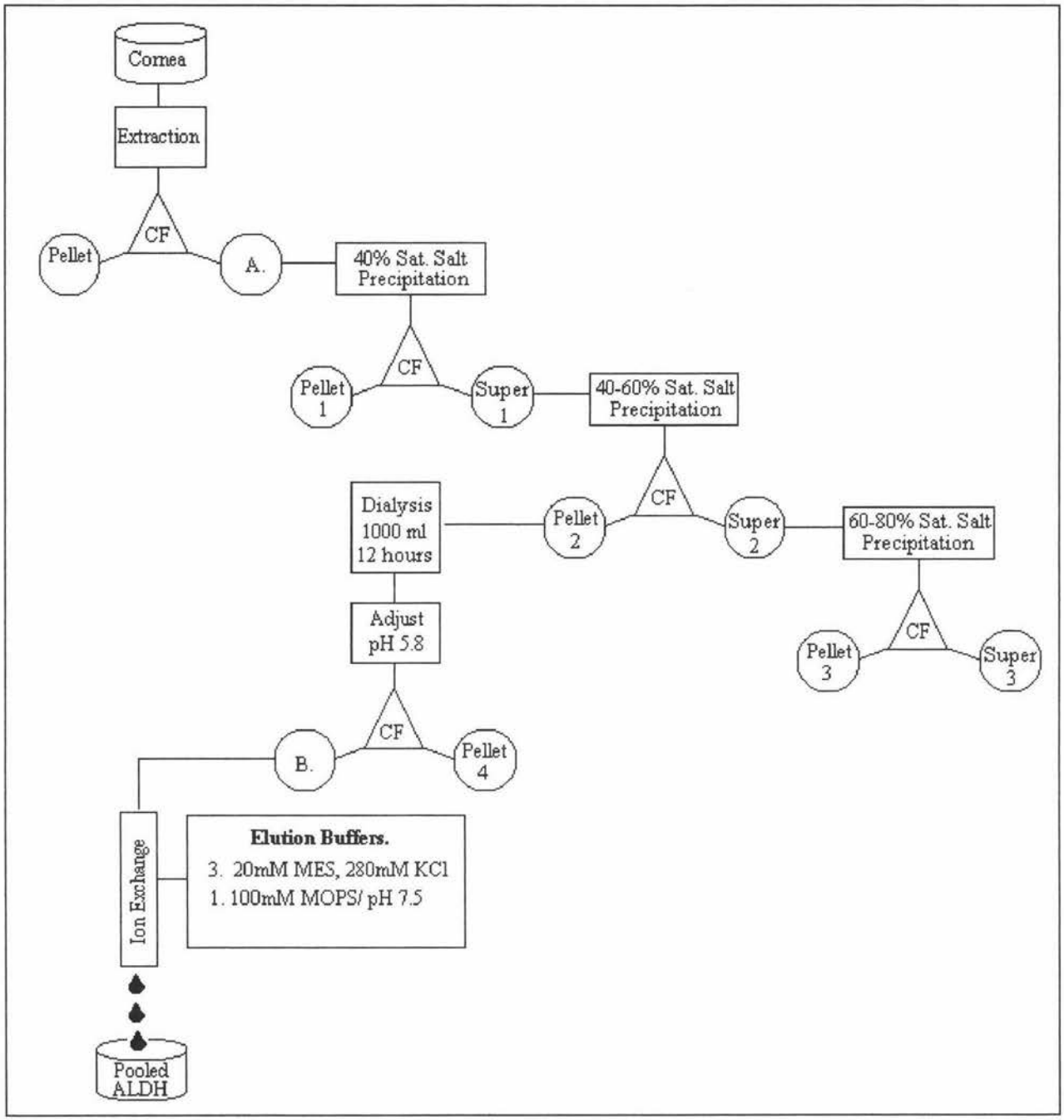

Figure 13. Procedure summary for protein purification 2.

Preliminary purification of ALDH involved the extraction of soluble protein with extraction buffer, followed by centrifugation (CF). The protein was then separated by stepwise salt fractionation using ammonium sulphate. Ammonium sulphate was added to the supernatant (sample A) to give a 40 % saturation of this salt and the precipitated protein (pellet 1) removed by centrifugation. A second ammonium sulphate fractionation step was then carried out by increasing the salt concentration to 60 % saturation and removing the precipitated protein (pellet 2) by centrifugation. A third and final ammonium sulphate fractionation step was achieved by increasing the salt concentration to 80 % saturation, followed by removal of the precipitated protein (pellet 3) by centrifugation. The pellets (1-3) were then dissolved separately in 5 ml of extraction buffer (pH 7.5) and along with the supernatants (super 1-3) assayed for ALDH activity. Pellet 2 contained the most ALDH activity and was dialysed overnight against 1000 ml extraction buffer (pH 7.5). Following acid denaturation and centrifugation, the sample was loaded onto a pre-equilibrated CM-Sepharose CL-6B chromatography column using extraction buffer (pH adjusted to pH 5.8). Initially a salt gradient generated using elution buffer 3 was applied to the column but no active ALDH fractions were collected, only when the pH was changed with elution buffer 1 did ALDH elute. The ALDH active fractions were then pooled and frozen in small aliquots.

2.2.9 Protein Purification 3, Methods and Results.

Examination of samples from the previous purifications 1a, b, c and 2 by SDS-PAGE revealed that the purified protein contained a number of extra bands or protein contaminants. Protease activity may be causing some degradation of the protein, which may have resulted in these extra bands. To attempt to resolve this problem a 'cocktail' of protease inhibitors such as EDTA and phenylmethylsulfonyl fluoride (PMSF) was employed to combat proteolytic degradation. But first PMSF had to be tested to see whether it had any detrimental affects on ALDH activity.

Effect of Phenylmethylsulfonyl Fluoride on ALDH Activity

A stock solution of 100 mM PMSF was made using acetone because of the low solubility and instability of PMSF in aqueous solutions. 6 µl of stock PMSF (final concentration 200 µM) was added to a quartz curvette containing 2.634 ml sodium phosphate buffer (50 mM, pH 7.5), 0.300 ml NAD^+ (0.5 mM) and 10 µl hexanal (2 mM). The curvette was placed in a CARY UV-spectrophotometer and blanked at 340 nm. The reaction was initiated by the addition of 50 µl of purified ALDH and the production of NADH was followed at 340 nm over a 3 minute period. A control reaction containing all reactants except PMSF was also carried out.

Pre-incubation experiments were performed, whereby 6 µl of stock PMSF was mixed with 2.634 ml sodium phosphate buffer (50 mM, pH 7.5) and 50 µl enzyme. The enzyme-PMSF solution was then left for 10, 15 and 120 minutes, after which 10 µl hexanal (2 mM) and 0.3 ml NAD^+ (0.5 mM) were added and the rate of NADH production was followed at 340 nm over a 3 minute period.

The addition of PMSF has little effect on the long term activity of the ALDH enzyme, but initial addition of PMSF causes a slight decrease in activity. As the preincubation time increases so does activity (Table 7). These results were as expected, because of the instability of PMSF in aqueous solutions (half-life of only 55 minutes at pH 7.5 and 25°C (James, 1978)) and demonstrate the importance of adding fresh PMSF at different stages of purification.

Table 7. Effect of phenylmethylsulfonyl fluoride on ALDH activity

Sample	Concentration PMSF (μM)	Pre-incubation Time (min)	Activity (μmol min^{-1} ml^{-1})
1	-----	0	0.0718
2	200	0	0.0505
3	200	10	0.0571
4	200	15	0.0602
5	200	120	0.0689

As PMSF had little effect on the long term activity of the ALDH enzyme, it was included in the extraction buffers for protein purifications 3a and 3b. Both methods use the same pool of corneas and only after protein extraction, acid denaturation and centrifugation do the purification procedures differ.

Corneal Extraction

Corneal extraction was carried out in a similar manner as outlined in purification 1a, except that 200 μM of PMSF was added to the extraction buffer. The homogenate was placed on ice for 25 minutes before being centrifuged (16000 rpm for 30 minutes at 4°C). The pH of the supernatant (sample A) was adjusted to pH 5.8 with dilute acetic acid and then kept on ice for 25 minutes. The acid-denatured protein was removed by centrifugation (16000 rpm for 15 minutes at 4°C) before being split into two volumes, B1 and B2, to be used in purifications 3a and 3b respectively. See Figure 14 for a summary of the purification procedure.

Protein Purification 3a

Protein purification 3a is almost identical to Procedure 1a, except for the inclusion of PMSF to the purification protocol and sample B1 being loaded onto a pre-equilibrated CM-Sepharose CL-6B chromatography column with equilibration buffer (20 mM MES, pH 5.8) not extraction buffer (pH 5.8). The protein was then eluted from the column by a change in pH using elution buffer 1 (pH 7.5). See Figure 14 for a summary of the purification procedure.

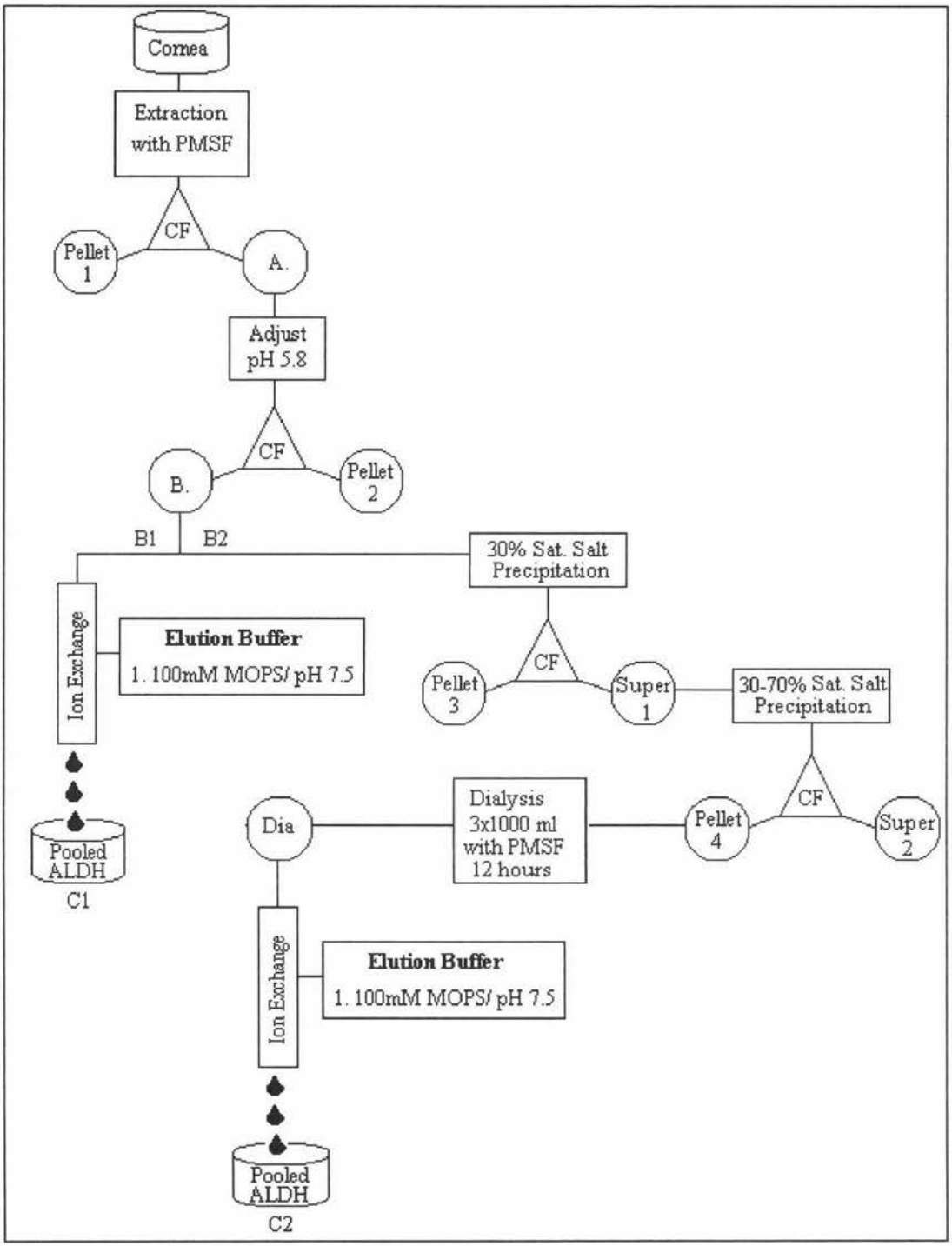

Figure 14. Procedure summary for protein purifications 3a and 3b.

Initial purification of ALDH involved protein extraction with buffer containing PMSF, followed by centrifugation (CF) and then acid denaturation. The supernatant (sample B) was split into two volumes, B1 and B2 and used in purification 3a and 3b respectively. Purification 3a involved sample B1 being loaded onto a pre-equilibrated CM-Sepharose CL-6B chromatography column with equilibration buffer (20 mM MES, pH 5.8). The protein was eluted from the column by a change in pH with elution buffer 1 (pH 7.5). The ALDH active fractions were pooled (sample C1) and frozen in small aliquots. Purification 3b involved sample B2 being subjected to a stepwise salt fractionation using ammonium sulphate. Ammonium sulphate was added to give a 30 % saturation of this salt and the precipitated protein (pellet 3) removed by centrifugation. A second ammonium sulphate fractionation was carried out by increasing the salt concentration to 70 % saturation and the precipitated protein (pellet 4) removed by centrifugation. Both pellets 3 and 4 were dissolved in 10 ml of equilibration buffer and along with the supernatants (Super 1 and 2) assayed for ALDH activity. Pellet 4 contained the most ALDH activity and was dialysed overnight against 3 x 1000 ml equilibration buffer (20 mM MES, pH 5.8) containing PMSF. Following dialysis a further 10 ml of equilibration buffer was added to the sample. The sample (Dia) was then loaded onto a pre-equilibrated CM-Sepharose CL-6B chromatography column with equilibration buffer. The protein was eluted from the column by a change in pH with elution buffer 1 (pH 7.5). The ALDH active fractions were pooled (C2) and then frozen in small aliquots.

Only one peak of ALDH activity was obtained (A_{280} maximum at 180 minutes) (Fig. 15). The active fractions were pooled to give sample C1 with an ALDH percentage recovery of approximately 52 % and a degree of purification of 6.9 (Table 8). When examined by SDS-PAGE, the purified pooled protein has a major band with a subunit molecular weight of approximately 54 kDa and contains minute amounts of protein contaminant (Fig.16, lane 4).

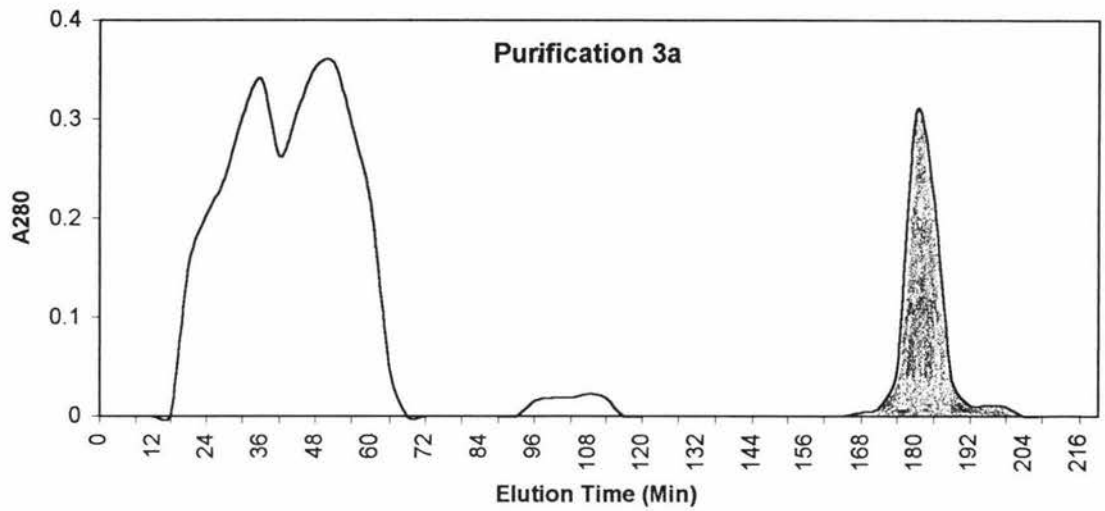

Figure 15. A_{280} versus elution time for the purification of bovine corneal ALDH using purification 3a.

Sample B1 was loaded onto a equilibrated CM-Sepharose CL-6B chromatography column using equilibration buffer (pH 5.8) at time 0 minutes. At 88 minutes protein elution was initiated by changing the pH using elution buffer 1 (pH 7.5). One peak of ALDH activity was recovered (A_{280} maximum at 180 minutes). Shaded area indicates ALDH activity. Flow rate: 2 ml/min

Table 8. Results of protein purification 3a.

Sample	Total Protein (mg)	Total Activity (μmol min^{-1})	Specific Activity (μmol min^{-1} mg^{-1})	% Recovery	Degree of Purification
A	561.60	11.95	0.0213	100.0	1.0
B	298.91	11.03	0.0369	92.3	1.7
C1	21.00	3.10	0.1476	51.8*	6.9

* % recovery values were multiplied by 2 as sample B was split into two equal volumes (B1 and B2)

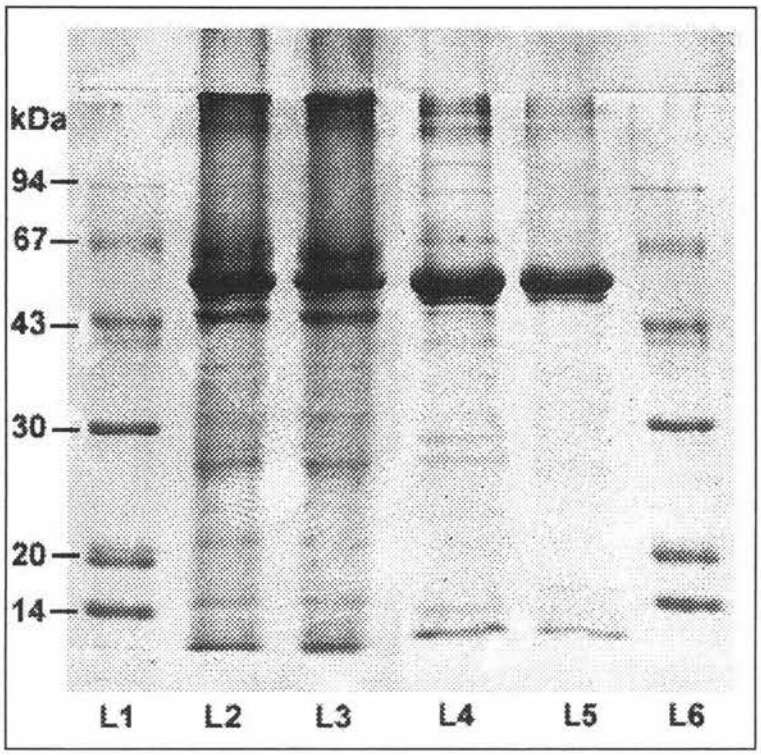

Figure 16. SDS-PAGE of purified and crude bovine corneal ALDH from purification 3a.

Lane 1 and 6, Standard low molecular weight markers. Lane 2, 5 µl crude extract of bovine cornea (sample A). Lane 3, 5 µl sample B1. Lane 4, 10 µl purified bovine corneal ALDH (sample C1). Lane 5, 10 µl purified bovine corneal ALDH from purification 3b (sample C2).

Protein Purification 3b

Protein purification 3b is similar to purification 2, in that they both have a salt fractionation step, dialysis and cation exchange chromatography. However, in purification 3b, PMSF has been added to the extraction buffer and the salt fractionation steps modified.

Following protein extraction and acid denaturation, sample B2 was further purified by salt fractionation using ammonium sulphate. Ammonium sulphate was added to give a 30 % saturation of this salt and the precipitated protein (pellet 3) removed by centrifugation (16000 rpm for 20 minutes at 4°C). A second ammonium sulphate fractionation was carried out by increasing the salt concentration to 70 % saturation and then removing the precipitated protein (pellet 4) by centrifugation (16000 rpm for 20 minutes at 4°C). Both pellets 3 and 4 were dissolved in 10 ml of equilibration buffer (20 mM MES, pH 5.8) and, along with the supernatants (super1 and 2), assayed for ALDH activity and analysed by SDS-PAGE (Fig. 17).

Most of the ALDH protein (54 kDa) from the first salt fractionation step was located within the supernatant (super 1, lane 5) but pellet 3 (lane 4) contained a small amount of ALDH and other protein contaminants. The second salt fractionation step resulted in almost all of the ALDH precipitating out in pellet 4 (lane 6), as indicated by the absence of protein in the supernatant (super 2, lane 7) and was subsequently used for further purification steps. Pellet 4 was dialysed overnight against 3 x 1000 ml equilibration buffer (20 mM MES, pH 5.8) containing 200 μM PMSF. After dialysis, an additional 10 ml of equilibration buffer was added to the sample before being loaded onto a pre-equilibrated CM-Sepharose CL-6B chromatography column with equilibration buffer (20 mM MES, pH 5.8). The protein was then eluted from the column by a change in pH using elution buffer 1 (pH 7.5). See Figure 14 for a summary of the purification procedure.

Only one peak of ALDH activity was obtained (A_{280} maximum at 124 minutes) (Fig. 18). The active fractions were pooled to give sample C2 with an ALDH percentage recovery of approximately 56 % and a degree of purification of 8.1 (Table 9). SDS-PAGE of the purified pooled protein (Fig. 17, lane 9) showed a single homogeneous protein with an approximate subunit molecular weight of 54 kDa.

Table 9. Results of protein purification 3b.

Sample	Total Protein (mg)	Total Activity ($\mu M\ min^{-1}$)	Specific Activity ($\mu M\ min^{-1} mg^{-1}$)	% Recovery	Degree of Purification
A	561.60	11.95	0.0213	100.0	1.0
B	298.91	11.03	0.0369	92.3	1.7
Pellet 3	7.35	0.16	0.0216	2.6*	1.0
Super 1	58.46	5.11	0.0873	85.4*	2.0
Pellet 4	30.40	3.73	0.1222	62.4*	5.7
Super 2	4.56	0.00	0.0000	0.0	0.0
Dia	29.44	3.61	0.1250	60.4*	5.8
C2	19.38	3.35	0.1730	56.2*	8.1

* % recovery values were multiplied by 2 as sample B was split into two equal volumes (B1 and B2)

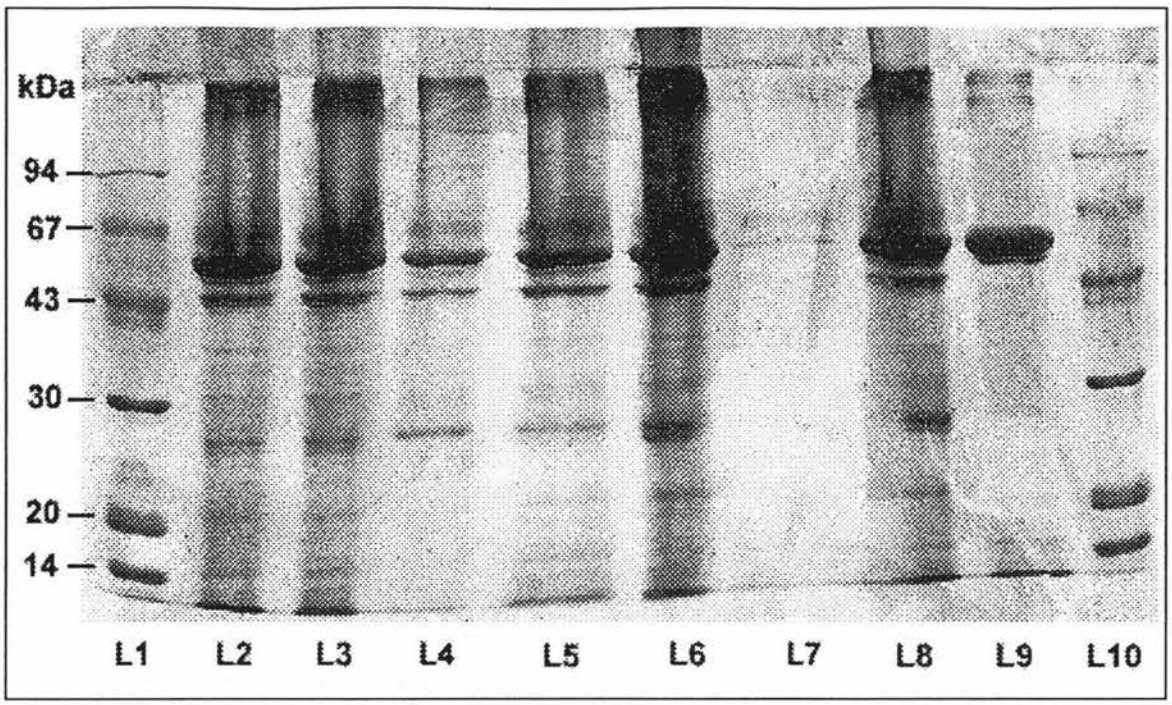

Figure 17. SDS-PAGE of purified and crude bovine corneal ALDH from purification 3b.

Lane 1 and 10, Standard low molecular weight markers. Lane 2, 5 µl Crude extract of bovine cornea (sample A). Lane 3, 5 µl sample B. Lane 4, 5 µl pellet 3 Lane 5, 5 µl super 1. Lane 6, 5 µl pellet 4. Lane 7, 10 µl super 2. Lane 8, 5 µl sample Dia. Lane 9, 5 µl purified bovine corneal ALDH (sample C2).

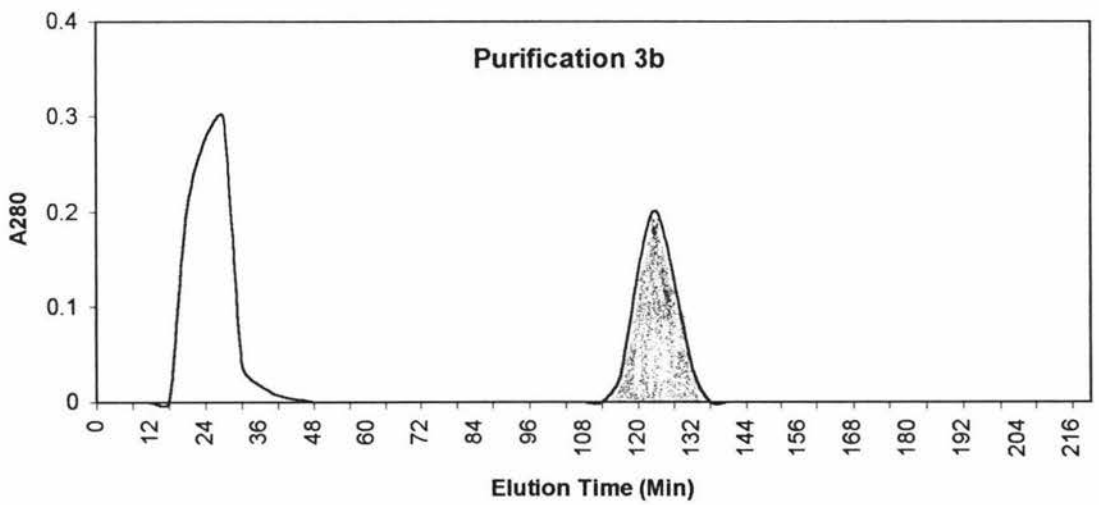

Figure 18. A_{280} versus elution time for the purification of Bovine corneal ALDH using purification 3b.

Sample (B2) was loaded onto a equilibrated CM-Sepharose CL-6B chromatography column with equilibration buffer (20 mM MES, pH 5.8) at time 0 minutes. At 64 minutes protein elution was initiated by changing the pH with elution buffer 1 (pH 7.5). One peak of ALDH activity was recovered (A_{280} maximum at 124 minutes). Shaded area indicates ALDH activity. Flow rate: 2 ml/min.

2.3 Discussion.

In purification 1a, bovine corneal aldehyde dehydrogenase was purified by a procedure based on that of previous investigators (Abedinia *et al*, 1990; Riley, 1993). This method resulted in the elution of two overlapping peaks of ALDH activity from a cation exchange column by changing the pH of the column. The method of elution was changed to a salt gradient in purifications 1b and 1c, allowing the separation of the two active ALDH peaks but it was found that the first peak of ALDH activity eluted before application of the salt gradient. It was originally thought that the occurrence of these two peaks may have resulted by loading the protein onto the column with extraction buffer (pH 5.8) instead of equilibrium buffer. However, results have shown that elution of the first active peak is affected more by the ionic strength of the equilibrium buffer than the buffer used to load the enzyme onto the column. The second active peak was eluted from the column using a salt gradient.

The purification protocol was modified in purification 2 to include a salt fractionation step, involving three salt precipitations (0-40%, 40-60% and 60-80%). The addition of this step allowed a large proportion of the contaminating protein to be removed before application to the cation exchange column, in case column overloading was causing the observed elution patterns. The ALDH protein could be found in all three pellets from the salt fractionation steps but the majority was located in the second step. Dialysis against extraction buffer (pH 7.5) without frequent buffer changes may have led to the non-elution of active ALDH from the column by application of a salt gradient. Only when the pH of the column was changed did elution of ALDH protein occur. The introduction of the salt fractionation step resulted in less protein being applied to the cation exchange column. Approximately 80 % of the extracted protein from purification 1c was applied to the column but in purification 2 this was reduced to about 20 %. The number of peaks of ALDH activity eluted also parallels the reduction in applied protein, from two peaks for purification 1a, 1b and 1c to only one peak for purification 2, 3a and 3b. This supports the proposal that the occurrence of two peaks could be a result of column overloading.

The addition of a protease inhibitor in purification 3a, which is similar to purification 1a, resulted in the elution of only one peak of ALDH activity from the cation exchange column. Purification 3a did not contain a salt fractionation step but it still resulted in only one active ALDH peak. However, it must be noted that sample B was divided equally into B1 and B2 and used in purifications 3a and 3b respectively, which lowered the amount of extracted protein applied to the column. It is more likely that the lower column loading is responsible for only one peak of ALDH activity being eluted, rather than the inclusion of PMSF to the purification protocol. Though the addition of PMSF to the purification buffers was effective in improving the degree of purification and the specific activity of the extracted corneal ALDH enzyme.

Protein recovery and purity was further improved by combining the addition of PMSF to the buffers with a preliminary protein purification step by salt fractionation, followed by dialysis and then cation exchange column chromatography.

In purification 3b the salt fractionation was changed to two steps, a 0-30 % and a 30-70 % salt saturation. This allowed almost all of the ALDH protein to be precipitated in the 30-70 % pellet. The dialysis buffer was changed from extraction buffer (pH 7.5) as in purification 2, to equilibration buffer (pH 5.8), with more frequent changes to the buffer reservoir. As a result of the salt fractionation step, the amount of protein loaded onto the cation exchange column was significantly reduced to approximately 5 % of the total extracted corneal protein, and ALDH was eluted from the column in one peak.

As purifications 3a and 3b use protein extracted from the same pool of corneas, direct comparisons can be made between the 2 procedures. Both methods have PMSF included in their buffers and result in only one peak of ALDH activity. However the addition of a salt fractionation and dialysis step in purification 3b resulted in a higher specific activity, percentage recovery and degree of purification relative to any of the purification procedures. Table 10 summarises the purification results from the various purifications.

Table 10. Summary of the results from the protein purification procedures

Purification Procedure	Sample	Specific Activity (μmol min^{-1} mg^{-1})	% Recovery	Degree of Purification
1a	C	0.0989	61.8	2.4
1b	C	0.0268	39.6	1.2
1c	C	0.0940	44.5	2.9
2	C	0.1003	25.5	2.3
3a	C1	0.1476	51.8	6.9
3b	C2	0.1730	56.2	8.1

SDS gel electrophoresis of the protein obtained from the different purifications 1a, 1b, 1c, 2 and 3a showed that the purified protein was not homogeneous, as there were protein contaminants, but the major protein band had an approximate subunit molecular weight of 54 kDa. However, purification 3b yielded a homogeneous purified protein with an approximate subunit molecular weight of 54 kDa.

The molecular weight forms and IEF patterns for corneal ALDH vary depending on the species from which the enzyme was obtained (Table 11). These differences may be accounted for by divergent evolution from a common ancestor, or by the "gene sharing phenomenon" both of which would allow the corneal ALDHs to have differing biological functions within the mammalian cornea.

From Table 11, it can be seen that the reported molecular weight of bovine corneal ALDH differs between studies. In this thesis the subunit molecular weight was found to be approximately 54 kDa but other studies have reported it between 52 and 65 kDa and the dimeric molecular weight between 88 and 130 kDa.. These differences are most likely due to experimental errors, The general consensus is that the approximate molecular weight of bovine corneal ALDH is 54 kDa. However, biochemical studies of human and bovine corneal ALDH performed by Gondhowiardjo *et al.* (1992a) have shown that the enzymatically active form is only located in the "dimeric" 88 kDa form and the dissociation of the active form into its 54 kDa subunit was related to the thermolability of the enzyme. Pretreatment of corneal ALDH at various temperatures showed that as the temperature increased, the 88 kDa species shifted towards the monomeric 54 kDa form with an associated

decrease in enzymatic activity. The apparent dimeric molecular weight of 88 kDa is lower than would be expected for subunits with molecular weights of 54 kDa. A possible reason for this difference could be that dimerisation of the monomers leads to conformational changes resulting in an apparent smaller complex than would be expected in SDS-PAGE analysis. Regardless of the cause, of all the oligomeric molecular weight forms observed for bovine corneal ALDH (88, 110, 154, and 210 kDa), only the 88 kDa possessed ALDH activity (Gondhowiardjo *et al.*, 1992a).

Gondhowiardjo *et al.* (1992a) also showed that the oligomeric forms of ALDH were not susceptible to dithiotheritol (DTT), a disulphide bridge reducing agent, suggesting that disulphide bonds are not involved in the oligomerisation of corneal ALDH (Gondhowiardjo *et al.*, 1992a). This agrees with the information obtained from the crystal structure of ALDH (see section 1.11), where association of the two ALDH subunits is mainly through intra-molecular hydrogen bonds between the bridging domain of one subunit and the catalytic domain of the other.

Table 11. Molecular weight forms and IEF patterns for mammalian corneal ALDH

Mammalian ALDH	Subunit Molecular Weight (kDa)	Dimeric Molecular Weight (kDa)	IEF Bands (pI)	Reference
Human Stomach	55			*a*
Mouse Stomach	65	141		*b*
Tumor-associated	51	110		*c*
Rat Corneal	51			*c*
Mouse Corneal	59	110	major pI 6.8	*d*
Human Corneal	54	88	5 bands 6.5 - 7.2	*e*
Baboon Corneal	63		3 - 4 bands	*f*
Bovine Corneal	65	130		*g*
Bovine Corneal	52		5 bands	*h*
Bovine Corneal	54	88	4 bands 6.5 - 7.0	*e*
Bovine Corneal	54		6.60, 6.78, 6.80, 6.90	*i*
Bovine Corneal	54		6.16, 6.22, 6.32, 6.41	*j*
Bovine Corneal	54		6.27, 6.38, 6.49, 6.69	*this work*

a, Wang *et al.*, (1990). ***b***, Algar & Holmes, (1989). ***c***, Evces & Lindahl, (1989). ***d***, Downes & Holmes, (1993). ***e***, Gondhowiardjo *et al.*, (1991, 1992a, b). ***f***, Algar *et al.*, (1990). ***g***, Abedinia *et al.*, (1990). ***h***, Riley, (1993). ***i***, Alexander *et al.*, (1981). ***j***, Konishi & Mimura, (1992).

The dimeric molecular weight was not determined in this thesis, but has been reported in other studies by Sephadex gel filtration. In future experiments, the dimeric and monomeric molecular weight could be determined by ultracentrifugation. This would allow for the characterisation and accurate molecular weight determination of the monomeric and oligomeric forms of corneal ALDH.

In this research four active ALDH bands with different isoelectric points were observed upon isoelectric focusing: 6.27, 6.38, 6.49, and 6.69. These values differ from those reported by Alexander *et al.* (1981), but are similar to those determined by Konishi & Mimura (1992). The differences in isoelectric focusing patterns could be related to post-translational events due to different sugar attachments. It was originally thought that class 3 ALDH was not a glycoprotein (Holt & Kinoshita, 1973; Alexander *et al.*, 1981), but it has been shown that there are at least two potential N-glycosylation sites based on the amino acid sequence of tumor-associated ALDH (Jones *et al*, 1988). Lectin binding studies performed by Gondhowiardjo *et al.* (1992b) indicate that corneal ALDH is a glycoprotein containing N-glycosylation sites and differences in glycosylation may have influenced the IEF migration patterns. Another example of a protein exhibiting this type of microheterogeneity as revealed by IEF is α_1-antitrypsin, which shows eight different isoforms on IEF, which can be differentiated by their oligosaccharide side chains, the degree of sialylation and post-translational cleavage of N-terminal amino acids (Karn *et al.*, 1973; Vaughn *et al.*, 1982; Jeppsson & Johansson, 1985).

In future studies, purified bovine corneal ALDH could be subjected to preparative isoelectric focusing to allow for the separation and recovery of the different isoforms, which in turn could be used in future kinetic investigations.

Section 3. Ligand Binding Studies.

3.1 Introduction and Ligand Binding Theory

Aldehyde dehydrogenase catalyses the oxidation of an aldehyde to its corresponding acid using NAD^+ as a cofactor, which in turn is reduced to NADH. The difference between the ultraviolet absorption spectrum of free NADH and that of enzyme-bound allows the enzyme-cofactor complex formation on NADH binding to be monitored. In this way, the number of coenzyme binding sites per molecule and the NADH dissociation constant can be determined.

Any species which binds to an enzyme or protein is a ligand, regardless of whether or not it is a substrate and undergoes a subsequent reaction. Consider the binding of a ligand (in this case NADH) to a protein, the dissociation constant, K_d , is defined by the equation;

$$K_d = \frac{[F]\,[U]}{[B]} \qquad [1]$$

where [F] is the molar concentration of free binding sites

[U] is the molar concentration of unbound ligand (NADH)

[B] is the molar concentration of bound ligand (or ligand-occupied binding sites)

Since the total binding site [S] concentration is equal to the sum of the free and ligand-occupied binding sites, i.e.,

$$[S] = [F] + [B]$$

then equation [1] can be rewritten as;

$$K_d = \frac{([S]-[B]).[U]}{[B]} \qquad [2]$$

For an enzyme molecule with *n* binding sites the total concentration of binding sites [S] can be written as;

$$[S] = n \,.\, [E]$$

where [E] is the total enzyme concentration and the total ligand concentration

If n molecules of enzyme each have, on average, one site occupied this is equivalent to one molecule of enzyme having n sites occupied. R, the fractional saturation, is defined as the proportion of the total number of binding sites that are occupied or as the fraction of completely liganded enzyme concentration.

$$R = \frac{[B]}{[S]} = \frac{[D]}{[E]}$$

where [D] is the concentration of liganded enzyme and n.[D] is equivalent to [B] the concentration of bound ligand.

As often only the enzyme concentration [E] is known the switch in nomenclature from binding site concentration [S] to enzyme concentration is made to determine the number of ligand binding sites per molecule. In this case equation [2] can be written as

$$K_d = \frac{([E]-[D])([L]- n.[D])}{[D]} \qquad \textbf{[3]}$$

Where [L] is equal to the sum of the bound and unbound ligand

i.e., $[L] = [B] + [U] = n.[D] + [U]$

Substituting R.[E] for [D] gives;

$$K_d = \frac{([E]- R[E])([L]- nR[E])}{R[E]} \qquad \textbf{[4]}$$

$$K_d = [L]\left(\frac{1}{R} - 1\right) - n[E](1 - R)$$

$$K_d \frac{1}{1 - R} = \frac{[L]}{R} - n[E]$$

Rearrangement of this equation gives

$$\frac{1}{1 - R} = \frac{[L]}{K_d.R} - \frac{n.[E]}{K_d} \qquad \textbf{[5]}$$

R can be determined experimentally by the difference in UV absorption between a solution of buffer and the enzyme solution on the addition of ligand, in this case NADH.

$$R = \frac{\Delta Abs}{A_{Max}} \qquad [6]$$

where ΔAbs is the absorbance difference between the buffer and the enzyme solution after the addition of an aliquot of NADH. A_{Max} is the absorbance value at which addition of NADH causes no further absorbance change.

Using equation [5] a Scatchard plot (Scatchard, 1949) can be obtained by plotting $1/(1 - R)$ against $[L] / R$ to allow for the determination of n, the number of binding sites per enzyme molecule and the dissociation constant K_d. Linearity of the plot indicates that all the ligand binding sites are identical and act independently of one another.

If more than one ligand-binding site is present on the protein, there is the possibility of interaction or cooperativity between the binding sites during the binding process. Positive cooperativity is said to occur when the binding of one molecule of a ligand increases the affinity of the protein for other molecules of the same or different ligand. Negative cooperativity occurs when the binding of one molecule of a ligand decreases the affinity of the protein for other molecules of the same or different ligand.

In the case of a dimeric protein (M_2) having two identical binding sites for a ligand (L):

$M_2 + L \rightleftharpoons M_2L$ with an apparent binding constant K_{b1}

$M_2L + L \rightleftharpoons M_2L_2$ with an apparent binding constant K_{b2}

The fractional saturation,

$$R = \frac{\text{number of protomers per unit volume which have bound ligand}}{\text{total number of protomers per unit volume}}$$

$$= \frac{[ML]}{[ML + M]}$$

However, as there are no isolated protomers, it is necessary to express R in terms of the various protein-ligand complexes present;

M_2, which consists of 2 protomers, both unbound.

M_2L, which consists of 1 bound and 1 unbound protomer.

M_2L_2, which consists of 2 protomers, both bound.

$$\therefore \quad R = \frac{[ML]}{[ML + M]} = \frac{[M_2L] + 2[M_2L_2]}{2([M_2] + [M_2L] + [M_2L_2])}$$

$$K_{b1} = \frac{[M_2L]}{[M_2][L]} \quad \text{so } [M_2L] = K_{b1}[M_2][L]$$

$$K_{b2} = \frac{[M_2L_2]}{[M_2L][L]} \quad \text{so } [M_2L_2] = K_{b2}[M_2L][L] = K_{b1}K_{b2}[M_2][L]^2$$

Substituting for $[M_2L]$ and $[M_2L_2]$ in the expression of R gives the Adair equation for the binding of a ligand to a dimeric protein.

$$R = \frac{K_{b1}[L] + 2K_{b1}K_{b2}[L]^2}{2(1 + K_{b1}[L] + K_{b1}K_{b2}[L]^2)} \qquad [7]$$

Where there is no interaction between the binding sites the plot of R against [L] will be hyperbolic (Fig. 19(a)) and the binding constants for the binding of ligand to a dimeric protein would be; $K_{b1} = 2K_b$ and $K_{b2} = \frac{1}{2} K_b$. Hence $K_{b1} = 4 K_{b2}$.

Where there is positive homotropic cooperativity between the binding sites. The second step of the binding process will be faster than it is in the situation where there is no interaction between the binding sites, i.e. where $K_{b1} = 4 K_{b2}$. Hence for positive homotropic cooperativity, $K_{b1} < 4 K_{b2}$ and according to the Adair equation, this relationship would result in a sigmodial plot of R against [L] (Fig. 19(a)). The sigmodial character of the curve is more marked the greater the degree of cooperativity.

Negative cooperativity results in the second step of the binding process being slower than it would be if there were no interaction between the binding sites. Hence for negative homotropic cooperativity, $K_{b1} > 4 K_{b2}$. In this case the plot of R against [L] is neither sigmodial nor a true rectangular hyperbola (Fig. 19(a)).

A qualitative indicator of the type of cooperativity between the binding sites can be obtained from the plots of R (Fractional Saturation), against [L] (Fig. 19(a)), 1/R against 1/[S] (Lineweaver-Burk plot, Fig. 19(b)), plot of R against R/[L] (Eadie-Hofstee plot, Fig. 19(c)) and [L]/R against [L] (Hanes plot, Fig. 19(d)). Linearity of the Lineweaver-Burk, Eadie-Hofstee and Hanes plot indicates the absence of cooperativity between the binding sites, i.e. that all the ligand binding sites are identical and non-interacting and function independently of one another, while non-linear plots is an indication that a cooperative relationship occurs which may be either positive or negative. In general, Eadie-Hofstee and Hanes plots are better qualitative indicators for the type of cooperativity than Lineweaver-Burk plots as departures from linearity are more obvious.

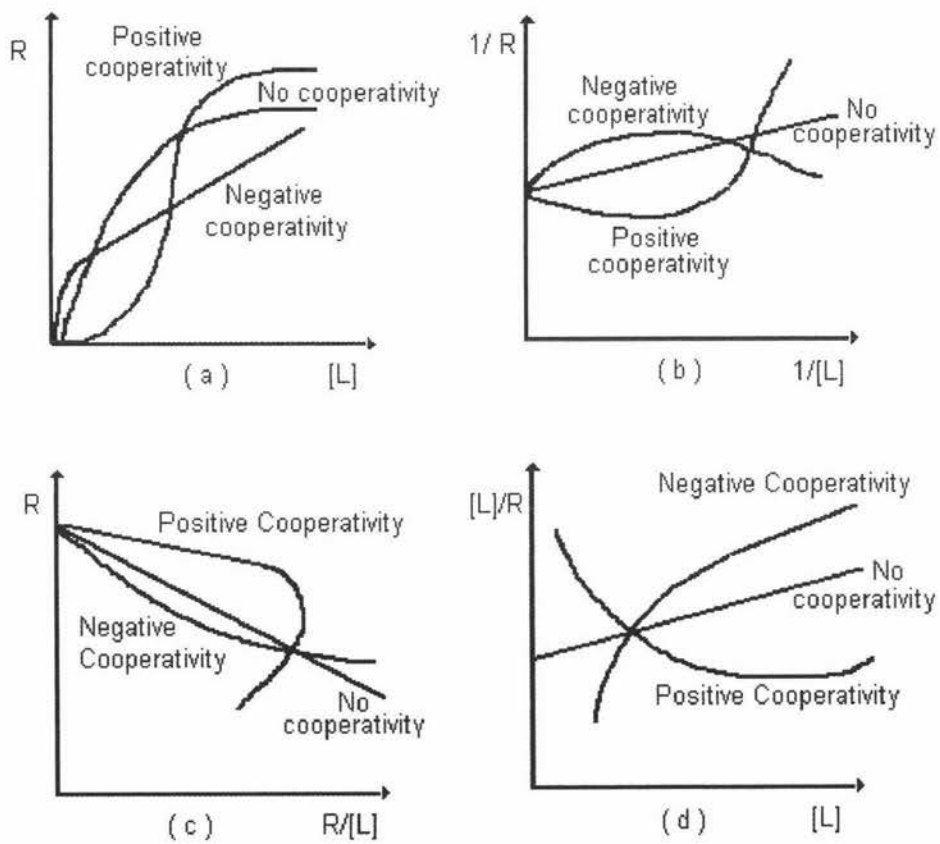

Figure 19. Plots showing the effects of cooperativity

(a) Plot of R (Fractional Saturation), against [L]. This is the titration curve.
(b) Plot of 1/R against 1/[S] (Lineweaver-Burk plot).
(c) Plot of R against R/[L] (Eadie-Hofstee plot).
(d) Plot of [L]/R against [L] (Hanes plot).

3.2.0 Methods

3.2.1 Ultraviolet Difference Spectrum between Enzyme-bound and Free NADH

The ultraviolet (UV) spectra of the following solutions were obtained using the Hewlett Packard 8452A diode array spectrophotometer.

1. Free NADH; 1.0 ml (0.2 mM stock) NADH + 1.0 ml sodium phosphate buffer (50 mM, pH 7.5).
2. Purified ALDH; 1.0 ml Purified ALDH + 1.0 ml sodium phosphate buffer (50 mM, pH 7.5).
3. NADH and Purified ALDH; 1.0 ml Purified ALDH + 1.0 ml (0.2 mM stock) NADH

Using the spectra obtained from the solutions described above, the UV spectrum for NADH bound to the enzyme was calculated by subtracting the sum of the spectra of solutions 1 and 2 from the spectrum of solution 3.

3.2.2 NADH Titration

The absorbance difference at 348 nm between enzyme-bound and free NADH allows the enzyme-NADH complex formation to be monitored after each subsequent addition of NADH. NADH is added to the enzyme until the relative absorbance between the two solutions at 348 nm ceases to change. The total concentration of NADH added to this point is equal to the concentration of NADH binding sites. Using this value the number of NADH binding sites per ALDH dimer can be calculated.

The stock NADH solution (0.2 mM or 0.4 mM) was made up using 50 mM sodium phosphate buffer, pH 7.5 which had been filtered and degassed before use. Prior to use in the NADH titrations the protein concentration of purified ALDH was determined by the Bradford method (see section 2.2.1) and the mg/ml values converted to μM dimers by dividing by the molecular weight of the enzyme dimer, 88 000 Da (refer section 2.3). The enzyme concentration was assumed to be constant throughout the titration; however the total NADH concentration was

corrected after each aliquot addition to account for the changes in volume. The NADH titrations were carried out using one of the following methods on a CARY spectrophotometer under differing conditions.

Method 1.

Two quartz curvettes were set up, one containing 2.00 ml sodium phosphate buffer (50 mM, pH 7.5) and the other containing 1.00 ml purified ALDH + 1.00 ml sodium phosphate buffer (50 mM, pH 7.5). As there is a decrease in absorbance on NADH binding the curvette containing the purified ALDH was placed in the reference cell holder and the curvette containing the buffer in the sample cell holder in order to obtain positive absorbance values. 10.0 µl aliquots of stock NADH were added to each curvette until the absorbance readings between aliquots ceased to change. The changes in absorbance values between the buffer and enzyme solutions were then converted to fractional saturation values (R) using equation [6] and fitted using equation [5] and the Enzfitter program to obtain values for n and K_d.

Method 2.

10.0 µl aliquots of stock NADH were added to a single quartz curvette containing 2.00 ml sodium phosphate buffer (50 mM, pH 7.5) and the absorbance values after each aliquot addition were measured at 348 nm. The titration was then repeated using another curvette containing 1.00 ml purified ALDH + 1.00 ml sodium phosphate buffer (50mM, pH 7.5) to which 10.0 µl aliquots of stock NADH were added and the absorbance values were measured at 348 nm. For each addition of NADH, the absorbance difference (ΔAbs) between the buffer and the enzyme solution was calculated using equation [8]

$$\Delta Abs = A_{BUF} - A_{ENZ} \qquad \textbf{[8]}$$

where A_{BUF} is the absorbance reading from the curvette containing buffer

A_{ENZ} is the absorbance reading from the curvette containing enzyme

The ΔAbs values were then converted to fractional saturation values (R) using equation [6] and fitted using equation [5] and the Enzfitter program to obtain values for n and K_d.

3.3.0 Results

3.3.1 Ultraviolet Difference Spectrum between Enzyme-bound and Free NADH

Free NADH has an ultraviolet absorption maximum at 340 nm. A difference spectrum between enzyme-bound and free NADH, calculated as described in section 3.2.1, showed a maximum absorbance change at 348 nm. This absorbance change was very small, about 0.015 absorbance units (Fig. 20). This absorbance difference at 348 nm allows the titration of enzyme with NADH to be monitored.

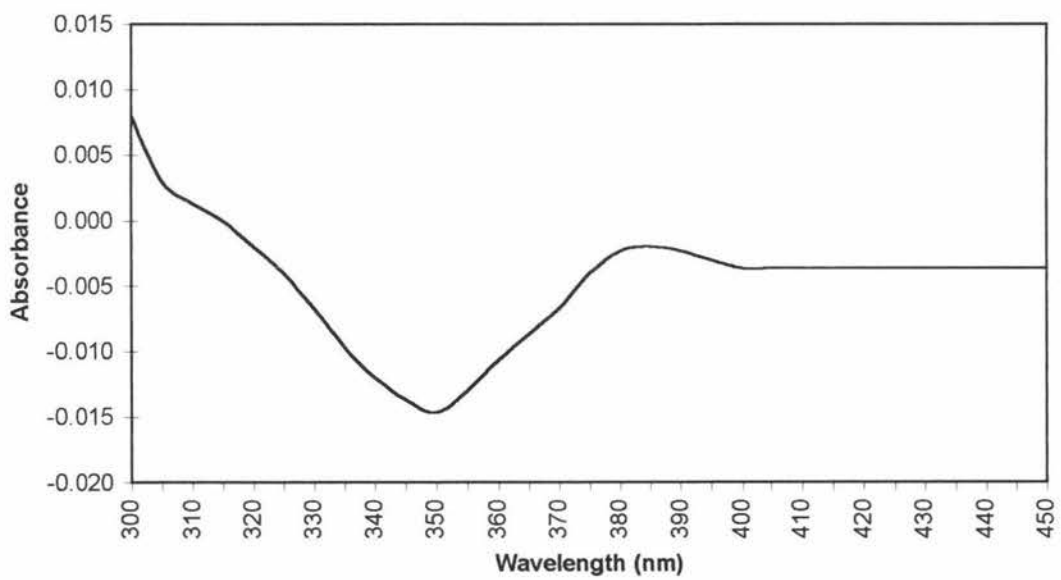

Figure 20. Difference spectrum between enzyme-bound and free NADH

The maximum absorbance change is seen at 348 nm and is very small, about 0.015 absorbance units.

3.3.2 NADH Titrations

A series of NADH titration experiments which utilised the difference in absorbance of NADH on binding to the enzyme were carried out to determine the number of NADH binding sites per dimer under differing conditions.

All titrations reported in this thesis were carried out using enzyme purified from protein purification 3b. Though initially the titrations were performed using enzyme from purification 1a the results were rejected as the NADH stock solution was made using distilled water instead of buffer causing the NADH to rapidly decompose.

Titration 1 (Fig. 21) and titration 2 (Fig. 22) were performed using method 1 and method 2 respectively. Both titrations used dialysed enzyme and 0.2 mM NADH stock solution. By performing the NADH titrations using two different methods the sensitivity and reliability of the methods could be compared.

For titration 1, the plot of absorbance at 348 nm against total NADH concentration (Fig. 21(a)) gave a hyperbolic curve as did the plot of R, the fractional saturation values against total NADH concentration (Fig. 21(b)). The final stage of the titration should have been horizontal to give an absolute A_{max} value, but instead there is a slight linear slope of $3.8 \pm 0.4 \times 10^{-4}$ μM^{-1} which may affect the fractional saturation values after each NADH addition. This slope is probably the result of experimental error, which would seem likely considering the very low absorbencies being measured. To test if the sloping A_{max} has any significant affect on the titration results new R values were calculated based on the A_{max} slope. For each NADH concentration an individual A_{max} value was found using equation [9]

$$\text{new } A_{max} = m[\text{NADH}] + c \qquad \textbf{[9]}$$

where m is the slope of final stage of the titration ($m = 3.8 \pm 0.4 \times 10^{-4}$ μM^{-1})

[NADH] is the total concentration of NADH after each aliquot addition

c is the intercept on the absorbance axis when [NADH] = 0 ($c = 0.04395$ a.u.)

These new A_{max} values were then used to recalculate the R values using equation [6] after each NADH addition.

Without taking the sloping A_{max} into account the Scatchard plot (Fig. 21(c)) constructed from the titration data gave an apparent NADH dissociation constant (K_d) of 1.57 ± 0.14 μM and a binding site concentration of 18.83 ± 0.19 μM, which corresponds to 2.01 ± 0.02 NADH binding sites per dimer for an enzyme solution of concentration 9.375 μM dimers. Taking the sloping A_{max} into account a Scatchard plot (Graph not shown) using the recalculated fractional saturation values gave an apparent NADH dissociation constant of 1.39 ± 0.15 μM and a binding site concentration of 17.96 ± 0.37 μM, which corresponds to 1.92 ± 0.04 NADH binding sites per dimer for the enzyme solution. It can be seen from these results that the sloping A_{max} does not significantly alter the values for the NADH dissociation constant nor the number of NADH binding sites per dimer.

The Hanes plot (Fig. 21(d)) was linear indicating the absence of cooperativity between the binding sites, i.e. that the two NADH binding sites are identical and non-interacting and function independently of one another.

For titration 2, the plot of the fractional saturation values against NADH concentration (Fig. 22(a)) gave a hyperbolic curve. The Scatchard plot (Fig. 22(b)) gave an apparent NADH dissociation constant of 1.34 ± 0.05 μM and a binding site concentration of 11.70 ± 0.24 μM, which corresponds to 1.94 ± 0.04 NADH binding sites per dimer for an enzyme solution of concentration 6.023 μM dimers. The Hanes plot (Fig. 22(c)) for titration 2 was also linear indicating the absence of cooperativity between the two NADH binding sites.

The results obtained by the two different titration methods were similar, i.e. K_d of about 1.3 - 1.6 μM and two binding sites per dimer. This indicates that either method can be used to obtain accurate and reproducible values for K_d and n (the number of binding sites per dimer). The values for K_d and n from titrations 1 and 2 differ from those reported in earlier investigations, where only one NADH binding site per dimer was determined with a K_d of about 0.3 μM (Riley, 1993), but in these earlier studies the titrations were performed using undialysed enzyme and a different buffer.

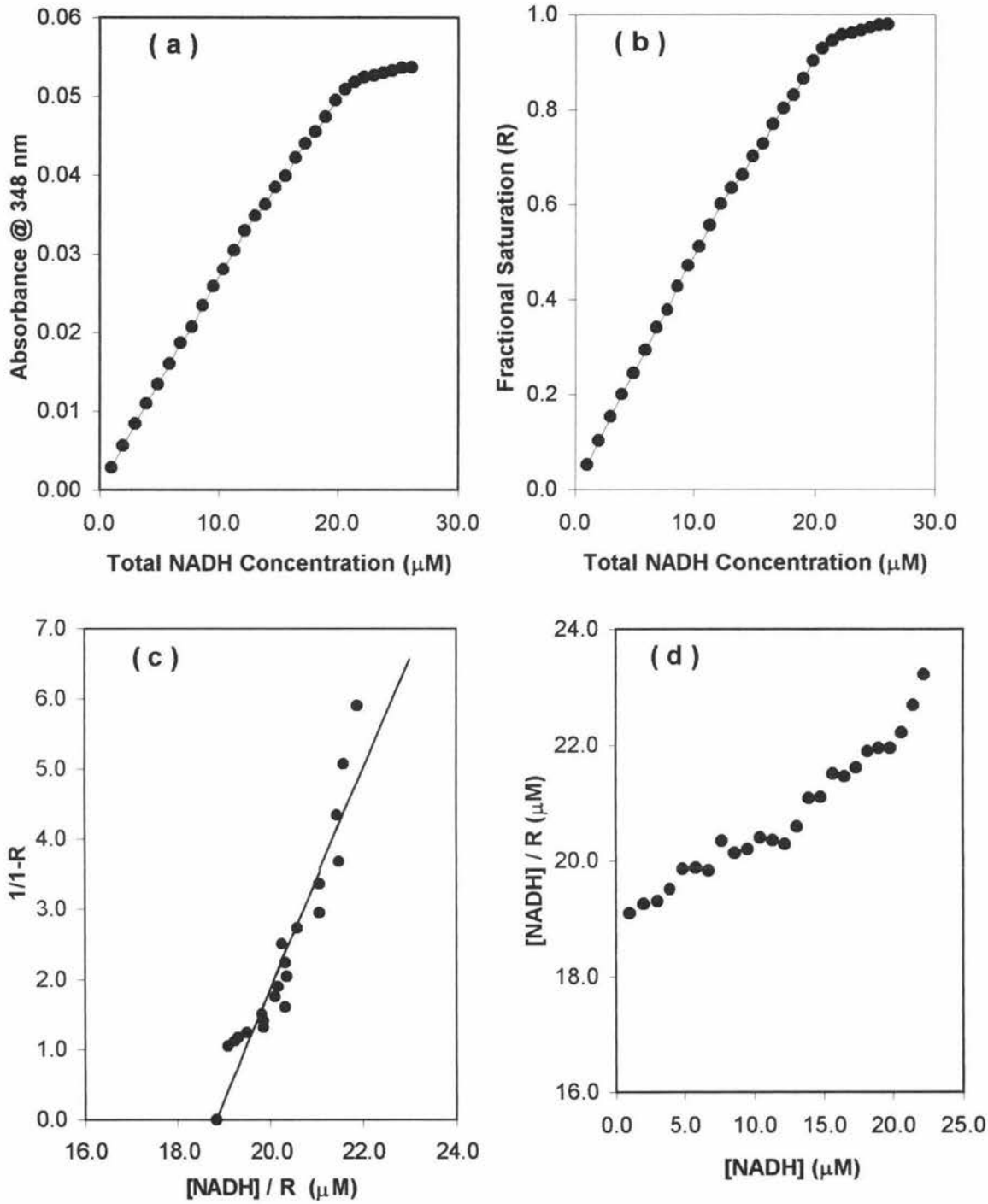

Figure 21. Titration 1 of purified aldehyde dehydrogenase with NADH.

(a) The plot of absorbance at 348 nm against total NADH concentration after each NADH aliquot addition using method 1 and 0.2 mM NADH stock solution.

(b) The plot of R, the fractional saturation values calculated using the data shown in Fig. 21(a) against the total NADH concentration

(c) A Scatchard plot constructed from the data shown in Fig. 21(b). The NADH dissociation constant K_d was calculated as 1.57 ± 0.14 μM while the intercept gave a binding site concentration of 18.83 ± 0.19 μM, which corresponds to 2.01 ± 0.02 NADH binding sites per dimer for an enzyme solution of concentration 9.375 μM dimers.

(d) Hanes plot of [NADH]/R against [NADH] to determine the type of cooperativity that may exist between the NADH binding sites.

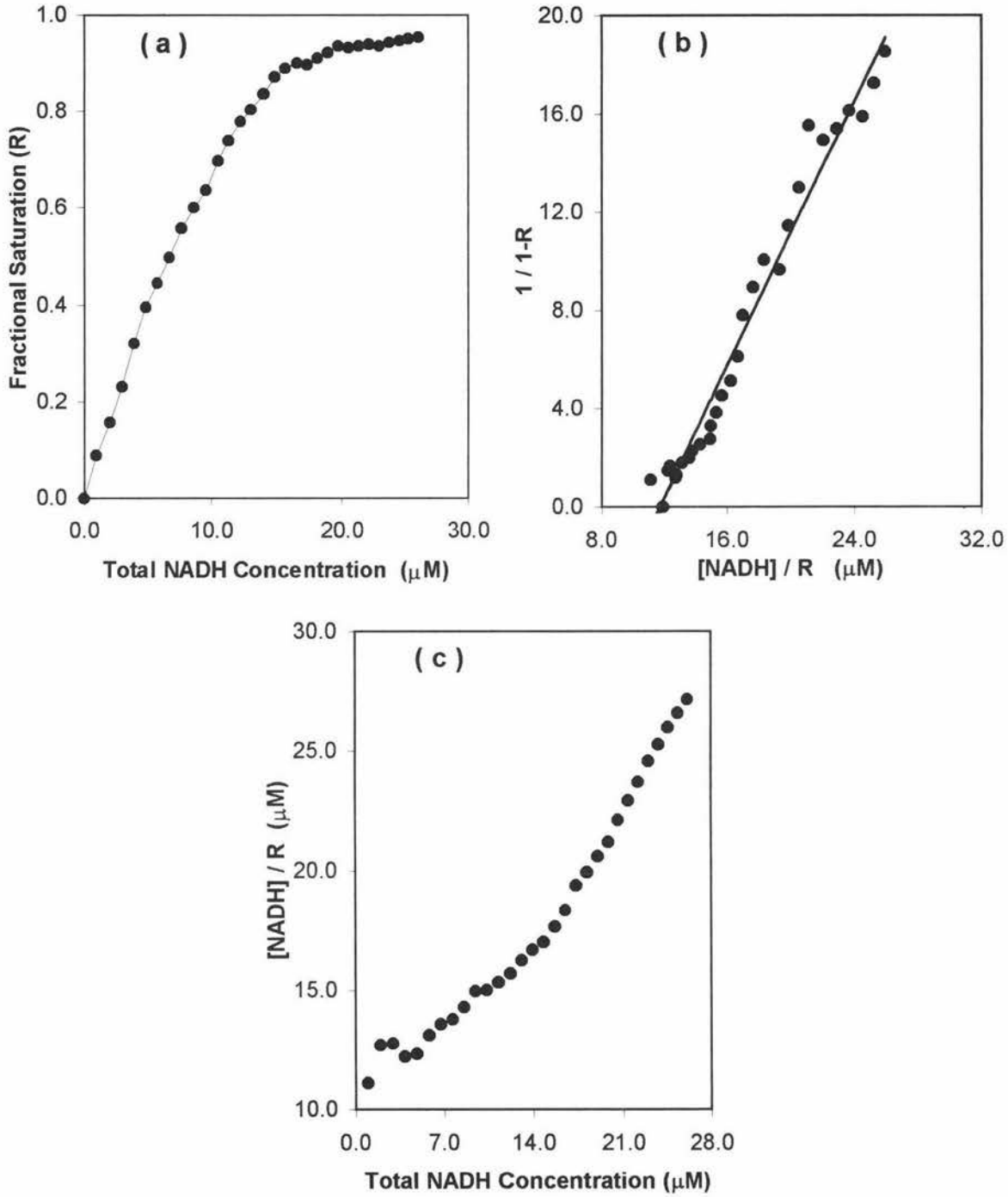

Figure 22. Titration 2 of purified aldehyde dehydrogenase with NADH.

(a) The plot of R, the fractional saturation values against the total NADH concentration after each NADH aliquot addition using method 2 and 0.2 mM NADH stock solution.

(b) Scatchard plot constructed from the data shown in Fig. 22(a). The NADH dissociation constant K_d was calculated as 1.34 ± 0.05 μM while the intercept gave a binding site concentration of 11.70 ± 0.24 μM, which corresponds to 1.94 ± 0.04 NADH binding sites per dimer for an enzyme solution of concentration 6.023 μM dimers.

(c) Hanes plot of [NADH]/ R against [NADH] to determine the type of cooperativity that may exist between the NADH binding sites.

Titration 3 was performed under similar conditions to those reported in earlier studies (Riley, 1993) (method 1, 0.2 mM NADH stock solution and MOPS buffer (100 mM, pH 7.5)) to investigate if the choice of buffer is the cause of the observed differences between the titration results. Note, however, that titration 3 used dialysed enzyme not undialysed enzyme, which was used in earlier studies. The plot of R, the fractional saturation values against NADH concentration (Fig. 23(a)) gave a hyperbolic curve. The Scatchard plot (Fig. 23(b)) gave an apparent NADH dissociation constant of 1.03 ± 0.06 μM and a binding site concentration of 19.47 ± 0.10 μM, which corresponds to 2.02 ± 0.01 NADH binding sites per dimer for an enzyme solution of concentration 9.659 μM dimers. The Hanes plot (Fig. 23(c)) for titration 3 was linear indicating the absence of cooperativity between the two NADH binding sites.

Titration 3 resulted in similar values for the number of binding sites per dimer and the NADH dissociation constant to those of titrations 1 and 2 but different from those reported in earlier studies (Riley, 1993). This suggests that the choice of buffer is not a likely cause of the observed differences between the results. It is more likely that the differences could be due to dialysis of the enzyme or as a result of a change in the purification procedure.

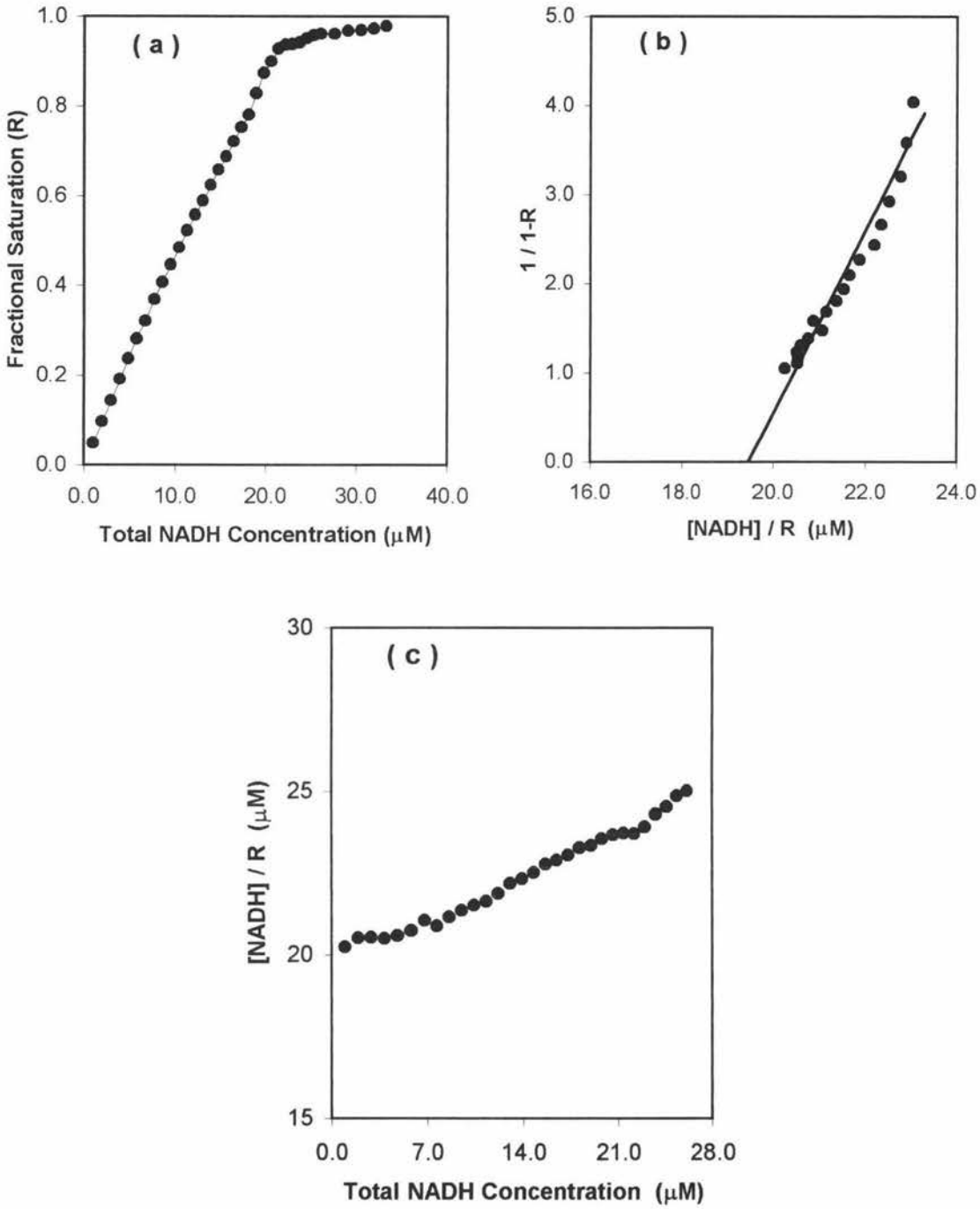

Figure 23. Titration 3 of purified aldehyde dehydrogenase with NADH.

(a) The plot of R, the fractional saturation values against the total NADH concentration after each NADH aliquot addition using method 1 and 0.2 mM NADH stock solution.

(b) Scatchard plot constructed from the data shown in Fig. 23(a). The NADH dissociation constant K_d was calculated as 1.03 ± 0.06 μM while the intercept gave a binding site concentration of 19.47 ± 0.10 μM, which corresponds to 2.02 ± 0.01 NADH binding sites per dimer for an enzyme solution of concentration 9.659 μM dimers.

(c) Hanes plot of [NADH]/ R against [NADH] to determine the type of cooperativity that may exist between the NADH binding sites.

The effect of dialysis of the enzyme on the NADH titration was investigated by repeating the titrations using dialysed (titration 4) and undialysed (titration 5) enzyme, method 2, 0.4 mM NADH stock solution and sodium phosphate buffer.

Titration 4 using dialysed ALDH gave a hyperbolic curve for the plot of R, the fractional saturation values against NADH concentration (Fig. 24(a)). The Scatchard plot (Fig. 24(b)) gave an apparent NADH dissociation constant of 1.64 $\pm$ 0.05 μM and a binding site concentration of 9.41 $\pm$ 0.25 μM, which corresponds to 1.51 $\pm$ 0.04 NADH binding sites per dimer for an enzyme solution of concentration 6.250 μM dimers.

The NADH titration performed using undialysed ALDH enzyme (titration 5), gave a hyperbolic curve for the plot of R, the fractional saturation values against NADH concentration (Fig. 25(a)). The Scatchard plot (Fig. 25(b)) gave an apparent NADH dissociation constant of 1.43 $\pm$ 0.06 μM and a binding site concentration of 12.41 $\pm$ 0.31 μM, which corresponds to 1.99 $\pm$ 0.05 NADH binding sites per dimer for an enzyme solution of concentration 6.227 μM dimers.

At low NADH concentrations the Hanes plots for titrations 4 and 5 (Fig. 24(c) and Fig. 25(c) respectively) were non linear, but at higher NADH concentrations the plots were linear indicating the absence of cooperativity between the two calculated NADH binding sites. A possible reason for the lack of linearity at low NADH concentrations could be due to the low protein concentration. This made the monitoring of the titration difficult, as absorbance readings were very small. The NADH titrations of dialysed and undialysed ALDH resulted in similar values for the number of binding sites per dimer and the NADH dissociation constant, which suggests that dialysis of the purified enzyme has little or no effect on binding of NADH to the enzyme.

In earlier investigations (Riley, 1993) it has been shown that undialysed enzyme contains bound aldehyde, as an absorbance burst is observed when ALDH and NAD^+ are mixed in a stopped flow spectrophotometer. Enzyme which had been dialysed against buffer exhibited no burst when mixed with NAD^+, indicating that the bound aldehyde had been removed.

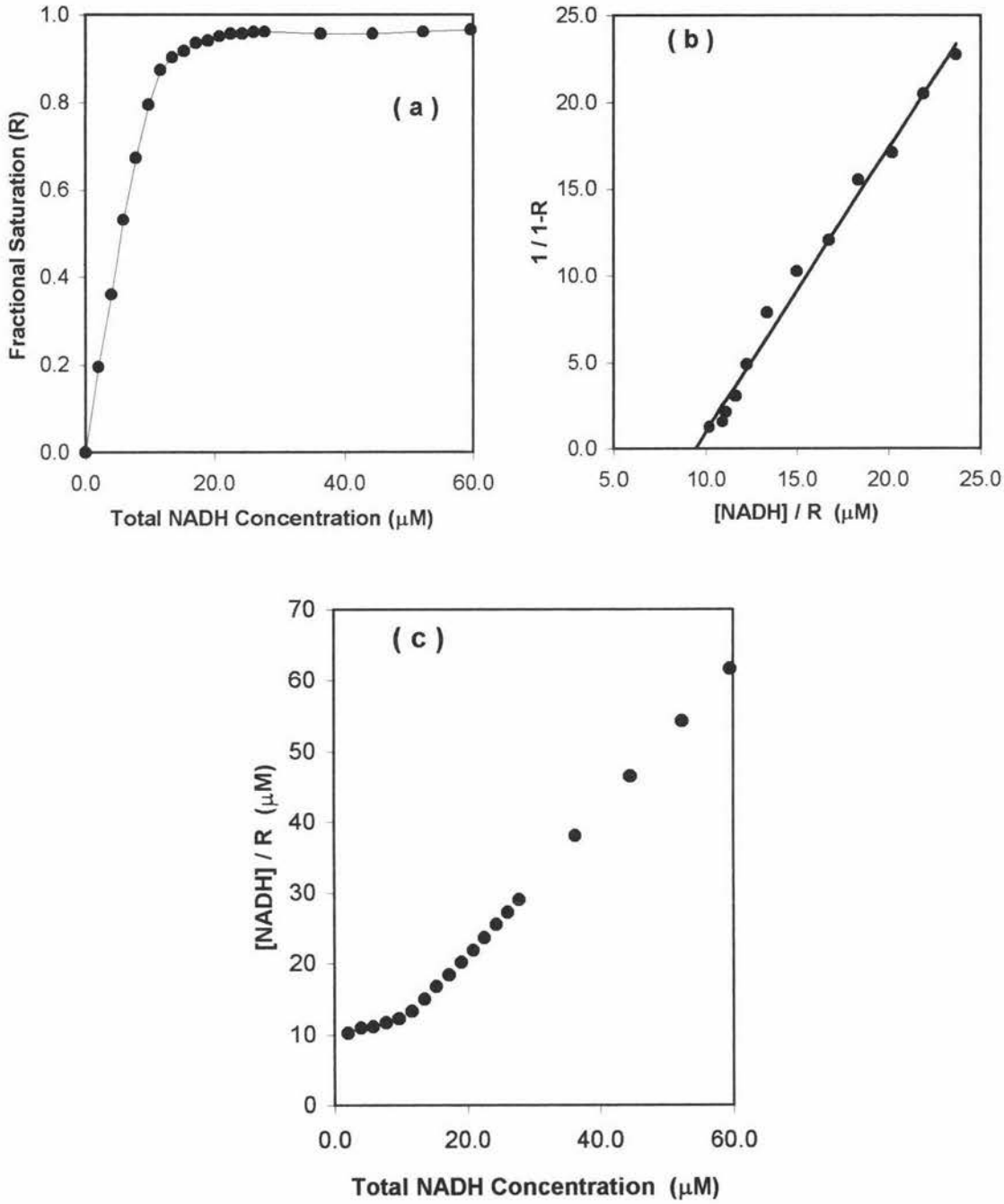

Figure 24. Titration 4 of purified aldehyde dehydrogenase (dialysed) with NADH.

(a) The plot of R, the fractional saturation values against the total NADH concentration after each NADH aliquot addition using method 2 and 0.4 mM NADH stock solution.

(b) Scatchard plot constructed from the data shown in Fig. 24(a). The NADH dissociation constant K_d was calculated as 1.64 ± 0.05 μM while the intercept gave a binding site concentration of 9.41 ± 0.25 μM which corresponds to 1.51 ± 0.04 NADH binding sites per dimer for an enzyme solution of concentration 6.250 μM dimers.

(c) Hanes plot of [NADH]/ R against [NADH] to determine the type of cooperativity that may exist between the NADH binding sites.

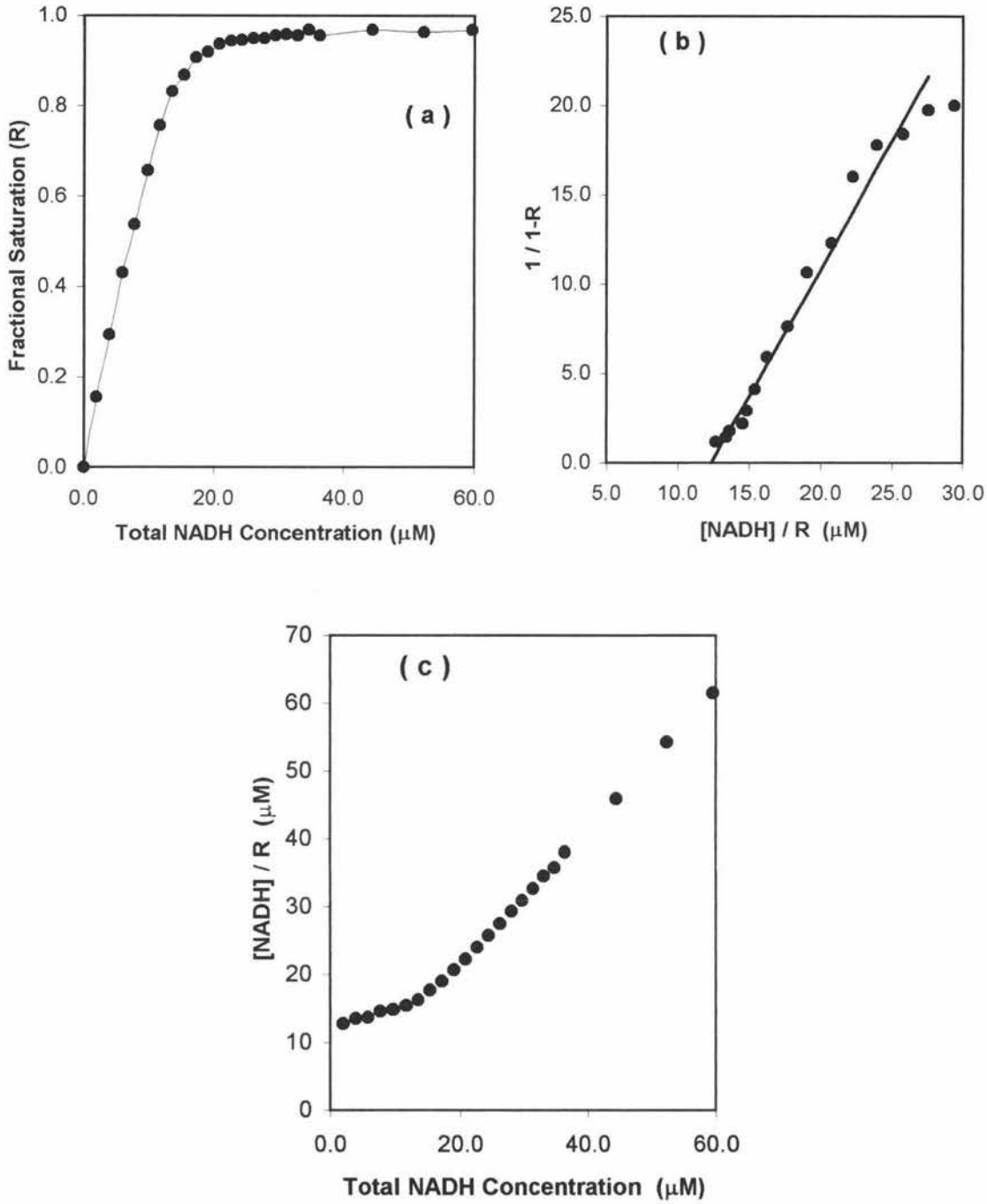

Figure 25. Titration 5 of purified aldehyde dehydrogenase (undialysed) with NADH.

(a) The plot of R, the fractional saturation values against the total NADH concentration after each NADH aliquot addition using method 2 and 0.4 mM NADH stock solution.

(b) Scatchard plot constructed from the data shown in Fig. 25 (a). The NADH dissociation constant K_d was calculated as 1.43 ± 0.06 μM while the intercept gave a binding site concentration of 12.41 ± 0.31 μM which corresponds to 1.99 ± 0.05 NADH binding sites per dimer for an enzyme solution of concentration 6.227 μM dimers.

(c) Hanes plot of [NADH]/ R against [NADH] to determine the type of cooperativity that may exist between the NADH binding sites.

To investigate how aldehyde effects the binding of NADH to the enzyme the titration (titration 6) was repeated using method 2, with dialysed enzyme mixed with excess aldehyde (5 µl of 800 mM hexanal added to curvette), 0.4 mM NADH stock solution and sodium phosphate buffer.

When excess aldehyde is mixed with dialysed ALDH and the NADH titration performed, NADH binding is disrupted, as shown by the plot of absorbance against NADH concentration (Fig. 26). Where in previous titrations an absorbance decrease was observed on binding NADH, now the reverse occurs. As the amount of NADH added to the curvette increases so does the absorbance.

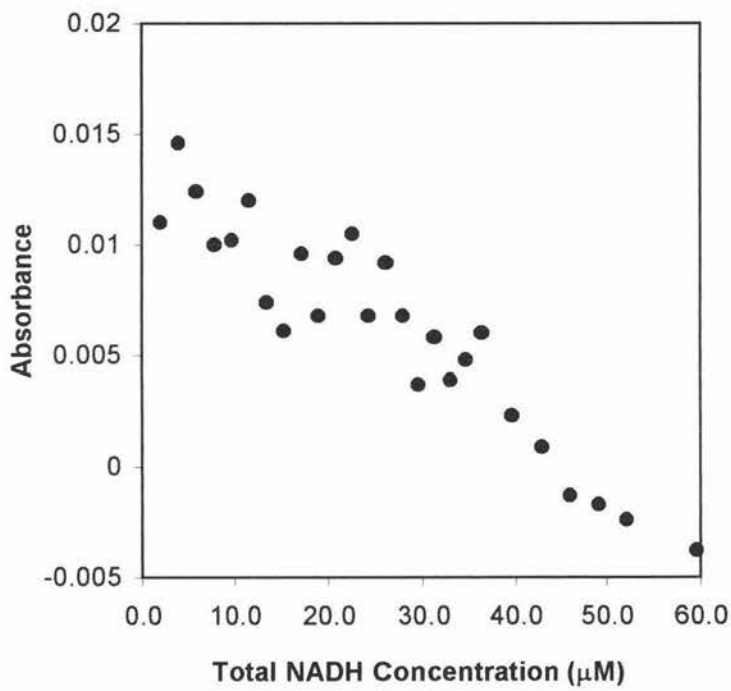

Figure 26. Titration 6 of purified ALDH (dialysed and mixed with excess aldehyde) with NADH.

plot of the difference in absorbance between the buffer/aldehyde and enzyme/aldehyde solution against total NADH concentration after each NADH aliquot addition using method 2 and 0.4 mM NADH stock solution.

3.4 Discussion

The difference spectrum between enzyme-bound and free NADH showed that the wavelength at which the highest absorbance change on NADH binding occurs is 348 nm (Fig. 19). This difference in absorbance allows the enzyme present in solution to be monitored on NADH binding at this wavelength. NADH was added

to the enzyme until the absorbance readings between aliquots ceased to change. The total concentration of NADH added to this point is equal to the NADH binding site concentration which can be used to calculate the number of NADH binding sites per enzyme dimer.

As the absorbance difference between enzyme-bound and free NADH is very small the accuracy and reliability of the titrations is of great importance. For this reason the titrations were performed using two different methods. Both methods resulted in similar values for the NADH dissociation constant and the number of NADH binding sites per dimer. However, the values were different from those reported in earlier studies (Riley, 1993)(Table 12). Titrations performed to try and account for these differences showed that neither the choice of buffer nor dialysis of the purified enzyme had any effect on the final titration results (titrations 3-5). It is more likely that the differences are as a result of a change in the purification procedure from that used in previous studies (Riley, 1993) to those employed in this thesis (see section 2).

NADH titrations using the same buffer as that used in earlier investigations as well as titrations using undialysed and dialysed enzyme gave values between 1.0 and 1.6 μM for the NADH dissociation constant and 1.5 and 2.0 for the number of NADH binding sites per dimer. See Table 12 for a summary of the NADH titration results.

Table 12. Summary of the NADH titration results

Titration	Method	Dialysed / Undialysed	Buffer	[Enzyme] (μM dimer)	NADH binding site conc (μM)	NADH dissociation constant (μM)	No.of NADH binding sites per dimer
1	1	Dia	Phos	9.375	18.83 ± 0.19	1.57 ± 0.14	2.01 ± 0.02
2	2	Dia	Phos	6.023	11.70 ± 0.24	1.34 ± 0.05	1.94 ± 0.04
3	1	Dia	MOPS	9.659	19.47 ± 0.10	1.03 ± 0.06	2.02 ± 0.01
4	2	Dia	Phos	6.25	9.41 ± 0.25	1.64 ± 0.05	1.51 ± 0.04
5	2	Undia	Phos	6.227	12.41 ± 0.31	1.43 ± 0.06	1.99 ± 0.05
6	2	Dia + Ald	Phos	7.215	----	----	----
Riley	1	Undia	MOPS	14.23	13.2 ± 0.4	0.29 ± 0.08	approximatey 1

Prev is the titration result of an earlier investigation (Riley 1993)
Dia and Undia refers to dialysed and undialysed ALDH respectively
Dia + Ald refers to dialysed ALDH and excess aldehyde (hexanal)
Phos is 50 mM sodium phosphate buffer (pH 7.5) and MOPS is 100 mM MOPS buffer (pH 7.5)

It is assumed that the number of NADH binding sites per dimer equals the number of NAD^+ binding sites per dimer. If this is indeed the case, then there are possibly two NAD^+ binding sites per dimer. Recently the crystal structure of a class 3 ALDH has been determined (refer section 1.11) and it was revealed that there are indeed two NAD^+ binding sites per dimer, which supports the results reported in this thesis.

Analysis of the titration results using Hanes plots showed that there is no cooperativity between the two calculated NADH binding sites, indicating that they are identical and act independently of one another.

The NADH titration performed using dialysed enzyme which had been premixed with excess aldehyde demonstrated the effect of the presence of aldehyde on NADH binding. When enzyme and excess aldehyde are premixed it is proposed that aldehyde binds to the enzyme to form a E_{Ald}^{NADH} complex and the remaining aldehyde stays in solution (Fig. 27(a)). On adding NADH to the premixed solution no NADH binding was observed, indicating that the E_{Ald} did not form. If the aldehyde does not bind to the enzyme during premixing, then on the addition of NADH a E^{NADH} complex would have been formed., and the E^{NADH} complex would have been observed (Fig. 27(a)). This complex was not observed, which implies that on the addition of NADH, either the E_{Ald} complex or free aldehyde in solution prevents NADH binding to the enzyme. Yet, NADH can bind to undialysed enzyme which has been shown to possess bound aldehyde (Fig. 27(b)). This suggests that the concentration of aldehyde plays an important part in determining the effects on NADH binding. In undialysed enzyme the concentration of bound aldehyde must be low as NADH binding can occur (titration 5), but at a high concentration of aldehyde, NADH binding to dialysed ALDH is disrupted (titration 6).

These results are not entirely unexpected as we would expect that if aldehyde is bound to the free enzyme, the formation of the non-productive complex E_{Ald}^{NADH} would not be favoured. In this way, the binding of aldehyde to the enzyme decreases the affinity of the E_{Ald} complex for NADH but increases it for NAD^+, as NAD^+ is required to allow the oxidation of the aldehyde to its respective acid.

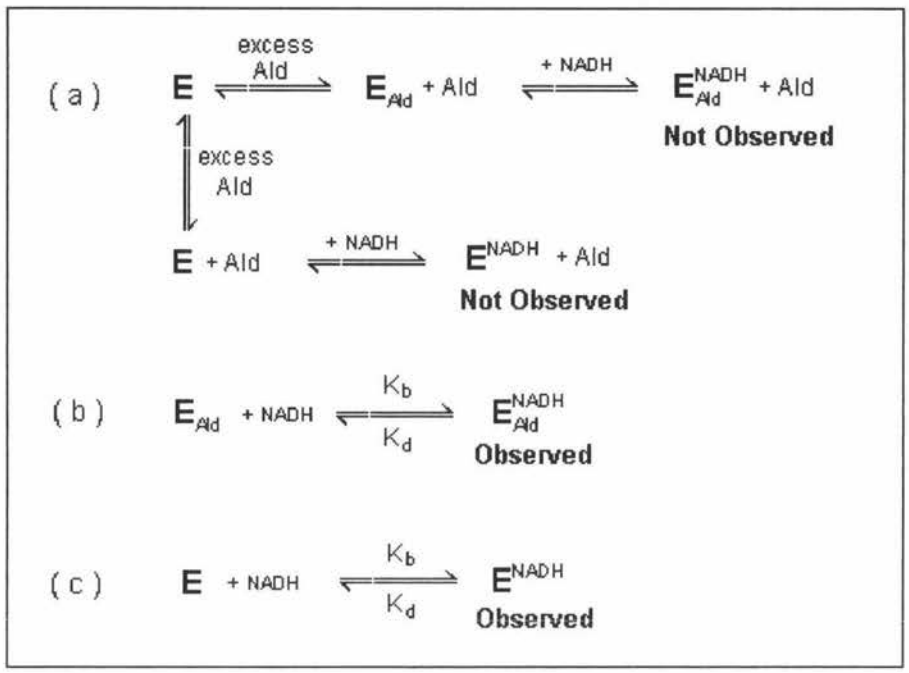

Figure 27. A kinetic model which rationalises the observed NADH titration results

(a) When dialysed enzyme and excess aldehyde are premixed, aldehyde is either bound or not bound. In either case, no enzyme-NADH complex is observed when titrating with NADH.

(b) When undialysed enzyme possessing bound aldehyde is titrated with NADH, NADH binding is observed. K_b and K_d are the NADH binding and dissociation constant respectively.

(c) When dialysed enzyme is titrated with NADH, NADH binding is observed. K_b and K_d are the NADH binding and dissociation constant respectively.

The ability of bovine corneal ALDH to bind aldehydes in the absence of NAD^+ supports the proposed functional role of the enzyme in protecting the cornea from the rapid build up of aldehydes produced by UV light . As well, NADH can bind to free ALDH to form a E^{NADH} complex, which can function as a UV-B filter protecting the retina from damage.

In the future ligand binding studies could also be performed by ultracentrifugation or gel filtration techniques, both of which involve moving an initially ligand-free protein through a solution of ligand and observing the changes which take place as it binds ligand.

Section 4. Presteady-State Kinetics.

4.0 Introduction.

Steady-state experiments give information about the rate-determining step, while presteady-state experiments allow study of steps in the reaction pathway other than the rate-determining step. The instrument used for presteady-state kinetic investigations was a Hi-Tech model stopped-flow spectrophotometer. The reactants are placed in separate syringes and an air-actuated plunger pushes the two solutions through a mixing jet into the observation chamber, where changes in absorbance or fluorescence are monitored. The mixing time is about 2 ms and 0.15 ml of each reactant is used in each push. For nucleotide (NADH) absorbance measurements, the wavelength on the monochromator is set at 340 nm. Using the inbuilt fitting program of the Hi-Tech model stopped-flow spectrophotometer data was fitted using the equation for a single exponential and slope [1] or the equation for a straight line [2], as appropriate.

$$Y = -dY*\exp(-k*X) + m*X + Y(inf) \quad [1]$$

$$Y = m*X + c \quad [2]$$

Presteady-state experiments were carried out under different reactant mixing conditions using different aldehyde substrates to help in the elucidation of the kinetic mechanism of bovine corneal aldehyde dehydrogenase.

4.1.0 Methods

4.1.1 Buffer and Reagents

Sodium phosphate buffer (50 mM, pH 7.5) was the standard buffer used. Before use the buffer was filtered and degassed for at least 20 minutes. All reagents used were made up using this degassed buffer solution. Unless otherwise stated the concentrations of all reagents are quoted as the final concentration in the observation chamber of the stopped-flow spectrophotometer after mixing.

4.1.2 Aldehydes

Some of the aldehydes used in this research needed repurifiying before they could be used as substrates. Others such as hexanal and octaldehyde were new stock and needed no further purification.

The procedure used for purifying the aldehydes is shown below. All purified aldehydes were stored under Argon and IR and NMR analyses were performed on all aldehydes to determine their purity. Stock aldehyde solutions were made up by diluting the purified aldehydes to the required concentrations with acetonitrile.

Aldehyde Purification Procedure.

Stock aldehyde was shaken for 30 minutes with a 10 % $NaHCO_3$ solution, washed with distilled water and then dried with $CaSO_4$. The aldehyde was then distilled either under vacuum or at normal atmospheric pressure and collected at its boiling point.

The pressure and boiling points for the aldehydes purified

- Propionaldehyde was collected at normal pressure at approximately 47°C.
- Butyraldehyde was collected at normal pressure at approximately 76°C.
- Valeraldehyde was collected at normal pressure at approximately 106°C.
- Heptaldehyde was collected under vacuum (12 mm Hg) at approximately 42°C.
- Benzaldehyde was collected under vacuum (10 mm Hg) at approximately 62°C.

The Effect of Acetonitrile on ALDH Activity

To determine whether acetonitrile is a suitable solvent for diluting the aldehyde concentration, the effect acetonitrile has on ALDH activity was investigated. Using a stock solution of 800 mM hexanal (acetonitrile, 97 % v/v) the following solutions (Table 13) were made up in quartz curvettes and assayed using the ALDH activity assay as described in section 2.2.4.

Table 13. The effect of acetonitrile on ALDH activity

Solution	Vol NAD^+ (ml)	Vol buffer (ml)	Vol hexanal (μl)	Vol extra acetonitrile (μl)	Vol ALDH (μl)	% acetonitrile	ALDH activity ($\mu M\ min^{-1}ml^{-1}$)
a	0.3	2.64	10	-----	50	0.3	0.0734
b	0.3	2.54	10	100	50	3.7	0.0511
c	0.3	2.44	10	200	50	7.0	0.0311
d	0.3	2.34	10	300	50	10.3	0.0212
e	0.3	2.24	10	400	50	13.7	0.0191
f	0.3	2.64	10	-----	50	0.3	0.0705
g	0.3	2.55	100	-----	50	3.3	0.0496
h	0.3	2.45	200	-----	50	6.6	0.0312

The ALDH activity of solutions a - e demonstrated that as the percentage of acetonitrile increases (v/v) activity decreases. The decrease in activity was not as a result of the aldehyde concentration decreasing, as activity for solutions f - h also decreased but with increasing aldehyde concentration.

These results show that it is the amount of acetonitrile which determines the affect on ALDH activity; for this reason the percentage (v/v) of acetonitrile in solution is limited to less than 1 % of the total volume.

4.1.3 Enzyme Concentration

The enzyme concentration is expressed in terms of the active site concentration in the observation chamber of the stopped-flow spectrophotometer after mixing.

For an enzyme with n binding sites the active site concentration, [S], is given by:

$$[S] = n\,.\,[E] \qquad \textbf{[3]}$$

where [E] is the total enzyme concentration (μM dimers) calculated by dividing the ALDH concentration (mg/ml) (found by the Bradford method, see section 2.2.1) by the dimeric molecular weight of the enzyme, 88 000 Da (refer to section 2.3).

n is the number of binding sites per dimer calculated from the ligand binding studies ($n = 2$, refer to section 3).

4.2.0 Results

4.2.1 Enzyme Mixed with NAD^+

Previous studies (Riley, 1993; Riley *et al.*, 1995) have shown that when undialysed enzyme is mixed with NAD^+ in the absence of any added aldehyde an absorbance burst is observed followed by a linear increase in absorbance. It was proposed that this burst represented the presteady-state production of NADH generated by the mixing of enzyme containing tightly bound aldehyde with NAD^+, while the linear phase was assumed to be the steady-state production of NADH. After extensive dialysis of the enzyme the tightly bound aldehyde was thought to have been removed as no absorbance burst was observed when the dialysed enzyme was rapidly mixed with NAD^+.

These initial stopped-flow experiments were repeated in this research to determine if purified ALDH contains tightly bound aldehyde and will produce the same burst patterns as those observed in earlier studies (Riley, 1993; Riley *et al.*, 1995).

Undialysed bovine corneal ALDH (11.5 μM) was rapidly mixed with a solution containing saturating NAD^+ (2 mM) in the stopped-flow spectrophotometer. A burst in absorbance was observed at 340 nm; the curve could be fitted to a single exponential before the absorbance leveled (Fig. 28). An average of five pushes gave a burst rate constant of $24.8 \pm 0.5\ s^{-1}$ and a very small burst amplitude of only 0.0030 ± 0.0003 absorbance units. After the burst the absorbance leveled at approximately 0.0247 ± 0.0005 absorbance units instead of increasing linearly, as in earlier investigations. The experiment was repeated, but this time absorbance was monitored over a 10 minute period following the burst. No slow increase in absorbance was observed. This supports evidence from ligand binding studies (refer section 3.4) that the concentration of aldehyde tightly bound to undialysed enzyme is low and non saturating. After the purification process only a small amount of aldehyde remains tightly bound to the enzyme. On mixing with NAD^+, an absorbance burst is observed, following which no more aldehyde remains to be oxidised.

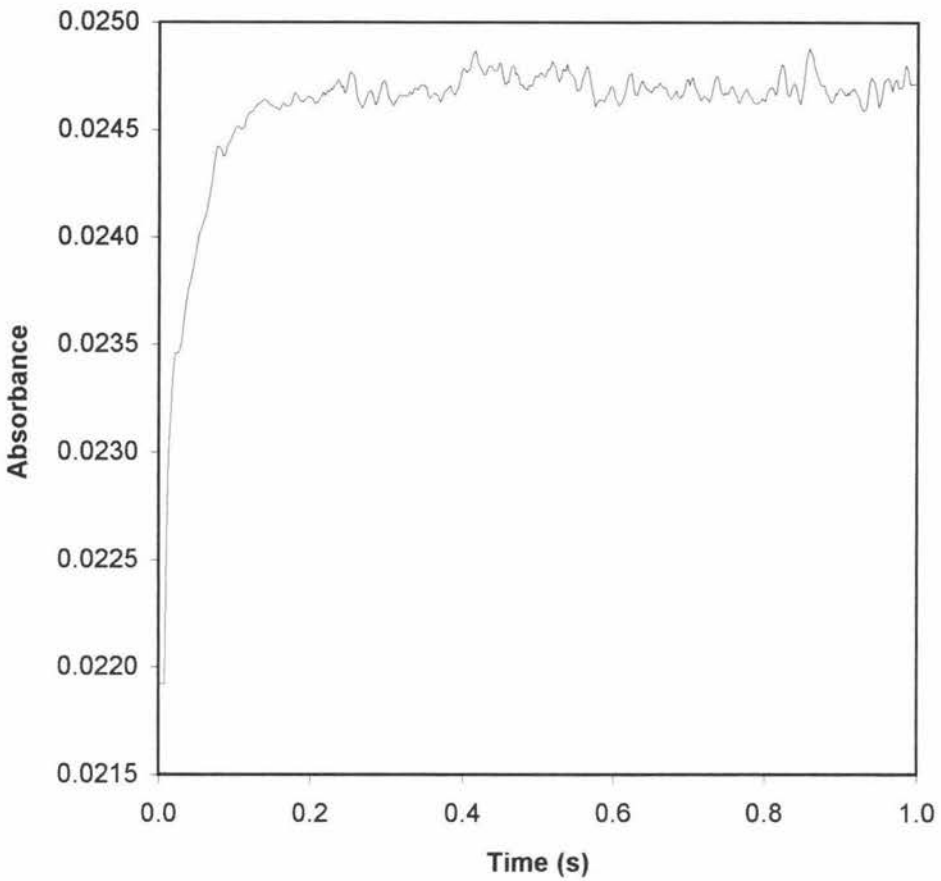

Figure 28. Time course of the absorbance change at 340 nm on mixing undialysed ALDH (11.5 μM) with NAD^+ (2 mM).

The trace shows an absorbance burst with a rate constant of $24.8 \pm 0.5\ s^{-1}$ and a very small burst amplitude of only 0.0030 ± 0.0003. Following the burst the absorbance leveled at approximately 0.0247 ± 0.0005 absorbance units.

When dialysed ALDH (11.5 μM) was rapidly mixed with a solution containing saturating NAD^+ (2 mM) neither an absorbance burst nor a linear increase in absorbance was observed. This indicates that the dialysis of purified ALDH against phosphate buffer (50 mM, pH 7.5) has removed whatever tightly bound aldehyde remained after the protein purification process.

4.2.2 Enzyme Premixed with Aldehyde and then Mixed with NAD^+

Dialysed ALDH (10 μM) was first premixed with one of the following aldehydes before being rapidly mixed with a solution containing saturating NAD^+ (2 mM) in the stopped-flow spectrophotometer. The aldehydes used under this mixing condition were: propionaldehyde (20 mM), butyraldehyde (1 mM), valeraldehyde (1 mM), hexanal (1 mM), heptanal (1 mM) and octaldehyde (1 mM).

Preincubation of the enzyme with butyraldehyde, valeraldehyde, hexanal, heptanal or octaldehyde followed by rapid mixing with NAD^+ resulted in an absorbance burst and then a steady-state increase in absorbance at 340 nm (Fig. 29). However, for enzyme preincubated with propionaldehyde there was no absorbance burst but a very slow steady-state phase was observed. Table 14 shows the affect preincubation of the enzyme with different aldehydes has on the burst parameters.

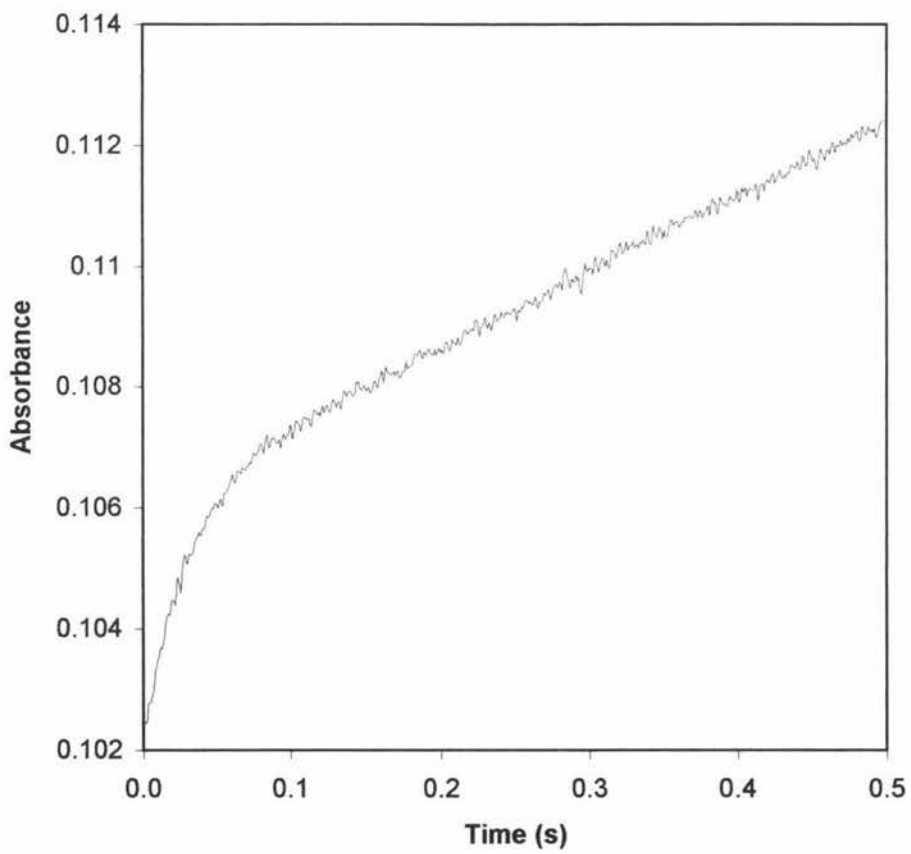

Figure 29. Time course of the absorbance change at 340 nm on mixing NAD^+ (2 mM) with dialysed ALDH (10 μM) which had been preincubated with aldehyde (hexanal, 1 mM).

The trace is an example of the burst followed by the steady-state phase observed when purified ALDH is preincubated with aldehyde (in this particular case hexanal) and then rapidly mixed with NAD^+. The burst rate constant was calculated to be 34.2 ± 0.5 s^{-1} and the burst amplitude 0.0043 ± 0.0002 absorbance units.

Table 14. Effect of preincubation of the enzyme with different aldehydes on the burst parameters

Aldehyde	[Aldehyde] (mM)	[NAD^+] (mM)	Burst rate constant (s^{-1})	Burst amplitude (a.u.)	Steady-state rate (a.u./s)
Propionaldehyde	20	2	-----	-----	0.0007 ± 0.0003
Butyraldehyde	1	2	30.8 ± 0.7	0.0020 ± 0.0002	0.0009 ± 0.0003
Valeraldehyde	1	2	31.7 ± 0.8	0.0032 ± 0.0003	0.0091 ± 0.0002
Hexanal	1	2	34.2 ± 0.5	0.0043 ± 0.0002	0.0122 ± 0.0002
Heptaldehyde	1	2	42.8 ± 1.2	0.0045 ± 0.0002	0.0258 ± 0.0002
Octaldehyde	1	2	42.5 ± 0.9	0.0047 ± 0.0001	0.0424 ± 0.0004

a.u. absorbance units. Enzyme concentration was 10 μM.

Table 14 shows that the burst rate constants were relatively similar for enzyme premixed with different aldehydes and then rapidly mixed with NAD^+, though the size of the burst and the rate of the steady-state phase increased slightly as the length of the aldehyde carbon chain increased. This is consistent with experimental evidence from other investigators that a physiological role of corneal ALDH is the oxidation of medium chain (C6 to C9) aliphatic aldehydes derived from lipid peroxidation (Holmes & VandeBerg, 1986b; Evces & Lindahl, 1989).

4.2.3 Enzyme Premixed with Aldehyde and then Mixed with $NADP^+$

For enzyme (10 μM) which had been premixed with heptaldehyde (1 mM) and then rapidly mixed with $NADP^+$ (2 mM) in the stopped-flow spectrophotometer an absorbance burst followed by a steady-state phase was observed, similar to the behavior shown in figure 29. An average of five pushes gave a burst rate constant of 27.6 ± 0.3 s^{-1}, a burst amplitude of 0.0034 ± 0.0004 absorbance units and a steady-state rate of 0.0125 ± 0.0001 absorbance units per second. This result indicates that $NADP^+$ can also act as a coenzyme in the catalytic conversion of an aldehyde to an acid by corneal ALDH.

4.2.4 Enzyme Mixed with Aldehyde and NAD^+ Together.

Dialysed ALDH (10 μM) was rapidly mixed with a solution containing saturating NAD^+ (2 mM) and one of the following aldehydes in the stopped-flow spectrophotometer. The aldehydes used were: propionaldehyde (20 mM), butyraldehyde (1 mM), valeraldehyde (1mM), hexanal (1 mM), heptanal (1 mM) and octaldehyde (1 mM).

Initial experiments resulted in an absorbance burst followed by a steady-state increase in absorbance for all the aldehydes used. The burst rate constants were all similar with an average of approximately 34 s^{-1}, though burst amplitudes and the steady-state rates did differ. This was unusual, as previous studies (Riley, *et al.*, 1995) observed only a steady-state phase under these mixing conditions. It is proposed that the observed burst may have been caused by aldehyde from previous experiments binding to the glass walls of the syringe. On the addition of fresh enzyme to the syringe, some of the aldehyde bound to the glass detaches to form a complex with the enzyme, i.e. E_{ALD}. When this complex was rapidly mixed with a solution of NAD^+ and aldehyde an absorbance burst similar to that shown in figure 29 was observed. To test this theory, dialysed enzyme in one syringe was mixed with a solution of NAD^+ in the other. If there was no aldehyde in the syringe containing enzyme, then no absorbance burst or linear increase in absorbance would be observed. However, an absorbance burst followed by a steady-state phase did occur. This is consistent with the proposed theory that aldehyde was remaining attached to the glass walls of the syringe even after vigorous cleaning with buffer.

Before the experiment was repeated the syringes were thoroughly cleaned using 95 % ethanol, purged with buffer and routinely checked to make sure no burst occurs when enzyme is mixed with a solution of NAD^+.

In the cleaned stopped-flow spectrophotometer dialysed ALDH (14.5 μM) was rapidly mixed with a solution containing saturating NAD^+ (2 mM) and hexanal (1 mM). This time no absorbance burst was observed, only the steady-state phase of the reaction (Fig. 30).

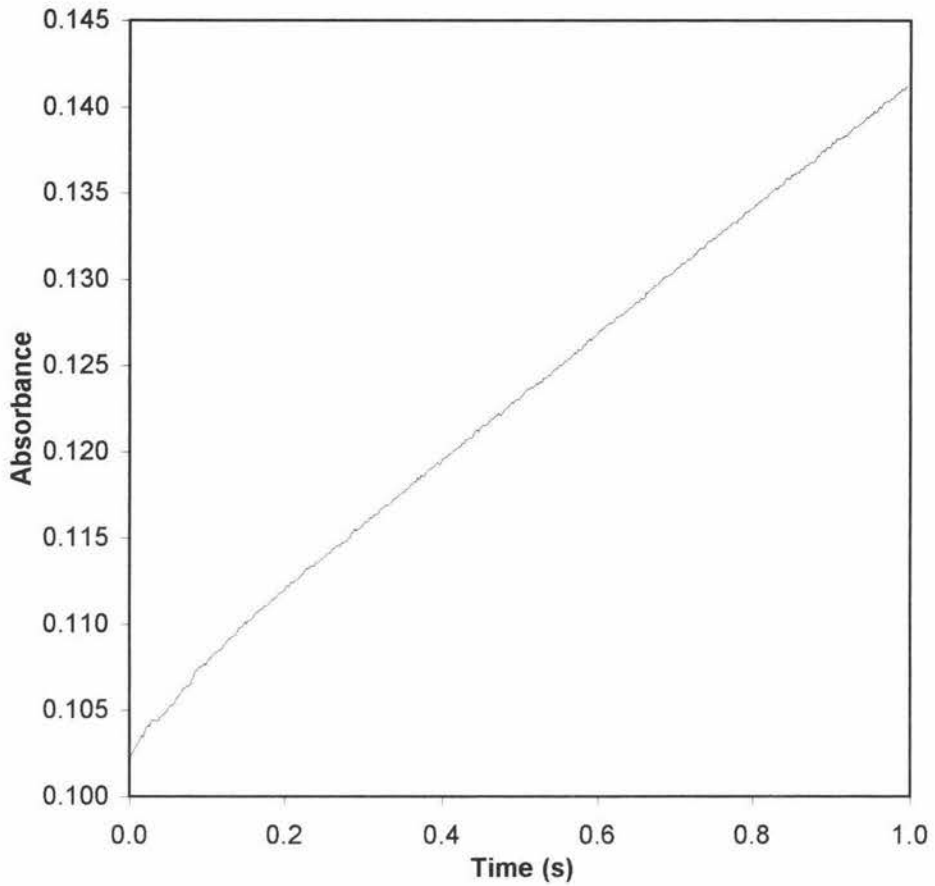

Figure 30. Time course of the absorbance change at 340 nm on mixing dialysed ALDH (14.5 μM) with a solution of NAD^+ (2 mM) and hexanal (1 mM) after cleaning the stopped-flow spectrophotometer.

The trace shows that only the steady-state phase of the reaction was observed after thorough cleaning of the stopped-flow spectrophotometer. The steady-state rate was found to be 0.0364 ± 0.0002 absorbance units per second.

4.2.5 Enzyme Premixed with NAD^+ and then Mixed with Aldehyde

Dialysed ALDH (10 μM) which had been premixed with a solution containing saturating NAD^+ (2 mM) was rapidly mixed with one of the following aldehydes in the stopped-flow spectrophotometer. The aldehydes used were: octaldehyde (1 mM), heptanal (1 mM), hexanal (1 mM), valeraldehyde (1mM), butyraldehyde (1 mM) and propionaldehyde (20 mM).

Using octaldehyde as a substrate under the mixing condition described above, the initial results showed the occurrence of a lag period of approximately 0.05 seconds in length before an absorbance burst and then a steady-state phase. In previous

studies (Riley, *et al.*, 1995) an initial lag period also occurred but there was no observed absorbance burst, only a steady-state phase. In section 4.2.4, it was found that there was aldehyde attached to the glass walls of the syringe, which may have been causing the occurrence of the absorbance burst. To see if this was occurring again, dialysed enzyme in one syringe was rapidly mixed with NAD^+ in the other. This time, no absorbance burst occurred, which suggests that the burst observed when a preincubated solution of enzyme and NAD^+ was rapidly mixed with octaldehyde was probably a result of the mixing condition.

The duration of preincubation between enzyme and NAD^+ was shown to affect the burst parameters (Table 15). The longer the preincubation the smaller the rate and amplitude of the burst, though the steady-state rate remained relatively constant (Fig. 31). This behaviour between the length of preincubation and the burst parameters was also observed when heptaldehyde (Fig. 32 & 33) and hexanal (Fig. 34 & 35) were used as substrates. The burst rate and amplitude decreased as the duration of preincubation increased until only the lag period and steady-state phase remained (Fig. 33 & 35). In figure 35 the lag period looks as if it has disappeared but as there is no burst it is difficult to distinguish where the lag finishes and where the steady-state starts.

Table 15. The effect the duration of preincubation between enzyme and NAD^+ has on the burst parameters using octaldehyde as the aldehyde substrate

Preincubation time (min)	Lag period (s)	Burst rate constant (s^{-1})	Burst amplitude (a.u.)	Steady-state rate (a.u./s)
2	0.05	38.0 ± 0.8	0.0268 ± 0.0034	0.0411 ± 0.0001
4	0.05	24.1 ± 1.2	0.0162 ± 0.0032	0.0433 ± 0.0002
6	0.05	12.9 ± 2.1	0.0098 ± 0.0010	0.0439 ± 0.0002

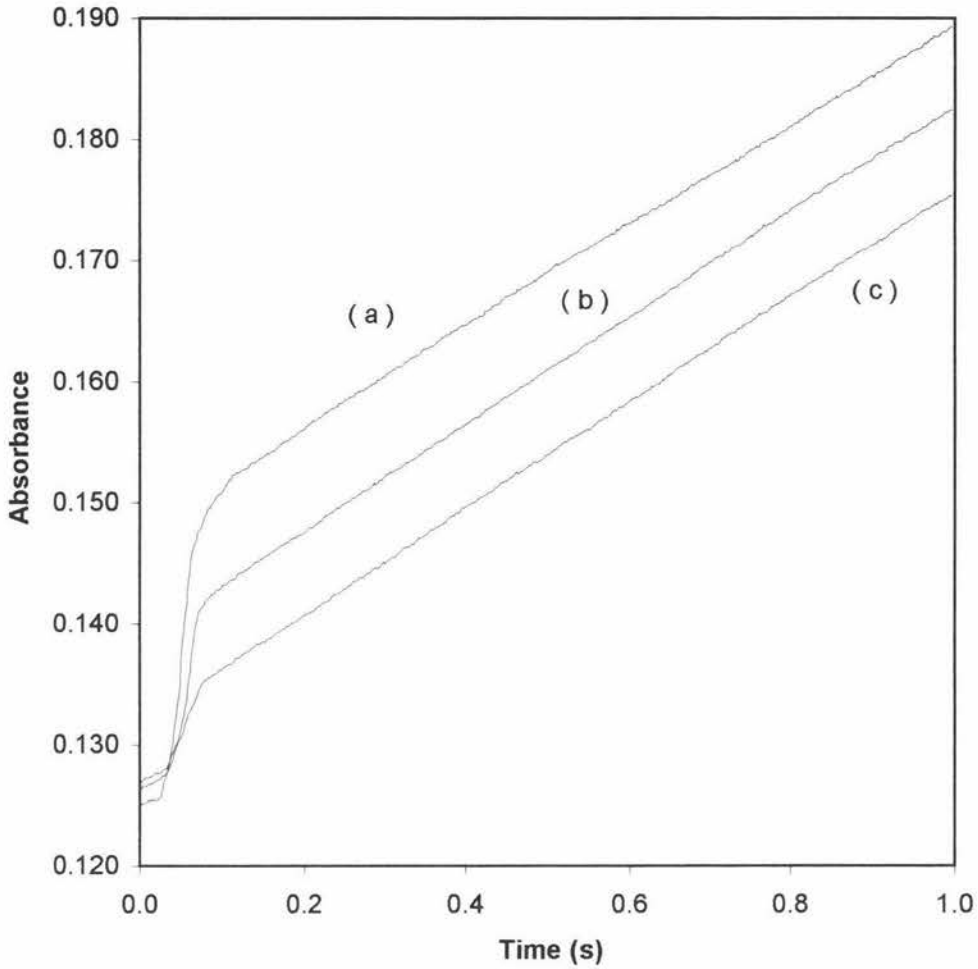

Figure 31. Time course of the absorbance change at 340 nm on mixing octaldehyde (1 mM) with dialysed ALDH (10 μM) which had been preincubated with NAD^+ (2 mM).

The traces show the time course of absorbance change after rapidly mixing octaldehyde with an enzyme solution which had been premixed with NAD^+ for (a) 2 minutes, (b) 4 minutes and (c) 6 minutes. An initial lag period of 0.05 seconds occurred before a burst in absorbance and a steady-state phase. The values for the burst parameters for the data shown are given in table 15.

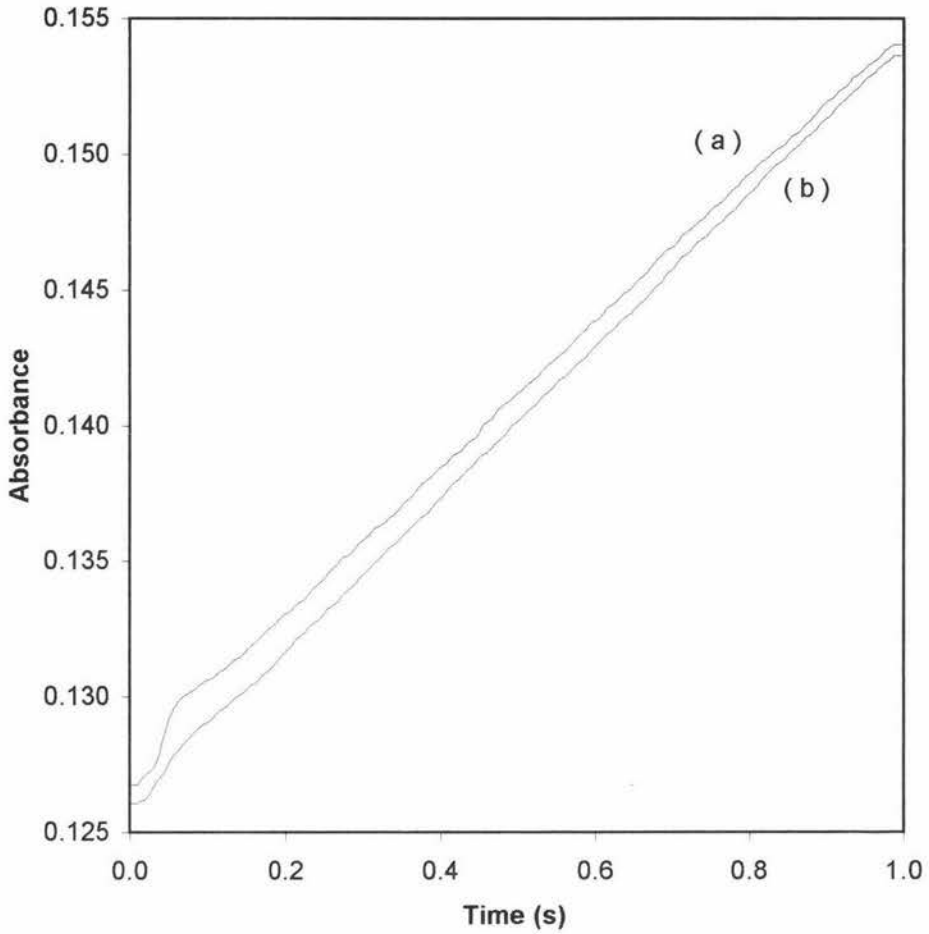

Figure 32. Time course of the absorbance change over 1 second at 340 nm on mixing heptaldehyde (1 mM) with dialysed ALDH (10 μM) which had been preincubated with NAD^+ (2 mM).

The traces show the time course of absorbance change after rapidly mixing heptaldehyde with an enzyme solution which had been premixed with NAD^+ for (a) 11 minutes and (b) 15 minutes. An initial lag period of 0.05 seconds occurred before a burst in absorbance and a steady-state phase.

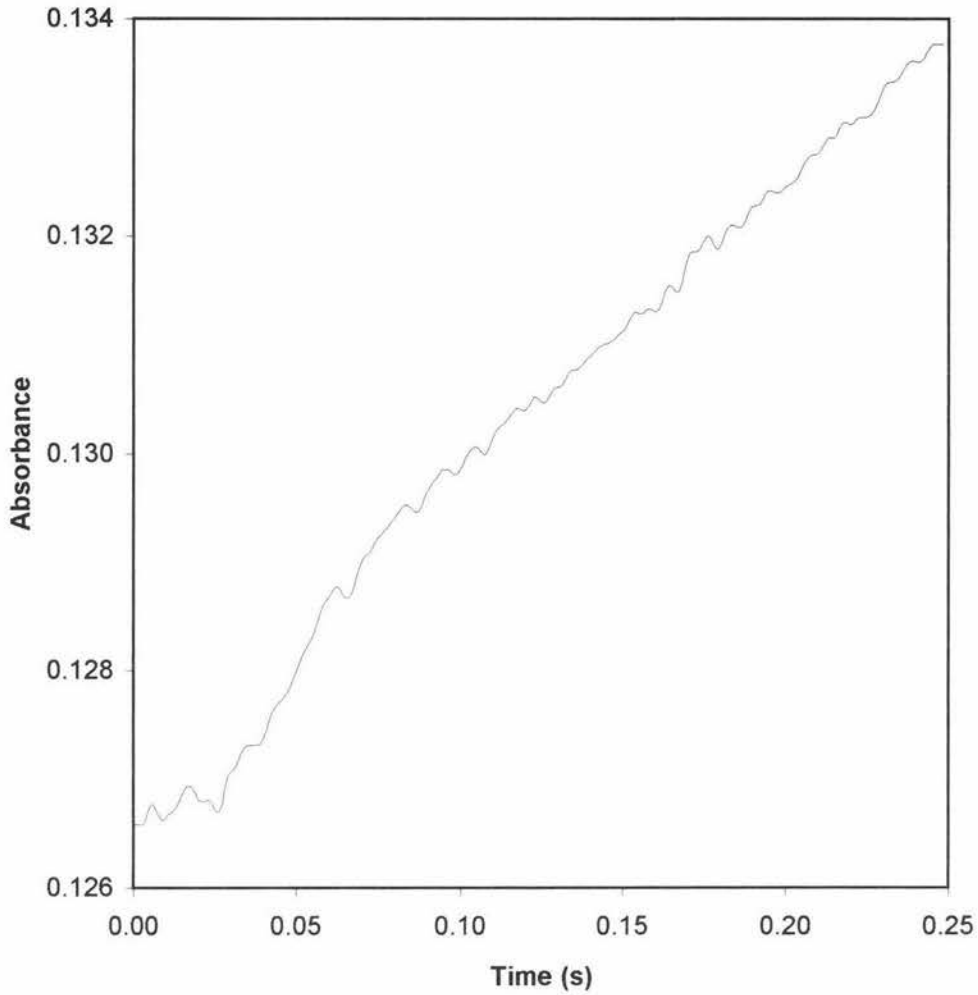

Figure 33. Time course of the absorbance change over 0.25 seconds at 340 nm on mixing heptaldehyde (1 mM) with dialysed ALDH (10 μM) which had been preincubated with NAD^+ (2 mM).

The trace shows the time course of absorbance change after rapidly mixing heptaldehyde with an enzyme solution which had been premixed with NAD^+ for 17 minutes. An initial lag period occurred before a very small burst and a steady-state phase.

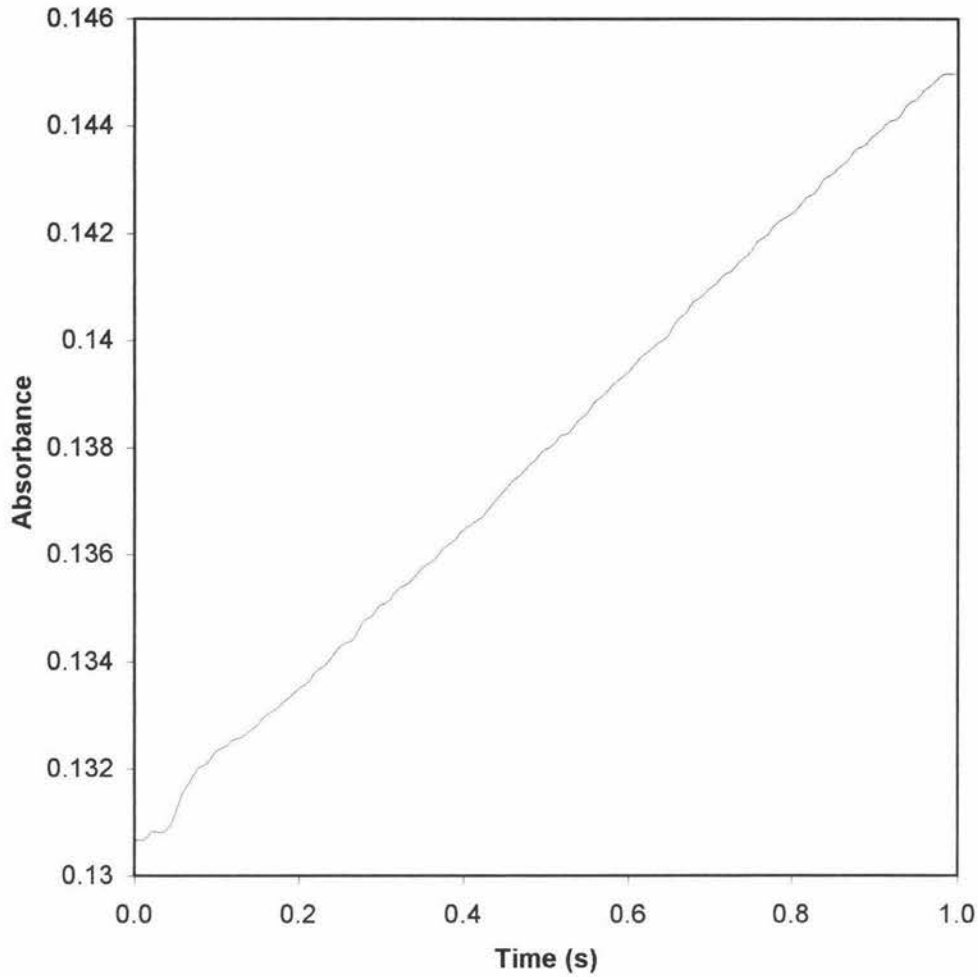

Figure 34. Time course of the absorbance change over 1 second at 340 nm on mixing hexanal (1 mM) with dialysed ALDH (10 μM) which had been preincubated with NAD^+ (2 mM).

The trace shows the time course of absorbance change after rapidly mixing hexanal with an enzyme solution which had been premixed with NAD^+ for 20 minutes. An initial lag period of 0.05 seconds occurred before a very small burst and a steady-state phase.

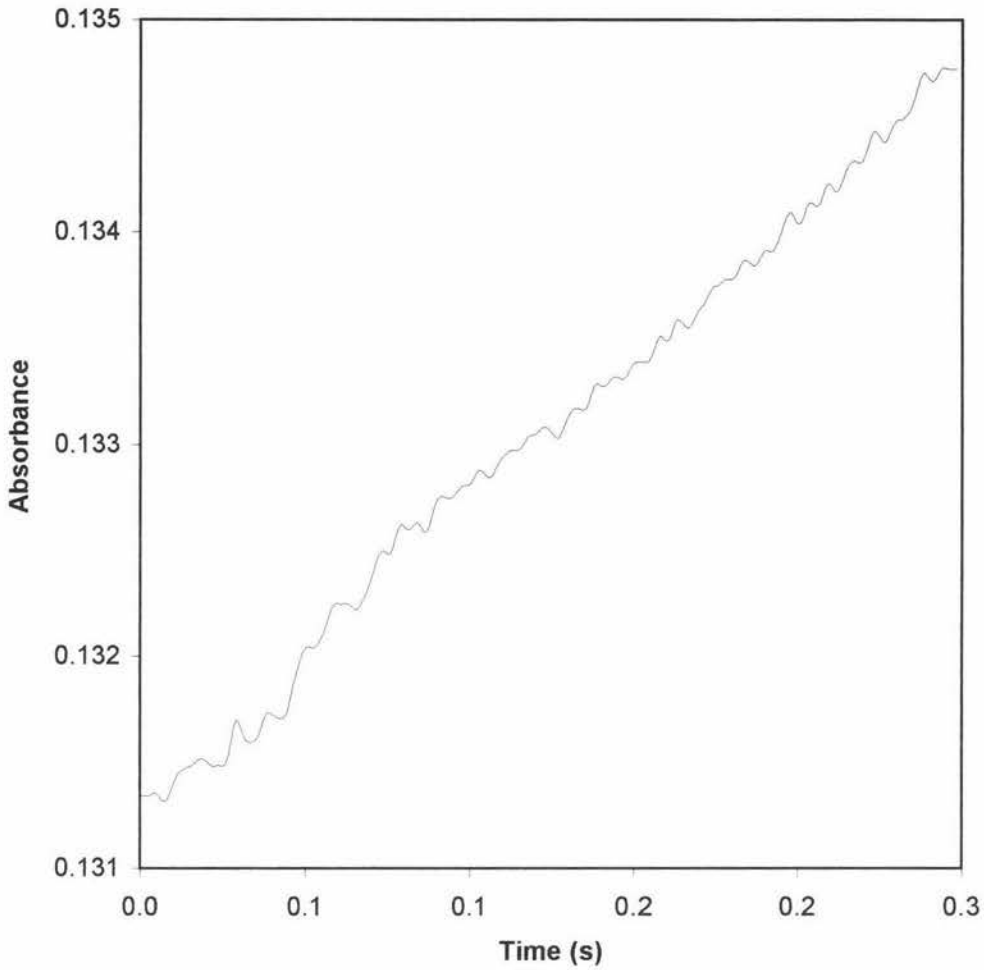

Figure 35. Time course of the absorbance change over 0.25 seconds at 340 nm on mixing hexanal (1 mM) with dialysed ALDH (10 μM) which had been preincubated with NAD^+ (2 mM).

The trace shows the time course of absorbance change after rapidly mixing hexanal with an enzyme solution which had been premixed with NAD^+ for 25 minutes. The lag period looks as if it has disappeared but as there is no burst it is difficult to distinguish where the lag finishes and where the steady-state phase starts

By the time valeraldehyde, butyraldehyde and propionaldehyde were used as substrates, the length of preincubation between enzyme and NAD^+ had been so long that only a lag period and a steady-state phase could be observed on mixing. Table 16 shows the steady-state rates obtained for enzyme preincubated with NAD^+ and then rapidly mixed with different aldehydes. These rates are similar to those obtained with enzyme which had been premixed with aldehyde and rapidly mixed with NAD^+ (Table 14). In both cases the steady-state rate increased with increasing length of the aldehyde carbon chain.

Table 16. Steady-state rates for different aldehyde substrates when rapidly mixed with enzyme preincubated with NAD^+

Aldehyde	[Aldehyde] (mM)	[NAD^+] (mM)	Steady-state rate (a.u./s)
Propionaldehyde	20	2	0.0007 ± 0.0002
Butyraldehyde	1	2	0.0017 ± 0.0002
Valeraldehyde	1	2	0.0112 ± 0.0001
Hexanal	1	2	0.0143 ± 0.0001
Heptaldehyde	1	2	0.0277 ± 0.0001
Octaldehyde	1	2	0.0428 ± 0.0001

Final enzyme concentration is 10 μM

The experiment was repeated using enzyme (14.5 μM) which had been preincubated with NAD^+ (2 mM) for 3 minutes and then rapidly mixed with hexanal (1 mM). A lag period occurred followed by an absorbance burst and then a steady-state phase. The burst rate constant was found to be 30.8 ± 0.5 s^{-1}, the burst amplitude 0.0151 ± 0.0021 a.u. and the steady state rate 0.0330 ± a.u. s^{-1}. The behaviour between the length of preincubation and the burst parameters was again observed. The longer the preincubation the smaller the rate and amplitude of the burst. This is consistent with the proposal that the length of premixing affects the appearance of the burst. In previous studies (Riley, *et al.*, 1995) the length of preincubation between enzyme and NAD^+ was of sufficient duration that a burst was not observed but was short enough to allow the observation of the lag period.

4.2.6 Enzyme Premixed with $NADP^+$ and then Mixed with Aldehyde

For enzyme (10 μM) which had been premixed with $NADP^+$ (2 mM) for 30 minutes and then rapidly mixed with heptaldehyde (1 mM) in the stopped-flow spectrophotometer a lag period of approximately 0.05 seconds occurred before a steady-state phase of 0.0352 a.u. s^{-1}. This result indicates that $NADP^+$ behaves similar to NAD^+ in terms of the observed absorbance characteristics after a long preincubation period and can act as a coenzyme in the catalytic conversion of an aldehyde to an acid by corneal ALDH.

4.3 Discussion

The results of the presteady-state studies using the stopped-flow spectrophotometer under different reactant mixing conditions can be summarised in table 17.

Table 17. Summary of the stopped-flow results under different mixing conditions.

Mixing conditions	Lag period	Burst	Steady-state phase	Comments
$E_{(undia)}$ vs NAD^+	-----	✓	-----	Absorbance levels after burst
$E_{(dia)}$ vs NAD^+	-----	-----	-----	May indicate no bound aldehyde
E + Ald vs NAD^+	-----	✓	✓	
E + Ald vs $NADP^+$	-----	✓	✓	
E vs NAD^+ + Ald	-----	-----	✓	
E + NAD^+ vs Ald	✓	✓	✓	Size and rate of burst is dependent on the preincubation time of E with NAD^+
E + $NADP^+$ vs Ald	✓	-----	✓	Burst may not have been observed because of long preincubation period

E: enzyme, undia: undialysed, dia: dialysed, Ald: Aldehyde,
✓ indicates a positive observation.
Example of mixing condition: E + Ald vs NAD^+ refers to enzyme and aldehyde premixed and then rapidly mixed with NAD^+.

A small amount of aldehyde was shown to be bound to undialysed enzyme by the presence of an absorbance burst when the enzyme was rapidly mixed with NAD^+. The fact that we don't see a steady-state phase proceeding the absorbance burst suggests that the concentration of bound aldehyde is less than or equal to the active site concentration and there is only enough aldehyde bound for a single enzyme turnover. After extensive dialysis of the purified enzyme the bound aldehyde was removed, as no burst nor steady-state phase was observed on mixing with NAD^+.

The observation of a burst when enzyme was premixed with aldehyde and then rapidly mixed with NAD^+ implies that aldehyde can bind to the free enzyme in the absence of bound NAD^+. The resulting E_{Ald} complex must form slowly, otherwise a burst would have also been observed when NAD^+ and aldehyde were both rapidly mixed with enzyme, instead of just the steady-state phase of the reaction. The burst observed is assumed to represent the presteady-state production of NADH while the linear phase is assumed to represent the steady-state production of NADH.

The size of the absorbance burst is a measure of the presteady-state formation of the E^{NADH} species. The concentration of this species produced during the presteady-state is therefore directly proportional to the burst amplitude and should be equal to the enzyme active site concentration, [S].

$$[E^{NADH}] = \frac{\text{Burst Amplitude}}{\varepsilon \cdot L} \qquad [4]$$

where L is the path length (1 cm) and assuming ε is 6220 $Lmol^{-1} cm^{-1}$ at 340 nm. The percentage of active sites with bound NADH is given by:

$$\% \text{ active sites with bound NADH} = \frac{[E^{NADH}]}{[S]} \times 100 \qquad [5]$$

When undialysed enzyme was rapidly mixed with NAD^+ there was only enough aldehyde bound for a single enzyme turnover. The absorbance change in the

presteady-state corresponded to NADH bound to only 4 % of the active sites (Table 18).

When enzyme was premixed with excess aldehyde (hexanal or octaldehyde), and then rapidly mixed with NAD^+, the absorbance change in the presteady-state corresponded to NADH being bound to approximately only 7 % or 8 % of the active sites respectively (Table 18). These values are similar to that obtained for undialysed enzyme and NAD^+ rapidly mixed together, which suggests that regardless of the type or concentration of aldehyde, only a small amount of aldehyde binds to the free enzyme. However, when enzyme was preincubated with NAD^+ for a short period and then rapidly mixed with aldehyde, the absorbance change in the presteady-state corresponded to NADH bound to approximately 17 % and 43 % of the active sites when hexanal and octaldehyde were used as substrates respectively (Table 18). Though the burst rate constant observed under different mixing conditions using different aldehydes were similar, the amount of NADH produced in the burst differed (Table 18). This suggests that the rate of NADH produced in the presteady-state may be dependent on NAD^+ binding, but the amount of NADH produced is dependent on the amount of aldehyde bound to the enzyme.

Table 18. Percentage of active sites with bound NADH produced in the presteady-state phase under different reactant mixing conditions.

Mixing conditions	Aldehyde	Burst rate constant (s^{-1})	Burst amplitude (a.u.)	$[E^{NADH}]$ (μM)	[S] (μM)	% active sites bound
$E_{(undia)}$ vs NAD^+	unknown	24.8 ± 0.5	0.0030 ± 0.0003	0.48	11.5	4
E + Ald vs NAD^+	hexanal	34.2 ± 0.5	0.0043 ± 0.0002	0.69	10.0	7
	octaldehyde	42.5 ± 0.9	0.0047 ± 0.0001	0.76	10.0	8
E + NAD^+ vs Ald	hexanal	30.8 ± 0.5	0.0151 ± 0.0021	2.43	14.5	17
	octaldehyde	38.8 ± 0.8	0.0268 ± 0.0034	4.31	10.0	43

$[E^{NADH}]$ values were calculated using equation [4] described in this section.
[S] values were calculated using equation [3] described in section 4.1.3
% active sites bound were calculated using equation [5] described in this section.

A short preincubation period for enzyme with NAD^+ followed by rapid mixing with aldehyde resulted in the formation of a species which allowed the observation of the rapid hydride transfer and then a steady-state production of NADH only after a lag period. However, as the duration of preincubation increased the size and rate of the burst decreased until only the lag period and steady-state phase remained. This implies that a long preincubation period between enzyme and NAD^+ results in a form which is unsuitable for the production of a burst. After the lag period, the enzyme recovers to give activity but it does so more slowly than the burst process, so that it effectively controls the rate at which the steady-state phase is setup and hence a burst is not observed.

The stopped-flow spectrophotometer results using $NADP^+$ instead of NAD^+ under different mixing conditions showed that $NADP^+$ can also act as the coenzyme in the catalytic conversion of an aldehyde to an acid by corneal ALDH.

Under the different reactant mixing conditions it could be seen that as the aldehyde chain length increased so did the corresponding steady-state rates. If the steady-state rates had been similar then this would imply that NADH dissociation was probably the rate limiting step; as it is for ALDH classes 1 and 2 (MacGibbon *et al.*, 1977) but as the steady-state rates were different then this suggests the rate limiting step may be aldehyde dependent.

A general mechanism based on the structure of a class 3 ALDH (Liu, *et al.*, 1996; 1997) was shown in figure 4 (section 1.11) but the actual order of substrate binding is not yet known. The reaction mechanism may be similar to that of the sheep liver enzyme (Fig. 36). This mechanism has ordered binding with NAD^+ as the lead substrate and NADH dissociation (k_5) as the rate-limiting step (Feldman & Weiner, 1972; Blackwell *et al.*, 1989; MacGibbon, 1977). However, experimental evidence reported in this thesis and from previous studies (Riley, 1993; Riley, *et al.*, 1995) suggests that bovine corneal aldehyde dehydrogenase may function by a different reaction mechanism from that of the sheep liver enzyme, with aldehyde being the leading substrate not NAD^+.

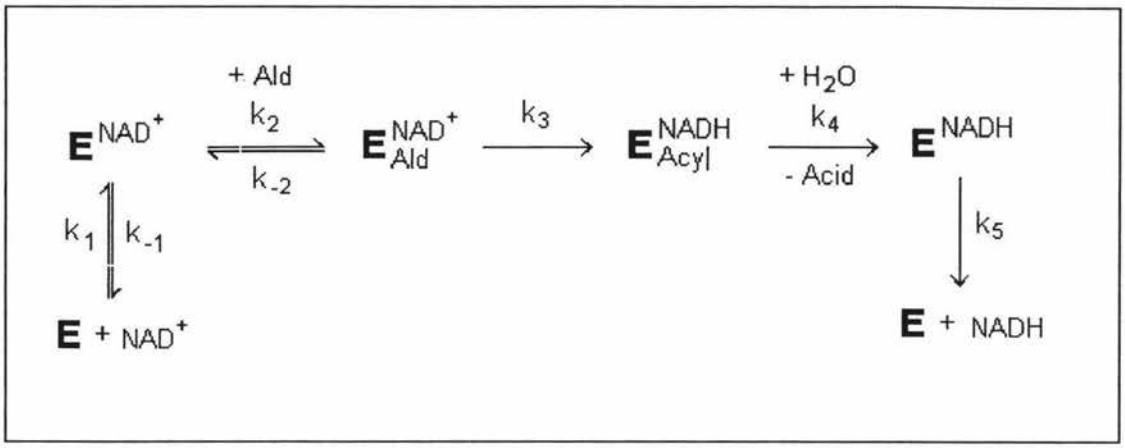

Figure 36. Reaction mechanism for the catalysed oxidation of an aldehyde by sheep liver ALDH.

Figure 37 shows the proposed kinetic model for bovine corneal aldehyde dehydrogenase catalysed oxidation of an aldehyde, based on experimental evidence reported in this thesis and from previous studies (Riley, 1993; Riley et al., 1995).

In this proposed model when enzyme and aldehyde are premixed, aldehyde binds readily to the free enzyme to form a E_{Ald} complex (step 1). This complex may then undergo a slow conformational change to form the $^*E_{Ald}$ species (step 2). When the enzyme-aldehyde equilibrium mixture is rapidly mixed with NAD^+ an absorbance burst is observed (step 3). This burst represents the presteady-state production of NADH controlled by the fast hydride transfer step. The overall rate-determining step must be after hydride transfer or early in the second cycle of the reaction pathway when the enzyme recycles. As mentioned earlier, NADH dissociation is probably not the overall rate-determining step; rather, it is the slow conversion of E_{Ald} to $^*E_{Ald}$ (step 2) which controls the steady-state production of NADH.

A short preincubation period between enzyme and NAD^+ results in the formation of a E^{NAD+} complex (step 4). When the E^{NAD+} complex is rapidly mixed with aldehyde a lag period followed by an absorbance burst and a steady-state phased is observed. The aldehyde binds relatively fast to the E^{NAD+} complex to form E^{NAD+}_{Ald} (step 5) but the conversion of E^{NAD+}_{Ald} to $^*E^{NAD+}_{Ald}$ is necessary before the burst can be observed. This conversion may be represented by the lag period. The occurrence of

a burst indicates that again the overall rate-determining step must be after hydrogen transfer or early in the second cycle of the reaction pathway, i.e. step 2.

When enzyme and NAD^+ are premixed they form a E^{NAD+} complex. As the duration of preincubation increases, the E^{NAD+} complex very slowly adopts a form ($^{**}E^{NAD+}$) which is catalytically unfavourable and lies off the normal pathway (step7, pathway C). After a long preincubation period a equilibrium is established, in which the concentration of the E^{NAD+} complex is almost zero relative to the $^{**}E^{NAD+}$ and **E** forms, i.e. $[E^{NAD+}] << [E] << [^{**}E^{NAD+}]$. When aldehyde is rapidly mixed with the enzyme-NAD^+ equilibrium solution, the aldehyde binds to the free enzyme resulting in a small amount of enzyme being converted to E_{Ald}; this causes the equilibrium to shift so that more free enzyme is produced. NAD^+ first detaches from the $^{**}E^{NAD+}$ complex to form $^{**}E$ (step 8), which is slowly converted to free enzyme, **E** (step 9) and is represented by a lag period. The reaction then proceeds down the aldehyde binding pathway (A), therefore, no absorbance burst is observed, only a steady-state rate, which is controlled by the slow conversion of E_{Ald} to $^{*}E_{Ald}$ (step 2).

When NAD^+ and aldehyde are rapidly mixed at the same time with free enzyme only the steady-state phase of the reaction is observed. This is consistent with the proposal, that aldehyde binds preferentially to the free enzyme and the reaction proceeds down the aldehyde binding pathway (A). By this pathway aldehyde binds to the free enzyme to form a E_{Ald} complex and the conversion of E_{Ald} to $^{*}E_{Ald}$ then controls the steady-state rate of the reaction. As this slow step precedes the rapid hydride transfer step, no burst would be observed, only the steady-state production of NADH.

If NAD^+ was to bind first as it does for ALDH classes 1 and 2 and the reaction was to proceed down pathway (B), then we would have expected to see a lag period followed by a burst and then a steady-state rate. This was not observed, which might suggest that aldehyde, not NAD^+ is the lead substrate and that the reaction pathway for class 3 bovine corneal aldehyde dehydrogenase is different from that of classes 1 and 2.

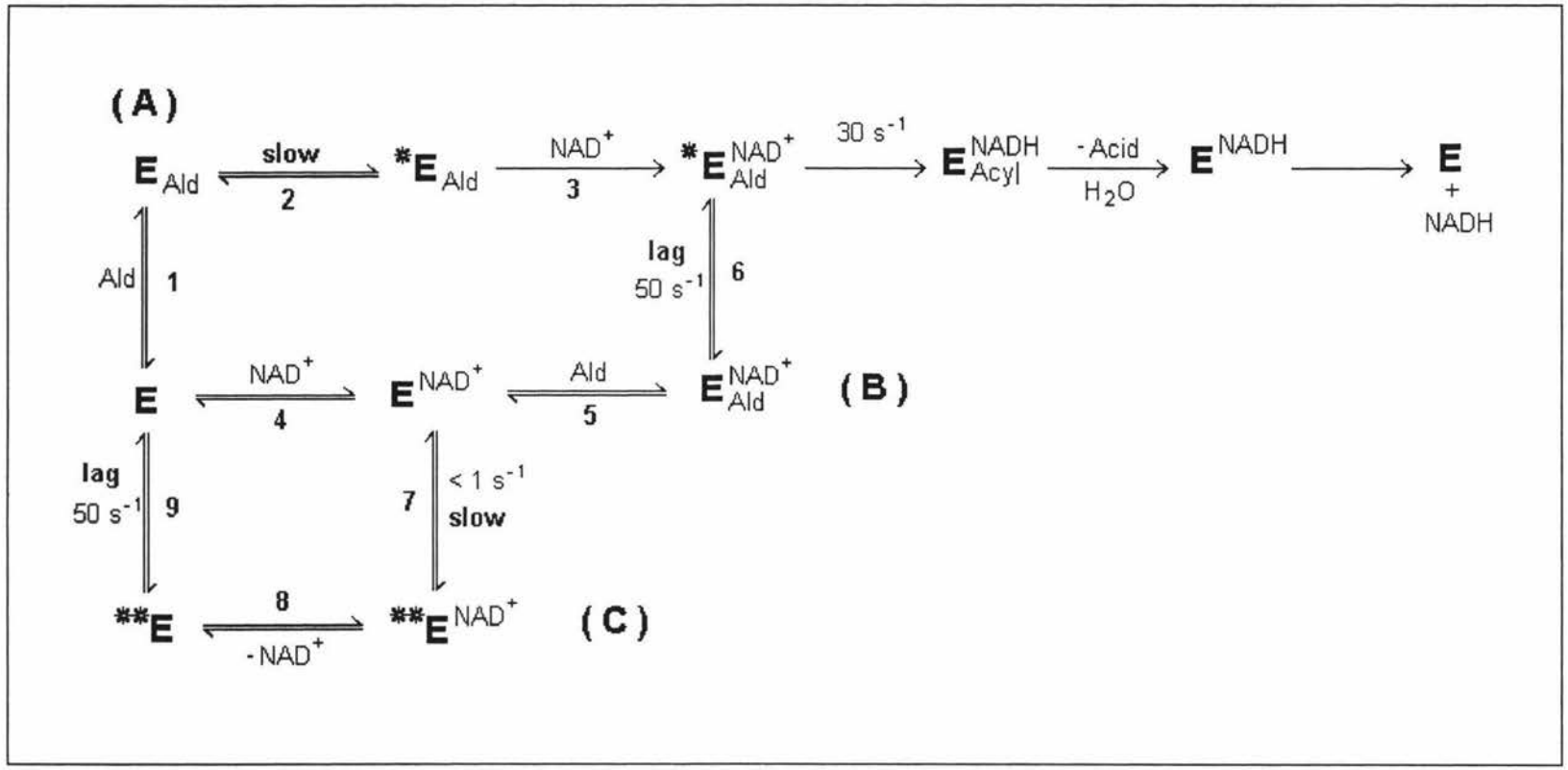

Figure 37. Proposed kinetic model for the reaction pathway for bovine corneal ALDH catalysed oxidation of an aldehyde based on experimental evidence.

[A] The reaction pathway if aldehyde binds to free ALDH first.
[B] The reaction pathway if NAD^+ binds to free ALDH first.
[C] The unfavorable reaction pathway after a long preincubation period between ALDH and NAD^+

The proposed kinetic model is consistent with the biological functions of class 3 ALDH in mammalian corneas (Abedinia *et al.*, 1990). The ability of free ALDH to bind aldehydes regardless of the levels of NAD^+, may provide a mechanism for the protection of the cornea from the rapid build up of aldehydes produced by the sudden exposure of the eye to ultraviolet light. As free ALDH can also bind NAD^+ and NADH, these enzyme-coenzyme complexes could also act as ultraviolet light filters, protecting the photosensitive retina cells from the damaging effects of ultraviolet light.

Section 5. Summary of Results and Conclusions

5.1 Purification of Class 3 Bovine Corneal Aldehyde Dehydrogenase

The purification of bovine corneal aldehyde dehydrogenase in this thesis was based on that of previous investigators (Abedinia *et al*, 1990; Riley, 1993). However, the procedure was modified by the inclusion extra purification steps.

In the final version of the purification procedure (purification 3b), PMSF was added to the buffers and a salt fractionation step was included in the purification protocol before application to a cation exchange column. These modifications to the purification procedure were effective in improving the degree of purification and the specific activity of the extracted corneal ALDH enzyme.

SDS gel electrophoresis of the protein obtained from the final purification procedure 3b, yielded a homogeneous purified protein with an approximate subunit molecular weight of 54 kDa. Earlier purifications showed that the purified protein was not homogeneous, as there were protein contaminants, but the major protein band did have an approximate subunit molecular weight of 54 kDa.

In this research four active ALDH bands with different isoelectric points were observed upon isoelectric focusing: 6.27, 6.38, 6.49, and 6.69. These values differ from those reported by Alexander *et al.* (1981), but are similar to those determined by Konishi & Mimura (1992).

5.2 Ligand Binding studies

The difference spectrum between enzyme-bound and free NADH showed that the wavelength at which the highest absorbance change on NADH binding occurs is 348 nm. This difference in absorbance allowed the enzyme present in solution to be monitored on NADH binding at this wavelength. NADH was added to the enzyme until the absorbance readings between aliquots ceased to change. The total concentration of NADH added to this point was equal to the NADH binding site

concentration, which was then used to calculate the number of NADH binding sites per enzyme dimer.

Values for the NADH dissociation constant and the number of NADH binding sites per dimer were found to be similar for NADH titrations performed using dialysed and undialysed enzyme, i.e. between 1.0 and 1.6 μM for the NADH dissociation constant and 1.5 and 2.0 for the number of NADH binding sites per dimer. However, the values were different from those reported in earlier studies (Riley, 1993). Recently the crystal structure of a class 3 ALDH has been determined (refer section 1.11) and it was revealed that there are indeed two NAD^+ binding sites per dimer, which supports the results reported in this thesis.

The NADH titration performed using dialysed enzyme which had been premixed with excess aldehyde showed that the presence of aldehyde disrupted NADH binding. Yet, NADH can bind to undialysed enzyme which has been shown to possess bound aldehyde. This suggests that the concentration of aldehyde plays an important part in determining the effects on NADH binding. In undialysed enzyme the concentration of bound aldehyde must be low as NADH binding can occur, but at a high concentration of aldehyde, NADH binding to dialysed ALDH is disrupted. This may indicate that there is an obligatory order of association/dissociation within the kinetic pathway. NADH can only bind/detach from the enzyme if no aldehyde is bound.

5.3 Kinetics

The resolution of individual steps of the overall reaction of an enzyme with its substrates and the evaluation of the rate constants associated with them is essential preliminary information for two lines of investigation. First, it serves as a basis for studies of the chemical mechanism through detailed analysis of the primary events responsible for each step. Secondly, it gives information about the particular step that is rate determining, and thus, where the control function of this particular enzyme lies.

Experimental evidence reported in this thesis and from previous studies (Riley, 1993; Riley, *et al.*, 1995) suggests that bovine corneal aldehyde dehydrogenase may function by a different reaction mechanism from that of the sheep liver enzyme, with aldehyde being the leading substrate not NAD^+. Based on the experimental evidence reported in this thesis a proposed kinetic model for bovine corneal aldehyde dehydrogenase catalysed oxidation of an aldehyde, is reported here (Fig. 37).

In this proposed model, aldehyde binds preferentially to the free enzyme to form a $\mathbf{E_{Ald}}$ complex and the then reaction proceeds down the aldehyde binding pathway (A). The conversion of $\mathbf{E_{Ald}}$ to $\mathbf{^*E_{Ald}}$ then controls the steady-state rate of the reaction. As this slow step precedes the rapid hydride transfer step, no burst would be observed, only the steady-state production of NADH. This was verified when NAD^+ and aldehyde were rapidly mixed at the same time with free enzyme, only the steady-state phase of the reaction is observed. If NAD^+ was to bind first, as it does for ALDH classes 1 and 2 and the reaction was to proceed down pathway (B), then we would have expected to see a lag period followed by a burst and then a steady-state rate. This was not observed and is consistent with the proposed kinetic model.

Free enzyme can bind NAD^+ in the absence of aldehyde, but as the duration of preincubation between enzyme and NAD^+ increases, this results in a form which is unsuitable for the production of a burst and lies off the normal pathway (pathway C). On the addition of aldehyde this unfavouable form is converted back to free enzyme and the reaction proceeds via the aldehyde binding pathway (A).

References.

Abedinia, M., Pain, T., Algar, E.M., Holmes, R.S. (1990). Bovine corneal aldehyde dehydrogenase: the major soluble corneal protein with a possible dual protective role for the eye. *Exp. Eye Res.* **51**, 419.

Alexander, R., Silverman, B. and Henley, W. (1981). Isolation and characterisation of BCP 54, the major soluble protein of bovine cornea. *Exp. Eye Res.* **32**, 205.

Algar, E.M. and Holmes, R.S. (1985). Mouse and mitochondrial aldehyde dehydrogenase isozymes: purification and molecular properties. *Int. J. Biochem.* **17**, 51.

Algar, E.M. and Holmes, R.S. (1986). Liver cytosolic aldehyde dehydrogenases from 'alcohol-drinking' and 'alcohol-avoiding' mouse strains: purification and molecular properties. *Int. J. Biochem.* **18**, 49.

Algar, E.M. and Holmes, R.S. (1989). Purification and properties of mouse stomach aldehyde dehydrogenase. Evidence for a role in the oxidation of peroxidic and aromatic aldehydes. *Biochim. Biophys. Acta*, **995**, 168.

Algar, E.M., Abedinia, M., VandeBerg, J.L., Holmes, R.S. (1990). Purification and properties of baboon corneal aldehyde dehydrogenase. Proposed UV protective role. In " Enzymology and Molecular Biology of Carbonyl Metabolism 3". Eds. Weiner, H., Flynn, T.G. Liss-Wiley, New York. pp53.

Ambach, W., Blumthaler, M., Schöpf, T., Ambach, E., Katzgraber, F., Daxecker, F., Daxer, A. (1994). Spectral transmission of the optical media of the human eye with respect to keratitis and cataract formation. *Doc Ophthalmol.* **88**, 165.

Ambroziak, W. and Pietruszko, R. (1987). Human aldehyde dehydrogenase: metabolism of putrsine and histamine. *Alcoholism: Clin. Exp. Res.*, **11**, 528.

Ames, G. (1974). Resolution of bacterial proteins by polyacrylamide gel electrophoresis on slabs. Membrane, soluble and periplasmic fractions. *J. Biol. Chem.* **249**, 634.

Bachem, A. (1956). Ophthalmic ultraviolet action spectra. *Am. J. Ophthalmol.*, **41**, 969.

Bakker, C., Pasmans, S., Verhagen, C., Van Haren, M., Van der Gaag, R., Hoekzema, R. (1992). Characterization of soluble protein BCP 11/24 from bovine corneal epithelium, different from the principal soluble protein BCP 54. *Exp. Eye Res.* **54**. 201.

Beekhuis, H.W. and McCarey, B.E. (1986). Corneal epithelial Cl-dependent pump quantified. *Exp. Eye Res.*, **43**, 707.

Bergmanson, J.P. (1990). Corneal damage in photokeratitis-why is it so painful? *Optom. Vis. Sci.* **67**, 407.

Blackwell, L.F., MacGibbon, A.K.H. and Buckley, P.D. (1989). Aldehyde dehydrogenases-kinetic characterisation, In "Human Metabolism of Alcohol, vol. II". Eds., Crow, K.E. and Batt, R.D., pp. 89-104, CRC Press, Boca Raton, Florida.

Blair, A.H. and Bodley, F.H. (1969). Human liver aldehyde dehydrogenase: partial purification and properties. *Can. J. Biochem.*, **47**, 265.

Boettner, E.A. and Wolters, J.R. (1962). Transmittance of the ocular media. *Invest. Opthalmol.* **1**, 776.

Borcherding, M., Blacik, L., Sittig, R., Breen, M., Weinstein, H. (1975). Proteoglycans and collagen fibre organisation in human corneoscleral tissue. *Exp. Eye. Res.* **21**, 59.

Bradford, M. (1976). A rapid and sensitive method for the quantitation of microgram quantities of protein utilising the principles of protein-dye binding. *Anal. Biochem.* **72**, 248.

Cannon, D. and Foster, C. (1978). Collagen cross linking in keratoconus. *Invest. Ophthalmol. Vis. Sci.* **17**, 63.

Cederbaum, A.I. and Rubin, E. (1977). The oxidation of acetaldehyde by isolated mitochondria from various organs of the rat and hepatocellular carcinoma. *Arch. Biochem. Biophys.*, **179**, 46.

Cogan, D.G. and Kinsey, V.E. (1946). Action spectrum of keratitis produced by ultraviolet radiation. *Acta Opthalmol.*, **35**, 670.

Cooper, D.L., Baptist, E.W., Enghild, J.J., Lee, H., Isola, N.R., Klintworth, G.K. (1990). Partial amino acid sequence determination of bovine corneal protein 54 K (BCP 54). *Curr. Eye Res .*, **9**, 781.

Cooper, D.L., Baptist, E.W., Enghild, J.J., Isola, N.R., Klintworth, G.K. (1991). Bovine corneal protein 54K (BCP54) is a homologue of the tumor-associated (class 3) rat aldehyde dehydrogenase (RATALD). *Gene.*, **98**, 201.

Cox, P.J., Phillips, B.J. and Thomas, P., (1975). The enzymatic basis of the selective action of cyclophophamide. *Cancer Res.*, 35, 3755.

Crow, K.E., Kitson, T.M., MacGibbon, A.K.H., Batt, R.D. (1974). Intracellular localisation and properties of aldehyde dehydrogenases from sheep liver. *Biochim. Biophys. Acta*, **350**, 121.

Cullen, A.P., Chou, B., Hall, M., Jany, S. (1984). Ultraviolet-B damages corneal endothelium. *Am. J. Optom. Physiol Optics.* **61**, 473.

Cuthbertson, R.A., Tomarev, S.I., and Piatigorsky, J. (1992). Taxon-specific recruitment of enzymes as major soluble proteins in the corneal epithelium of three mammals, chicken, and squid. *Proc Natl. Acad Sci.* **89**, 4004.

Dianzani, M. (1989). Lipid peroxidation and cancer: a critical reconsideration, *Tumori*, **75**, 351.

Deitrich, R.A. (1966). Tissue and subcellular distribution of mammalian aldehyde-oxidising capacity. *Biochem. Pharmacol.*, **15**, 1911.

Deitrich, R.A. (1971). Genetic aspects of increase in rat liver aldehyde dehydrogenase by phenobarbital. *Science*, **173**, 334.

Deitrich, R.A., Bludeau, P., Stock, T., Roper, M. (1977). Induction of different supernatant aldehyde dehydrogenases by phenobarbital and tetrachlorodibenzo-*p*-dioxin. *J. Biol. Chem.*, **252**, 6169.

Doughty, M. J. and Cullen, A. P. (1989). Long-term effects of a single dose of ultraviolet-b on albino rabbit cornea. *Photochem. Photobiol.* **49**, 185.

Downes, J. and Holmes, R. (1992). Development of aldehyde dehydrogenase and alcohol dehydrogenase in mouse eye: evidence for light-induced changes. *Biol. Neonate.* **61**, 118.

Downes, J.E. and Holmes, R.S. (1993). Purification and properties of murine corneal aldehyde dehydrogenase. *Biochem Molec Bio Int.* **30**, 525.

Downes J.E., Swann, P.G. and Holmes, R.S. (1993). Ultraviolet light-induced pathology in the eye: associated changes in ocular aldehyde dehydrogenase and alcohol dehydrogenase activities. *Cornea.* **12**, 241.

Downes, J.E., VandeBerg, J.L., Hubbard, G.B., Holmes R.S. (1992). Regional distribution of mammalian corneal aldehyde dehydrogenase and alcohol dehydrogenase. *Cornea.* **11**, 560.

Duley, J.A., Harris, O. and Holmes, R.S. (1985). Analysis of human alcohol- and aldehyde-metabolising isozymes by electrophoresis and isoelectric focusing. *Alcoholism: Clin. Exp. Res.*, **9**, 263.

Dunn, T.J., Lindahl, R. and Pitot, H.C. (1988). Differential gene expression in response to 2,3,7,8-tetrachlorodibenzo-*p*-dioxin (TCDD). Noncoordinate regulation of a TCDD-inducible aldehyde dehydrogenase and cytochrome P-450c in the rat. *J. Biol. Chem.*, **263**, 10878.

Eckfeldt, J.H. and Yonetani, T. (1976). Subcellular localisation of the F1 and F2 isozymes of horse liver aldehyde dehydrogenase. *Arch. Biochem. Biophys.*, **175**, 717.

Eckfeldt, J.H., Mope, L., Takio, K., Yonetani, T. (1976). Horse liver aldehyde dehydrogenase: purification and characterisation of two isozymes. *J. Biol. Chem.*, **251**, 236.

Esterbauer, H., Zollner, H. and Schaur, R. (1990). Aldehydes formed by lipid peroxidation: mechanisms of formation, occurrence and determination. In "Membrane Lipid Oxidation, Vol. 1", Vigo-Pelfrey, C., Ed., CRC Press, Boca Raton, FL.

Esterbauer, H., Zollner, H. and Lang, J. (1985). Metabolism of the lipid peroxidation product 4-hydroxynonenal by isolated hepatocytes and by liver cytosolic fractions. *Biochem J.* **208**, 129.

Evces S. and Lindahl R. (1989). Characterization of rat cornea aldehyde dehydrogenase. *Arch Biochem. Biophys.*, **274**, 518.

Eype, A., Kruit, P., Van der Gaag, R., Neuteboom, G., Broersma, L., Kijlstra, A. (1987). Autoimmunity against corneal antigens. II . Accessibility of the 54 kD corneal antigen for circulating antibodies. *Curr. Eye Res.*, **6**, 467.

Farres, J., *et al.* (1995). Investigation of the active site cysteine residue of rat liver mitochondrial aldehyde dehydrogenase by site-directed mutagenesis. *Biochem.* **11**, 2592.

Feinstein, R.N. and Cameron, E.C. (1972). Aldehyde dehydrogenase activity in rat hepatoma. *Biochem. Biophys. Res. Comm.*, **48**, 1140.

Feldman, R. and Weiner, H. (1972). Horse liver aldehyde dehydrogenase. I. Purification and characterisation. *J. Biol. Chem.*, **247**, 260.

Gondhowiardjo, T.D., van Haeringen, N.J., Hoekzema, R., Pels, L., Kijlstra, A. (1991). Detection of aldehyde dehydrogenase activity in human corneal extracts. *Curr. Eye Res.* **10** 1001.

Gondhowiardjo, T.D., van Haeringen, N.J. and Kijlstra, A. (1992a). Molecular weight forms of corneal aldehyde dehydrogenase. *Current Eye Res.* **11**, 377.

Gondhowiardjo, T.D., van Haeringen, N.J. and Kijlstra, A. (1992b). Isoelectric focusing pattern of human corneal aldehyde dehydrogenase. *Cornea.* **11**, 386.

Grafstrom, R.C. (1990). *In vitro* studies on aldehyde effects related to human respiratory carcinogenesis. *Mutat. Res.*, **238**, 175.

Greenfield, N.J. and Pietruszko, R. (1977). Two aldehyde dehydrogenases from human liver. Isolation via affinity chromatography and characterisation of the isozymes. *Biochim. Biophys. Acta*, **483**, 35.

Grunnet, N., (1973). Oxidation of acetaldehyde by rat liver mitochondria in relation to ethanol oxidation and the transport of reducing equivalents across the mitochondrial membrane. *Eur. J. Biochem.* , **35**, 23.

Harada, S., Agarwal, D.P. and Goedde, H.W. (1978). Isozyme variations in acetaldehyde dehydrogenase (e.c.1.2.1.3) in human tissues. *Hum. Genet.*, **44**, 181.

Harada, S., Agarwal, D.P. and Goedde, H.W. (1980). Electrophoretic and biochemical studies of human aldehyde dehydrogenase isozymes in various tissues. *Life Sci.* **26**, 1773.

Hedbys, B.O. (1961). The role of polysaccharides in corneal swelling. *Exp. Eye Res.*, **1**, 81.

Hemmingsen, E.A. and Douglas, E.L. (1970). Ultraviolet radiation thresholds for corneal injury in Antarctic and temperate-zone animals. *Comp. Biochem. Physiol.* **32**, 593.

Hempel, J. and Pietruszko, R. (1981). Selective chemical modification of human liver aldehyde dehydrogenases by iodoacetamide. *J. Biol. Chem.* **256**, 10889.

Hempel, J., Bahr-Lindstrom, H. and Jornvall, H. (1984). Aldehyde dehydrogenase from human liver. Primary structure of the cytoplasmic isoenzyme. *Eur. J. Biochem.* **141**, 21.

Hempel, J., Liu, Z.J., Perozich, J., Rose, J., Lindahl, R., Wang, B.C. (1996). Conserved residues in the aldehyde dehydrogenase family. Locations in the class 3 tertiary structure. *Adv. Exp. Med. Biol.* **414**, 9.

Hempel, J., Nicholas, H. and Lindahl, R. (1993). Aldehyde dehydrogenases: widespread structural and functional diversity within a shared framework. *Prot. Sci.* **2**, 1890.

Hjelle, J.T., Petersen, D.R. and Hjelle, J.J. (1983). Drug metabolism in isolated proximal tubule cells: aldehyde dehydrogenase. *J. Pharmacol. Exp. Ther.*, **224**, 699.

Holmes, R.S. (1978). Electrophoretic analysis of alcohol dehydrogenase, aldehyde dehydrogenase, aldehyde oxidase, sorbitol dehydrogenase and xanthine oxidase from mouse tissues. *Comp. Biochem. Physiol.* **61B**, 339.

Holmes, R.S. (1988). Alcohol dehydrogenases and aldehyde dehydrogenases of anterior eye tissues from humans and other mammals. In "Biomedical and Social Aspects of Alcohol and Alcoholism". Eds. Kuriyama, K., Takada, A. and Ishii, H. Elsevier Science Publishers; Amsterdam. 51.

Holmes, R.S., Popp, R.A. and VandeBerg, J.L. (1988). Genetics of ocular NAD-dependent alcohol dehydrogenase and aldehyde dehydrogenase in the mouse: evidence for genetic identity with stomach isozymes and localisation of *Ahd-4* on chromosome II near trembler. *Biochem. Genet.* **26**, 191.

Holmes, R.S. and VandeBerg, J.L. (1986a). Aldehyde dehydrogenases, aldehyde oxidase and xanthine oxidase from baboon tissues: phenotypic variability and subcellular distribution in liver and brain. *Alcohol.*, **3**, 205.

Holmes, R.S. and VandeBerg, J.L. (1986b). Ocular NAD-dependent alcohol dehydrogenase and aldehyde dehydrogenase in the baboon. *Exp. Eye Res.*, **43**, 383.

Holmes, R.S., Cheung, B. and VandeBerg, J.L. (1989). Isoelectric focusing studies of aldehyde dehydrogenases, alcohol dehydrogenases and oxidases from mammalian anterior eye tissues. *Comp. Biochem Physiol.* **93**, 271.

Holmes, R.S., van Oorschot, R.A. and VandeBerg, J.L. (1990). Genetics of alcohol dehydrogenase and aldehyde dehydrogenase from Monodelphis domestica cornea: further evidence for identity of corneal aldehyde dehydrogenase with a major soluble protein. *Genet. Res.*, **56**, 259.

Holt, W.S. and Kinoshita, J.H. (1973). The soluble proteins of the bovine cornea. *Invest. Ophthalmol.*, **12**, 114.

Horton, A.A. and Barrett, M.C, (1975). The subcellular localisation of aldehyde dehydrogenase in rat liver. *Arch. Biochem. Bioohys.*, **167**, 426.

Hsu, L.C., Bendel, R.E. and Yoshida, A. (1988). Genomic structure of the human mitochondrial aldehyde dehydrogenase gene. *Genomics.*, **2**, 57.

James, G. (1978). *Anal Biochem.* **86**, 574.

Jeppsson, J. and Johansson, M. (1985). Isolation of two minor fractions of α1-Antitrypsin by high performance liquid chromatography. *J. Chromatogr.*, **327**, 173-7

Jones, K., Lindahl, R., Baker, D., Timkovich, R. (1987). Hydride transfer stereospecificity of rat liver aldehyde dehydrogenases. *J. Bio. Chem.* **262**, 10911.

Jones Jr, D., Brennan, M.D., Hempel, J., Lindahl, R. (1988). Cloning and complete nucleotide sequence of a full length cDNA encoding a catalytically functional tumor-associated aldehyde dehydrogenase. *Proc. Natl. Acad. Sci. USA,* **85**, 1782.

Kangas, T., Edelhauser, H., Twinning, S., O'Brien, W. (1990). Loss of stromal glycosaminoglycans during corneal edema. *Arch. Biochem. Biophys.* **31**, 1994.

Kapoor, R., Bornstein, P. and Sage, E. (1986). Type VIII collagen from bovine Descemet's membrane: Structural characterisation of a triple-helical domain. *Biochem.* **25**, 3930.

Karn, R.C., Shulkin, J.D., Merritt, A.D., Newell, R.C. (1973). Evidence for post-transcriptional modification of human salivary amylase (amy_1) isozymes. *Biochem. Gen.*, **10**, 341-50.

King, G. and Holmes, R.S. (1993). Human corneal aldehyde dehydrogenase: purification, kinetic characterisation and phenotypic variation. *Biochem Mol Biol. Int.* **31**, 49.

Kitson. T., Hill, J. and Midwinter, G. (1991). Identification of a catalytically essential nucleophilic residue in sheep liver cytoplasmic aldehyde dehydrogenase. *Biochem. J.* **275**, 207.

Klyce, S.D. and Beuerman, R.W. (1988). Structure and function of the cornea. In " *The Cornea*" Eds. Kaufmann H.E., Barron, B.A., McDonald, M.B. and Waltman, S.R., Chapter 1, 3, Churchill Livingstone, New York, Edinburgh, London, Melbourne.

Koivula, T. and Koivusalo, M. (1975). Different forms of rat liver aldehyde dehydrogenase and their subcellular distribution. *Biochim. Biophys. Acta*, **397**, 9.

Konishi, Y. and Mimura, Y. (1992). Kinetic properties of the bovine corneal aldehyde dehydrogenase (BCP 54). *Exp. Eye Res.*, **55**, 569.

Kraemer, R.J. and Deitrich, R.A. (1968). Isolation and characterisation of human liver aldehyde dehydrogenase. *J. Biol. Chem.*, **243**, 6402.

Kurzel, R.B. (1978). On the nature of the action spectrum for ultraviolet photokeratitis. *Ophthalmic Res.* **10**, 312.

Laemmli, U.K. (1970). Cleavage of structural protein during the assembly of the head of bacteriophage T4. *Nature.* **227**, 680.

Leicht, W., Heinz, F. and Freimuller, B. (1978). Purification and characterisation of aldehyde dehydrogenase from bovine liver. *Eur. J. Biochem.*, **83**, 189.

Le Grand, Y. (1958). La protection des yeux contre l'ultraviolet. *Ann. Oculist.* **191**, 193.

Lesk, A.M. (1995). NAD-binding in dehydrogenases. *Curr. Opin. Struct. Bio.* **5**, 775.

Lindahl, R. (1986). Identification of hepatocarcinogenesis-associated aldehyde dehydrogenase in normal rat urinary bladder., *Cancer Res.*, **46**, 2502.

Lindahl, R. and Evces, S. (1984a). Comparative subcellular distribution of aldehyde dehydrogenase in rat, mouse and rabbit liver. *Biochem. Pharmacol.*, **33**, 3383.

Lindahl, R. and Evces, S. (1984b). Rat liver aldehyde dehydrogenase. II. Isolation and characterisation of four inducible isozymes. *J. Biol. Chem.*, **259**, 11991.

Lindahl, R. and Evces, S. (1984c). Rat liver aldehyde dehydrogenase. I. Isolation and characterisation of four high K_m normal liver isozymes. *J. Biol. Chem.*, **259**, 11986.

Lindahl, R. and Feinstein, R.N. (1976). Purification and immunochemical characterisation of aldehyde dehydrogenase from 2-acetylaminofluorene-induced rat hepatomas. *Biochim. Biophys. Acta*, **452**, 345.

Lindahl, R. and Petersen, D.R. (1991). Lipid aldehyde oxidation as a physiological role for class 3 aldehyde dehydrogenases. *Biochem. Pharmacol.*, **41**, 1583.

Liu, Z.J., Hempel, J., Sun, J., Rose, J., Hsiao, D., Chang, W.R,, Chun,g Y.J., Kuo, I., Lindahl, R., Wang, B.C., (1996). Crystal structure of a class 3 aldehyde dehydrogenase at 2.6 A resolution. *Adv. Exp. Med. Biol.* **414**, 1.

Liu, Z.J., Sun, Y.J., Rose, J., Chung, Y.J,, Hsiao, C.D., Chang, W.R., Kuo, I., Perozich, J., Lindahl, R., Hempel, J., Wang, B.C. (1997). The first structure of an aldehyde dehydrogenase reveals novel interactions between NAD and the Rossmann fold. *Nat Struct. Biol.* **4**, 317.

MacGibbon, A.K.H., *et al.* (1977). *Biochem. J.* **167**, 469.

MacKerrell, A.D., Blatter, E.E. and Pietruszko, R. (1986). Human aldehyde dehydrogenase: kinetic identification of the isozyme for which biogenic aldehydes and acetaldehyde compete. *Alcoholism: Clin. Exp. Res.* **10**, 266.

Mahoney, N.T., Doolittle, N.T. and Weiner, H. (1981). Genetic basis for the polymorphim of rat liver cytosolic aldehyde dehydrogenase. *Biochem. Genet.* **19**, 1275.

Manthey, C.L., Landkamer, G.J. and Sladek, N.E. (1990). Identification of mouse liver aldehyde dehydrogenases important in aldophosphamide detoxification. *Cancer Res.*, **50**, 4991.

Marjanen, L. (1972). Intracellular localisation of aldehyde dehydrogenase in rat liver. *Biochem. J.*, **127**, 633.

Marselos, M., Torronen, R., Koivula, T., Koivusalo, M. (1979). Comparison of phenobarbital and carcinogen-induced aldehyde dehydrogenases in the rat. *Biochim. Biophys. Acta*, **583**, 110.

Maurice, D.M. (1957). The structure and transparency of the cornea. *J. Physiol.*, **136**, 263.

Maurice, D.M. (1969). Cornea and sclera. In "The eye". Ed. Davson, H., Chapt. VII, 489. Academic Press, New York, London. Second edition.

Messiha, F. (1981). Species-dependent ocular aldehyde dehydrogenase. *Res. Comm. Chem. Pathol and Pharmacol.* **34**, 365.

Messiha, F. (1982). Developmental and kinetic aspects of rat eye aldehyde dehydrogenase. *Int. J. Biochem.*, **14**, 75

Messiha, F.S. and Price, J. (1983). Properties and regional distribution of ocular aldehyde dehydrogenase in the rat. *Neurobehav. Toxicol Teratol.* **5**, 251.

Millin, J.A., Galub, B.M. and Foster, C.S. (1986). Human basement membrane components of keratoconus and normal corneas. *Invest. Ophthalmol. Vis. Sci.*, **27**, 604.

Mitchell, J. and Cenedella, R.J. (1995). Quantitation of ultraviolet light-absorbing fractions of the cornea. *Cornea*, **14**, 266.

Mitchell, D.Y. and Petersen, D.R. (1987). The oxidation of α-β unsaturated aldehydic products of lipid peroxidation by rat liver aldehyde dehydrogenases. *Toxicol. Appl. Pharmacol.*, **87**, 403.

Nakanishi, S., Shiohara, E. and Tsukada, M. (1978). Rat liver aldehyde dehydrogenases: strain differences in the response of the enzymes to phenobarbital treatment. *Jpn. J. Pharmacol.*, **28**, 653.

Nakayasu, K., Tanaka, M., Konimi, H., Hayashi, T. (1986). Distribution of types I, II, III, IV and V collagen in normal and keratoconus corneas. *Ophthalmic Res.*, **18**, 1.

Nakayasu, H., Mihara, K and Sato, R. (1978). Purification and properties of a membrane-bound aldehyde dehydrogenase from rat liver microsomes. *Biochem. Biophys. Res. Comm.*, **83**, 697.

Newsome, D., Foidart, J., Hassel, J., Krachmer, J., Rodrigues, M., Katz, S. (1981). Detection of specific collagen types in normal and keratoconus corneas. *Invest. Ophthalmol. Vis. Sci.*, **20**, 738.

Olsen, T. (1980). The endothelial cell damage in acute glaucoma. On the corneal thickness response to intraocular pressure. *Acta Opthalmol.*, **58**, 257.

Oxlund, H. and Andreassen, T. (1980). The roles of hyaluronic acid, collagen and elastin in the mechanical properties of connective tissues. *J. Anat.*, **35**, 413.

Piatigorsky, J., O'Brien, W., Norman, B., Kalumuck, K., Wistow, G., Borras, T., Nickerson, J., Wawrousek, E. (1988). Gene sharing by δ-crystallin and argininosuccinate lyase. *Proc. Natl. Acad. Sci. USA* **85**, 3479.

Piatigorsky, J. and Wistow, G. (1989). Enzyme/crystallins: gene sharing as an evolutionary strategy. *Cell.* **57**, 197.

Pitts, D.G. (1970). A comparative study of the effects of ultraviolet radiation on the eye. *Am. J. Optom. Arch. Am. Acad. Optom.* **47**, 535.

Pitts, D.G. (1973). The ocular ultraviolet action spectrum and protection criteria. *Health Phys.* **25**, 559.

Pitts, D.G., Bergmanson, J.P.G., Chu, L.W.F., Waxler, M. and Hitchins, V.M. (1987). Ultrastructural analysis of corneal exposure to UV radiation. *Acta Opthalmol.*, **65**, 263.

Rabaey, M. and Segers, J. (1981). Changes in the polypeptide composition of the bovine corneal epithelium during development. In " VIth Congress of the European Society of ophthalmology" Eds. Trevor-Roper, P.D. Academic Press, London, 41.

Riley, I.K. (1993). Purification and kinetic studies on class3 ALDH from bovine cornea. B.Sc. (Hons) "Project", Massey University.

Riley, I.K, Burrows, C.A, Hardman, M.J., Buckley, P.D. (1995). Kinetic studies on class 3 aldehyde dehydrogenase from bovine cornea. *Adv. Exp. Med. Biol.* **372**, 85.

Riley, M.V., Susan, S., Peters, M.I., Schwartz, C.A. (1987). The effects of UV-B irradiadtion on the corneal endothelium. *Curr. Eye Res.*, **6**, 1021.

Ringvold A. (1980). Cornea and ultraviolet radiation. *Acta Opthalmol.*, **58**, 63.

Rossmann, M., Moras, D. and Olsen, K. (1974). Chemical and biological evolution of a nucleotide binding protein. *Nature*. **250**, 194.

Rout, U.K. and Holmes, R.S. (1985). Isoelectric focusing studies of aldehyde dehydrogenases from mouse tissues: variant phenotypes of liver, stomach and testis isozymes. *Comp. Biochem. Physiol.*, **81B**, 647.

Rout, U.K. and Holmes, R.S. (1988). Postnatal development of mouse aldehyde dehydrogenases. Agarose-isoelectric focusing analyses of the heart, lung, skin and ocular isozymes. In " Biomedical and Social Aspects of Alcohol and Alcoholism" Eds. Kuriyama, K., Takada, A. and Ishii, H. Elsevier Science Publishers; Amsterdam. 139.

Rout, U.K. and Holmes, R.S. (1991). Postnatal development of mouse alcohol dehydrogenases: Agarose-isoelectric focusing analyses of the liver, kidney, stomach and ocular isozymes. *Biol. Neonate.* **59**, 93.

Ryzlak, M.T. and Pietruszko, R. (1987). Purification and characterisation of aldehyde dehydrogenase from human brain. *Arch. Biochem. Biophys.*, **255**, 409.

Scatchard, G. (1949). *Ann. N.Y. Acad. Sci.* **51**, 660.

Schauenstein, E., Esterbauer, H. and Zollner, H. (1977). *Aldehydes in Biological systems: Their Natural Occurrence and Biological Activities*, Pion, London.

Scholander, P., Irving, L., Hemmingsen, E., Bradstreet, E. (1969). Ultraviolet absorption in the cornea of arctic and alpine mammals. In "The biological effects of ultraviolet radiation, with emphasis on the skin". Ed. Urbach, F., Pergamon Press, New York, 469.

Sherashov, S.G. (1970). Spectral sensitivity of the cornea to ultraviolet radiation. *Biofizika*, **15**, 543.

Shum, G.T. and Blair, A.H. (1972). Aldehyde dehydrogenases in rat liver. *Can. J. Biochem.*, **50**, 741.

Siegenthaler, G., Saurat, J. and Ponec, M. (1990). Retinol and retinal metabolism. Relationship to the state of differentiation of cultured human keratinocytes, *Biochem. J.*, **268**, 371.

Siew, C., Deitrich, R.A. and Erwin, V.G. (1976). Localisation and characteristics of rat liver mitochondrial aldehyde dehydrogenase. *Arch. Biochem. Biophys.*, **176**, 638.

Silverman, B., Alexander, R.J. and Henley, W.L. (1981). Tissue and species specificity of BCP 54, the major soluble protein of bovine cornea. *Exp. Eye Res.*, **33**, 19.

Smith, L. and Packer, L. (1972). Aldehyde oxidation in rat liver mitochondria., *Arch. Biochem. Biophys.*, **148**, 270.

Sugimoto, E., Takahasi, N., Kitagawa, Y. Chiba, H. (1976). Intracellular localisation and characterisation of beef liver aldehyde dehydrogenase isozymes. *Agric. Biol. Chem.*, **40**, 2063.

Tank, A.W., Weiner, H. and Thurman, J.A. (1981). Enzymology and subcellular localisation of aldehyde oxidation in rat liver. Oxidation of 3-4-dihydroxyphenylacetaldehyde derived from dopamine to 3,4-dihydroxyphenylacetic acid. *Biochem Pharmacol.*, **30**, 3265.

Tomarev, S., Zinovieva, R. and Piatigorsky, J. (1991). *J. Biol. Chem.* **266**, 24226.

Torronen, R., Nousianinen, U. and Hanninen, O. (1981). Induction of aldehyde dehydrogenase by polycyclic aromatic hydrocarbons in rats. *Chem. Biol. Interactions.*, **36**, 33.

Tottmar, S.O.C., Pettersson, H. and Kiessling, K.H. (1973). The subcellular distribution and properties of aldehyde dehydrogenases in rat liver. *Biochem. Biophys.*, **135**, 477.

Uma, L., Balasubramanian, D. and Sharma, Y. (1994). In situ fluorescence spectroscopic studies on bovine cornea. *Photochem. Photobiol.* **59,** 557.

Uma. L., Hariharan, J., Sharma, Y., Balasubramanian, D. (1996). Effect of UVB radiation on corneal aldehyde dehydrogenase. *Curr. Eye Res.* **15**, 685.

Vaughan, L., Lorier, M. and Carrell, R. (1982). α_1-Antitrypsin microheterogeneity: isolation and physiological significance of isoforms. *Biochim. Biophys. Acta*, **701**, 330-45.

Verhagen C, Hoekzema R, Verjans GM, Kijlstra A. (1991). Identification of bovine corneal protein 54 (BCP 54) as an aldehyde dehydrogenase [letter]. *Exp. Eye Res.* **53**, 283.

Wang, S., Wu, C., Cheng, T., Yin, S. (1990). *Biochem Intl.* **22**, 199.

Wierenga, R., Terpstra, P. and Hol, W. (1986). Prediction of the occurrence of the ADP-binding βαβ-fold in proteins using an amino acid fingerprint. *J. Mol. Biol.* **187**, 101.

Williams, R. (1959). *Detoxification Mechanisms,* Chapman and Hall, London.

Wistow, G. and Kim, H. (1991). *J. Mol. Evol.* **32**, 262.

Wistow, G.J. and Piatigorsky, J. (1987). Recruitment of enzymes as lens structural proteins. *Science*, **236**, 1554.

Wurtman, R. J. (1975). The effects of light on the human body. *Sci. Am.* **233**, 68.

Yin, S.J., Wang, M.F., Han, C.L., Wang, S.L. (1995). Substrate binding pocket structure of human aldehyde dehydrogenases. A substrate specificity approach. *Adv. Exp. Med. Biol.* . **372**, 9.

Yoshida, A. (1990). Isozymes of human alcohol dehydrogenase and aldehyde dehydrogenase. In "Isozymes: Structure, Function and Use in Biology and Medicine". Ogita, Z.I. and Markert, C.L., Eds., Wiley-Liss, New York, 327.

Zigman, S.(1983). The role of sunlight in human cataract formation. *Surv. Opthalmol.*, **27**, 317.

Zigman, S. (1995). Environmental near-UV radiation and cataracts. *Optom. Vis. Sci.* **72**, 899.

Zimmermann, D., Trueb, B., Wintherhalter, K., Witmer, R., Fischer, R. (1986). Type VI collagen is a major component of the human cornea. *FEBS Lett.*, **197**, 55.

Zimmermann, D., Fischer, R., Wintherhalter, K., Witmer, R., Vaughan, L. (1988). Comparative studies of collagens in normal and keratoconus corneas. *Exp. Eye. Res.*, **46**, 431.